Universidad
Carlos III de Madrid

TESIS DOCTORAL

Active Neuro-Fuzzy Integrated Vehicle Dynamics Controller to improve the vehicle handling and stability at complicated maneuvers

Autor:
Rana Raouf Hasan Farag

Directores:
Prof. Dr. Beatriz Lopez Boada
Full Prof. Dr. Vicente Diaz Lopez

DEPARTAMENTO DE INGENIERÍA MECÁNICA

Leganés, Junio 2013

TESIS DOCTORAL

Active Neuro-Fuzzy Integrated Vehicle Dynamics Controller to improve the vehicle handling and stability at complicated maneuvers

Autor: Rana Raouf Hasan Farag

Directores:
Prof. Dr. Beatriz Lopez Boada
Full Prof. Dr. Vicente Diaz Lopez

Firma del Tribunal Calificador:

Firma

Presidente:
Vocal:
Secretario:

Calificación:

Leganés, de Julio de 2013 .

Dedicated to my Mom, my Dad, my Sister
and to Karim.

قال رسول الله صلى الله عليه وسلم :

"إذا مات ابن آدم انقطع عمله إلا من ثلاث: صدقة جارية، أو علم ينتفع به، أو ولد صالح يدعو له"
((رواه مسلم)).

El Profeta Muhammad dijo:

"Cuando un hombre muere, todas sus obras se terminan a excepción de tres tipos: una caridad continua y perpetua que deja atrás, o un conocimiento que él enseñó y difundió, o un hijo piadoso que pide perdón en su nombre."

Prophet Muhammad said:

"When a man dies, his deeds come to an end except for three things: a ceaseless charity, or a beneficial knowledge, or a virtuous descendant who prays for him."

Abstract

With the recent advancements in vehicle's industry, driving safety in passenger vehicles is considered one of the key issues in designing any vehicle. According to other studies Electronic Stability Control (ESC) is considered to be the greatest road safety innovation since the seatbelt. Yet ESC has its drawbacks, that encouraged the development of other stability systems to correct or compensate these draw backs. But to efficiently make up for the ESC problems the integration of various control systems is needed, which is a pretty complicated task on its own. Lately, solving this stability problem became a hot research topic accompanied by the market demands for improving the available stability systems.

Therefore, this thesis aims to add an innovative approach to help improve the vehicle stability. This approach consists of an intelligent algorithm that collects data about the vehicle characteristics and behavior. Then it uses an Artificial Neural Network to construct a fuzzy logic control system through learning from the optimum control values that was generated beforehand by the intelligent algorithm. This way, the proposed controller didn't depend only on experts' knowledge like the other controllers presented in the literature. This makes the controller more generic and reliable which is a very important aspect in designing a safety critical controller, like the presented one, where any fault in it can lead to a fatal accident.

Also using the technique of using an Artificial Neural Network to construct a fuzzy logic control allows benefiting from the learning and auto-adaption capability of neural networks and the smooth controlling performance that fuzzy logic controllers offers.

Simulations results show the effectiveness of the proposed controller for improving the vehicle stability in different driving maneuvers. Where the controller's results were compared to an uncontrolled vehicle and another vehicle

controlled by a controller from the literature.

Resumen

Cuando un vehículo entra en una curva a alta velocidad, la aceleración lateral producida hace que el vehículo tienda a ser más inestable y menos controlable desde el punto de vista del conductor. Esta inestabilidad, podría conllevar un comportamiento no deseado del vehículo, como el sub-viraje ó el sobre-viraje, que pueden llevar al vehículo a salirse de su curso previsto ó que vuelque. Además, las estadísticas concluyen que la inestabilidad lateral del vehículo es causa de accidentes de fatales consecuencias. Para hacer frente a este problema, se han propuesto varios sistemas de control, con el objetivo de generar una acción contraria que lleve de nuevo al vehículo a su curso deseado.

Estos sistemas pretenden alterar de una manera u otra las fuerzas centrífugas del neumático con el fin de producir fuerzas de compensación que ayuden a mantener el control lateral del vehículo. Estos controladores presentan estrategias de control diferentes: algunos intentan afectar directamente a los ángulos de dirección de los neumáticos, otros inciden en las fuerzas longitudinales de los neumáticos para crear un momento de guiñada alrededor del eje vertical del vehículo, y por último, otros intentan afectar a la distribución de la carga vertical entre los neumáticos. Por ello, debido a la diferencia de las características de cada uno de estos sistemas, sus capacidades de controlar también difieren. Sin desmerecer a ninguno de ellos, algunos demuestran mayor eficacia en situaciones de inestabilidad suaves; otros lo son cuando el vehículo llega a sus límites de adhesión, y los hay cuando la aceleración lateral supera un cierto valor.

Por esta razón, se recomienda el uso de más de un sistema de control para beneficiarse de las ventajas de sus diferentes conceptos de control. Sin embargo, la combinación de más de un controlador de estabilidad de un vehículo, no es tarea fácil, dado que podrían producirse conflictos entre los diferentes controladores, así como la superposición de los diferentes objetivos de control.

Adicionalmente, una simple combinación podría llevar a una mayor complejidad del *hardware* y el *software* usados, debido a la posible repetición de sensores y actuadores, y en consecuencia a una complejidad de cables de conexión. Por ello, se han propuesto sistemas de Dinámica de Vehículos de Control Integral (IVDC), para proporcionar una integración cuidadosamente diseñada con el objetivo de coordinar los diferentes sistemas de control del chasis. De esta manera, los conflictos de control podrían ser eliminados, y los resultados podrían reforzarse aún más mediante tal combinación. Igualmente el coste y la complejidad del sistema podrían reducirse debido al posible uso compartido de sensores, actuadores, unidades de control y cables. Recientemente, los sistemas de IVDC han sido un tema de investigación recurrente, existiendo distintos sistemas en la literatura que han intentado controlar varias combinaciones de los citados controladores utilizando una variedad de técnicas de control, muchos de los cuales han mostrado resultados prometedores en la mejora del manejo del vehículo a través de los resultados de simulaciones.

No obstante, estos sistemas eran manualmente diseñados y probados en un número limitado de maniobras y condiciones. Además, han sido testados en las mismas maniobras utilizadas para su diseño y, por tanto, su fiabilidad y previsibilidad son cuestionables. Por otra parte, los sistemas de control de estabilidad del vehículo son considerados como sistemas de seguridad crítica, donde cualquier error podría causar un accidente fatal. De este modo, como consecuencia de la imprecisión humana, un controlador diseñado manualmente que ha sido desarrollado a través de pruebas de situación limitada, es propenso a errores que generan deficiencias en ciertas zonas de control ó a inexactitudes en las decisiones de los valores de control.

Por otra parte, la selección manual del margen de control dedicado a cada sub-sistema integrado no asegura la optimización de las capacidades de los controladores. Además, dado que estos controladores son diseñados por el hombre, cualquier variación de las características del modelo del vehículo, como por ejemplo algo tan sencillo como el cambio en la rigidez de la suspensión, necesitaría de intervención humana para volver a calibrar ó volver a ajustar manualmente el sistema con el objetivo de adaptarse a la variación realizada.

Por lo tanto, en esta tesis se intentará reemplazar el conocimiento humano y los sistemas diseñados manualmente, por un sistema automatizado e inteligente, que autoconstruye el sistema de control sin intervención humana.

Este método utilizará una red neuronal inteligente que aprende los valores óptimos de control a través de un algoritmo extenso de minería de datos. En consecuencia, se autoconstruye un controlador de lógica difusa que corrige la estabilidad del vehículo a través de un sistema activo de corrección de la entrada al volante y un sistema de control de ángulo de guiñada mediante los frenos. Las entradas de control de estos sistemas serán la velocidad del ángulo de guiñada y el ángulo de deslizamiento lateral, siendo los controladores más eficaces presentados en la literatura.

Acknowledgments

I would like to sincerely thank my thesis supervisors *Prof. Dr. Beatriz Lopez Boada* and *Full Prof. Dr. Vicente Diaz Lopez* for guiding and helping me during the last five years of work. I would also like to express my deepest appreciation for the way they believed in me and in my capabilities and their encouragement that helped me a lot in finishing this work.

I would like to extend my gratitude to *Prof. Dr. Maria Jesus Lopez Boada* for all the valuable discussions and guidance that she provided me through out my thesis work. The suspensions control research would not have been realized without her recommendations and instructions.

The success of any project depends largely on the encouragement and guidelines of many others. I take this opportunity to express my gratitude to my colleagues of the MECATRAN Lab who have helped me through their valuable guidance and fruitful discussions and even through emotional support. I can say they became a family to me, the ones who are still working with us and the ones who left. Also a special thanks goes my office-mates for creating such a great work environment and cheering me up in the toughest moments.

Also I appreciate all the help and emotional support from other members of the university staff, either academic or non-academic, they have made my stay in a foreign country much easier and more delightful. But above all I'd like to thank *David Pedroche* for being my patient Spanish instructor, tireless encourager, such a great friend and such a great person.

I am also sincerely grateful for the University of Carlos III for providing the funds for my scholarship and facilitating various research funding supports. Also I would like to appreciate my gratitude for the funds provided by the Regional Government of Madrid through the project CCG10-UC3M/DPI-4614 and the funds provided by the Spanish Government through the CICYT project TRA2008-05373/AUT.

I would like to take the opportunity to dedicate a special thanks to *Dr. David Crolla* for all the contribution he have added to the research field and all the work he have published freely online to help and guide the other researchers. I would like to acknowledge that both thesis he supervised of *Mark Albert Selby* and *Junjie He* have been of a great guidance to my research work and dissertation writing. Unfortunately I have never got the chance to meet him but from the bottom of my heart I pray for his soul to rest in peace.

Out of the academic life their are people who have helped me along my thesis journey and their support was not of less importance to get this presented work done. They are *Susann Gobbin* who have provided me a great emotional support on my first year in Madrid, which would have been an unbearable year without her. And my beautiful friend *Nayla Belkhir* who have always believed in me, encouraged me and made my stay in Madrid much more delightful. Also my beautiful flat mates *Emma Diez*, *Maria Gascon* and *Veronica Ruiz* for being like a family to me, for supporting and encouraging and taking care of me. Also I would like to thank *Emma* and *Maria* for proof reading the Spanish part of my dissertation. And a very special thanks goes to my gorgeous and brilliant friend *Kamila Zwolinska* for being an inspiration in my life and for being such a great friend.

I am also very thankful for having my life time Egyptian friends *Nehal*, *Pasant*, *Mai*, *Yomna*, *Menna*, *Rana*, *Iman*, *Shimaa*, *Moe*, *Mido* and *Saleh* for being the best friends ever. For supporting and encouraging me and for not changing even when we are thousands of miles apart. I would also like to express my gratitude for my grandparents, my uncles and aunts and my cousins. For their belief in me, for their emotional support and for their prayers.

My deepest gratitude goes to my parents, *Hanan Abd el Wahed* and *Raouf Farag*, for everything they have done to me. Without their priceless support and guidance this work would not have even started. They supported and encouraged me to travel and start my Ph.D. program and have provided me with invaluable emotional and financial support throughout my thesis journey. Their belief in me was limitless and their satisfaction for me was the greatest motivator. Also my little sister, my best friend forever and my little angel *Sandra Raouf* have provided me with a rare emotional support. It has been very hard for me to spend all that time away and without her I would have not been able to make it.

Last but not least, I want to thank my lovely husband *Karim Moussa* for the endless love, tremendous support and encouragement he gave me through the past years. Without his understanding, his support and his selfless acts most probably this work would have never been finished.

Contents

List of Figures

List of Tables

Acronyms and Abbreviations

4WS Four Wheel Steering

4WD Four Wheel Drive

A4S Active Four Wheel Steering

ABS Anti-lock Braking Systems

ACV ANFIS Controlled Vehicle

AFS Active Front Steering

AI Artificial Intelligence

ANFIS Adaptive Neuro-Fuzzy Inference System

ANN Artificial Neural Network

ARC Active Roll Control

ARS Active Rear Steering

AS Active Steering

CL Change Lane

COG Center Of Gravity

DCL Double-change Lane

DOF Degrees of Freedom

DSC Dynamic Stability Control

DYC Direct Yaw moment Control

ECU Electronic Control Unit

ESC Electronic Stability Control

ESP Electronic Stability Program

FCV Fuzzy Controlled Vehicle

FLC Fuzzy Logic Control

FLS Fuzzy Logic System

GA Genetic Algorithms

IVDC Integrated Vehicle Dynamics Control

LSD Limited Slip Differential

NLVM Non-Linear Vehicle Model

RMSD Root Mean Squared Deviation

SBW Steer-By-Wire

TCS Traction Control Systems

VSC Vehicle Stability Control

Chapter 1

Introduction

Nowadays, high end vehicles look more like the intelligent vehicles of the fiction movies displayed 20 years ago. Some of these vehicles are now equipped with highly advanced user interfaces that react to the driver needs and decisions. They can provide the driver with addresses, directions and traffic information. They can also avoid collisions and improve the vehicle's dynamics depending on the driving situations. Also they can automatically park the car or help the driver to follow the correct speed limit or to keep the lane, etc.

This thesis addresses the intelligent control of the vehicle lateral stability. Aiming to improve the vehicle performance and therefore decrease the possibility of accidents and increase the passengers safety. This chapter will start by introducing the presence of electronic components in modern vehicles. Then, it will introduce the safety controllers that is mainly addressed in this thesis.

1.1 Electronic control in modern vehicles

In the last three decades and with the digital revolution, the vehicles manufacturing industry has been embracing more and more car mobile computers, also known as, Carputers, or known technically as Electronic Control Units (ECUs). In the 1980s, the main electronic devices found in a car was the radio and the engine controller. And the main car buying criteria were the engine power, car speed and body design [15]. But nowadays, automotive electronics are used to improve the comfort, safety, fuel consumption and even

for extra luxury options. Consequently car buyers choice is highly affected with these emerging options. In a study by Bosch® [16], they estimate that a modern upper class automobile would have up to 70 ECUs. Table 1.1 shows some examples of ECUs that can be found in nowadays cars. Needless to mention, the overhead cost that ECUs present, during 1980, the ratio between the "Cost of Electronic Embedded system" to the "cost of the car" was 1%, and raised up to 20% during 2005 and is expected to be 40% in 2015 [17].

1.2 Active Chassis Control

Specifically when it comes to vehicle dynamics, numerous active control systems have been developed to improve vehicle performance and active safety using different actuation concepts or advanced control methodologies. With the aim of increasing the passenger comfort and the vehicle ride handling. Most of these systems can be divided into three groups based on their control objectives; longitudinal control, lateral control and vertical (heave) control, see figure 1.1. Longitudinal control systems can include Anti-lock Braking Systems (ABS) and Traction Control Systems (TCS) that automatically modulate the braking or tractive force to improve the braking or traction performance of the vehicle. Lateral control systems come into action at cornering situations to maintain the vehicle stability and prevent it from over/under-steering, such as, Active Front Steering (AFS), Active Rear Steering (ARS) and Direct Yaw moment Control (DYC). As for vertical control, in such a type of control no driver intervention is needed as the control system intends to handle the vehicle automatically such as the active and semi-active suspensions controller, Active Roll Control (ARC) and damping controllers.

In this thesis, we are mainly interested in lateral control systems. Therefore, the main control systems that falls in this category will be discussed in the next chapters.

1.2.1 Driver, controller and vehicle dynamics interactions

A driver can control the vehicle dynamics through three ways; control the vehicle throttle, the braking pedals and the steering wheel. The first two control systems mainly address the vehicle's longitudinal motion, while

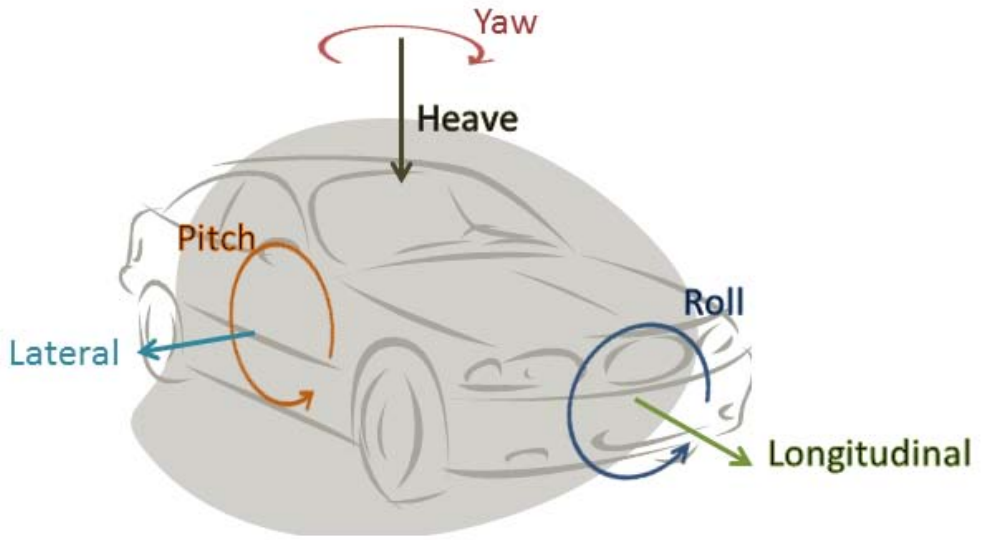

Figure 1.1: Chassis Dynamics Variables Using SAE Coordinates [1]

the latest controls the lateral motion (directional control). As we mentioned before, that this thesis focuses on the lateral control of the vehicle, therefore we will focus our attention on the driver steering input.

A driver steering input is influenced by two main factors: route following and vehicle stabilization. The first task presents the normal direction task, while the second represents the action of trying to compensate for any undesired maneuver or lateral instability. Both tasks are performed by the driver through monitoring the feedback information from the vehicle motion, e.g. position on the road and steering feel, see figure 1.2. Yet the second task is not a preferred one for the drivers [18] and the increase of its occurrence, decreases the feeling of safety and ride comfort.

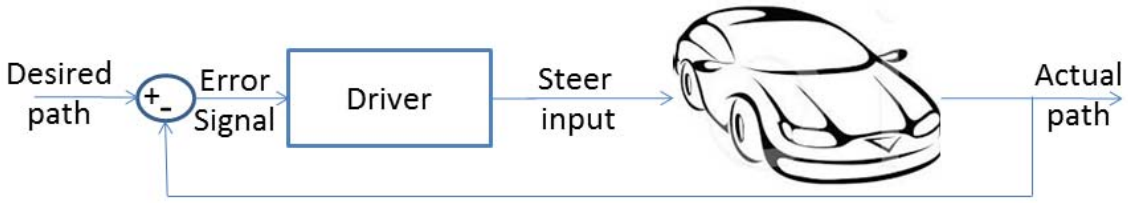

Figure 1.2: Block diagram of the driver-vehicle interaction

When such a task is left solely for the driver it gets affected by the driver's response time, driving expertise and chance of overreacting to the

situation. Moreover, when the vehicle endures complicated conditions, such as, driving on a high speed or on slippery surfaces or in hard weather conditions or even handling a sudden or difficult maneuver; the risk of the vehicle lateral instability increases, making the situation even harder for the driver to handle. At such situations, lateral control systems becomes very useful to avoid the probability of human-error through avoiding and recovering from any unwanted route disturbance.

For the control system to achieve a desired control, it monitors the feedback information from the vehicle motion just like the driver do, but this time through sensors and observers. The vehicle motion state is then compared with the desired state values that on their turn are decided by a reference model. The current and desired states are then used by the controller that decides the control action(s) that is carried on by the actuator(s). Figure 1.2 shows a block diagram of the generic concept of such control systems.

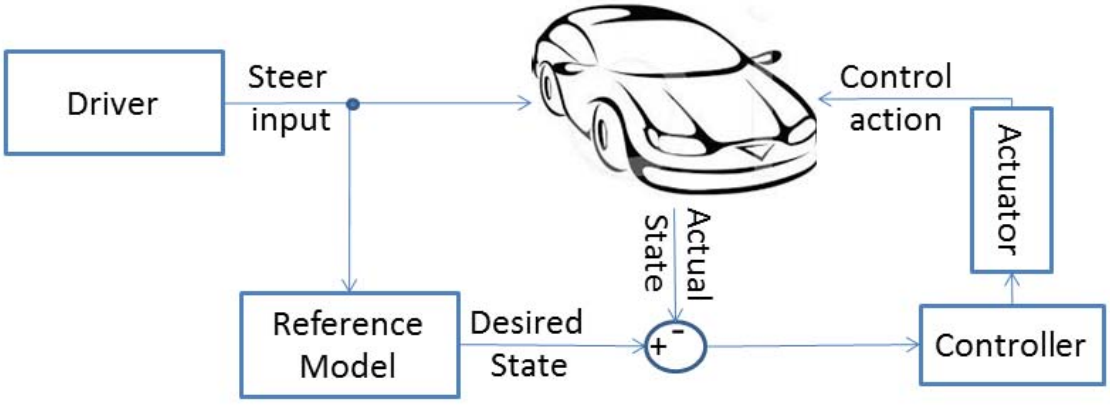

Figure 1.3: Block diagram of the driver-vehicle-controller interactions

1.2.2 Standalone Chassis Controllers

As mentioned above, there are numerous ECUs used in todays vehicles. Various controllers of them are standalone ones; where they work on their own without being a part of a controlling set or being connected to other ECUs. Many of these standalone controllers have been designed with the purpose of active control of vehicle handling. Each of such controllers has effective regions and a principal function and could be categorized, in terms of the tire forces they target as follows:

- **Active steering systems:** Active Front Steering (AFS), Active Rear Steering (ARS) and Active Four Wheel Steering (A4S).
- **Active roll moment distribution control systems:** Active Roll Bar, Active Suspension and Controllable Dampers.
- **Dynamic Stability Control (DSC):** driveline based DSC and brake based DSC.

The first group of ECUs affects the lateral tire forces, and is considered very effective in the linear handling, where the lateral tire forces are proportional to the corresponding slip angle. Yet as the car approaches the handling limit this system doesn't become as effective. Active roll moment distribution control systems, aims to change the roll moment distribution between the front and rear suspensions during cornering and thus vehicle handling behavior can be regulated through balancing the lateral forces between the front and rear ends of the vehicle. This technique's importance is only evident with the increase of the vehicle's lateral load displacement. And therefore, it can be effective at high lateral acceleration situations [19]. Then comes the Dynamic Stability Control systems that acts directly on the differential longitudinal tire forces between the right and left sides of the vehicle. In this way they generate a counter yaw moment to maintain the vehicle stability. These systems are pretty powerful when the vehicle reaches its handling limits of adhesion, yet in normal driving situations it has the major drawback of strongly influencing the longitudinal dynamics of the vehicle. Giving the drivers a feeling of uncontrollability over their vehicles and reducing the vehicle's speed in unnecessary situations. Section 3.2 provides a detailed explanation and literature review of these systems.

1.2.3 Integrated Chassis Control

As it can be seen, each of the discussed standalone chassis control techniques have their pros and cons. Which suggests the combination of various controllers to benefit from the advantages of each while trying to overcome their disadvantages. Nevertheless, combining these safety critical systems can not be done by a simple arithmetic operation; such that, such a combination can lead to a conflict between the submodules or even an overcorrection

behavior. Thus, a careful integration technique is required according to the behavior of each of the integrated controllers. Such an integration would add modularity, scalability and robustness [11].

This integration also allows to reduce the complexity of the controlling systems and in sometimes even reduce its cost; by sharing sensors and actuators between the different control system modules. Also this integration allows having a unique calculating processor that handles the different sensors and actuators through only a singular decision maker. Also it's suggested that this integration could increase the flexibility of the control system design, if the control target could be broken down to seperate tasks that each of which could be designed separately [20, 9]. A detailed description of the integrated chassis control will be detailed in section 3.3.

In this thesis, we will be mainly addressing an integration system of AFS and brake based DSC. A comparative study of the previously mentioned chassis controllers will be detailed later in chapter 3 along with our discussion of why we have chosen these controllers in particular. From those chosen controllers, the most widely used one in today's vehicles is the brake based DSC, also known as; Vehicle Stability Control (VSC) or Electronic Stability Program (ESP) or Electronic Stability Control (ESC). This system will take an important part of the motivation chapter (chapter 2) to show the impact of these used systems in improving the vehicles riding safety.

1.3 Thesis Outline

The organization of the next thesis's chapters will be as follows:

Chapter 2 presents the main motivating reason for realizing the presented work. It starts by displaying the vehicle accidents statistics from around the world, that verifies the effectiveness of the stability control systems. Then it reviews the laws and regulation that obligates the vehicles manufacturers to install these systems in all the modern vehicles. The chapter ends by highlighting the role of simulations in developing the vehicle control systems.

Chapter 3 is dedicated to review the state of the art of the thesis research scope. The chapter starts by briefly explaining the vehicle cornering dynamics and the most indicative characteristics that shows the vehicle stability state. Afterward, the chapter details the different standalone chassis controllers and

it refers to the academic and commercial attention that these systems have received. Then the chapter describes the integration techniques of these systems. Stressing on the importance of this integration and the challenges faced while integrating different systems. Finally the chapter provides a brief explanation of the concepts that lies beneath the used integration technique.

Chapter 4 defines the objectives of the Ph.D. thesis. It first states the addressed problem then it specifies the objectives of the thesis that shall be fulfilled along of the presented work.

Chapter 5 denotes the different phases that the presented work had to go through to fulfill the thesis objectives. The described phases are ordered chronologically, and make references to the document's different sections. The main objectives of this chapter is to orient the readers and give them a complete overview of the presented work.

Chapter 6 explains how the system was implemented. At the beginning, the chapter describes the system's modules and their interrelations. Then, the equations that defines the mechanical models that describes the vehicle are stated and explained. Afterward, the phases of the controller construction are detailed. The chapter ends by illustrating the way of integrating the designed controller in the vehicle, making it ready for the testing phase.

Chapter 7 displays the results obtained by the proposed controller in comparison to a passive uncontrolled vehicle and a vehicle from the literature. The three vehicles were tested together on different maneuvers at different velocities and in different road and weather conditions.

The controlling technique, explained in chapter 6, is thought to be generic and propitious to control more mechanical systems. Therefore, chapter 8 presents an experiment that tried the same presented algorithm and the controlling approach on a semi-active suspension model. Therefore, this chapter explains briefly the semi-active controlling problem. Then, it explains how the controller was adapted to control the suspensions systems. Finally, it ends by demonstrating this experiment's obtained results.

Last but not least, chapter 9 concludes the presented work and suggests future research possibilities to complete this research line.

ECU	**Description**
Active Steering systems	adds a steering correction value to improve the car handling and stability
Airbag Control Unit (ACU)	the control unit responsible of the deployment of the airbag
Anti-lock braking system (ABS)	a braking control system that prevents the wheels from locking up (ceasing rotation) and avoids uncontrolled skidding
Battery Management systems	in electric and hybrid vehicles
Body Control Module (BCM)	monitors and controls various car electronic accessories like; power windows, power mirrors, airconditioning, immobilizer system, central locking, etc
Electric Power Steering Control Unit (PSCU)	responsible for the managing of the power assisted steering
Electronic Stability Control (ESC)	a braking control system that detects and prevents skids, by varying the braking moment in different wheels
Electronically Controlled Suspension (ECS)	including control systems of active and semiactive suspensions
Engine Control Unit (ECU)	monitors and controls internal combustion engine to ensure its optimum running
Human Machine Interface (HMI)	responsible for the high level interactions between the car users and the car control units
Navigation systems	including GPSs, speed control units, radar based brake assist(BAS), park assist, lane keep assist, collision prevention assist, trafic sign assist, etc
Powertrain Control Module (PCM)	Sometimes the functions of the Engine Control Unit and Transmission Control Unit are combined into a single unit called the Powertrain Control Module
Radio system	including radios, music players, speakers and amplifiers
Transmission Control Unit	controls modern electronic automatic transmissions to calculate how and when to change gears in the vehicle for optimum performance, fuel economy and shift quality

Table 1.1: Examples of Electronic Control Units (ECUs)

Chapter 2

Motivation

With the recent advancements in the vehicle's industry, driving safety in passenger vehicles is considered one of the key issues in designing any vehicle. With the increased number of road accidents and the public awareness of its possible causes, people put car security and stability as one of the most important aspects while buying a new car. As manufacturers tend to meet this market demand, they invest large amounts of money in implementing more advanced security systems and compete between each other on providing the most secure and stable vehicle.

In this thesis, we will be mainly addressing an integrated control system of Active Front Steering (AFS) and brake-based Dynamic Stability Control (DSC). The integration of both systems together would allow us to profit from the advantages of each system while trying to compensate for its disadvantages. The brake-based DSC, also known as, Vehicle Stability Control (VSC) or Electronic Stability Program (ESP) or Electronic Stability Control (ESC) is considered one of the most widely used vehicle stability control systems.

Furthermore, the ESC is considered to be the greatest road safety innovation since the seatbelt [21]. This conclusion is supported by studies and statistics from various countries around the world [22, 23, 2, 24]. Even before a driver knows there's a problem, ESC senses when a vehicle strays from the intended travel path or begins to spin out. Then the system automatically brakes individual wheels and sometimes reduces throttle to keep the vehicle under control and moving in the intended travel direction [22].

Section 2.1 reviews some statistics and data that shows the effect of Electronic Stability Control on reducing the number of fatal accidents and will

take a look on some of the latest international standards that demands the installment of ESC.

2.1 Statistics and Norms

According to various studies of the evaluation of the efficiency of vehicle's security systems, ESC continues to be one of the most efficient developed techniques for the prevention of fatal accidents in passenger vehicles, specially in the accidents that includes a single car turn over. Even before the driver notices that there's a problem, ESC senses when the vehicle strays from the intended travel path or begins to spin out, then it starts automatically to brake individual wheels and sometimes reduces throttle to keep the vehicle under control, while moving in the intended direction of travel [22]. In this section, we'll outline some universal statistics that show the importance of ESC along with the latest standards that impose its employment.

2.1.1 USA statistics and standards

In the USA, according to a 10-years study realized by the "Insurance Institute for Highway Safety" of the USA [22] [25], with data taken from the year 1999 to 2008 in 50 states, comparing fatal crash involvement rates between identical vehicles with and without ESC installed. From the database constructed from this study, the ESC proved to reduce the risk of accidents by these percentages:

- Deadly crashes by 33%.
- Single vehicle rollover by 73%.
- Single vehicle fatal crash risk on wet or slippery roads by 59%.

Moreover when studying these statistics for SUV-cars, these percentages would even increment, since SUV-cars tend to have a higher center of gravity, therefore they are more likely to get into more situations of loss of control and roll-over crashes, which ESC helps to prevent.

Aware of these statistics, the "National Highway Traffic Safety Administration" of the USA issued a rule on 2007 [23], that demands the installation of ESC in 100% of all light vehicles by 2012 (with exceptions for some vehicles

manufactured in stages or by small volume manufacturers). And they estimate that the application of the new standard will help to prevent between 5300 and 9600 anual fatalaty, once all passenger vehicles gets equipped with ESC.

2.1.2 Spanish statistics and European Union standards

In Spain, starting the year 2000 the number of registered vehicles equipped by ESC began to increase year after year. And by June 2006, the percentage of these vehicles was 49%, which was the second largest percentage in Europe after Germany who had a percentage of 75% [2]. Although no dedicated study, like the one reviewed in the previous section was conducted to study the effect of ESC on the accidents in Spain. The data collected by the "Dirección General de Tráfico" DGT of the Ministry of Interior affairs, about the mortal accidents that took place in Spain between they years 1993 and 2010 can show a possible effect of ESC in reducing the number of mortal accidents starting from the year 2000, see figure 2.1. As you can see that although the number of registered vehicles increases yearly the number of fatal accidents decreases noticeably.

Affected by similar data from different countries of the European Union and by the decision made by the USA. On the 10th of March 2009, the European Parliament approved the standard of the compulsory introduction of ESC in all new types of vehicles from 1 November 2011, and for all new vehicles from 1 November 2014 [26]. This new decision is earlier than the originally foreseen one in the Commission's proposal (COM (2008) 316 final)[27] that planed it for the 2018 instead of 2014. The regulation is directly applicable in the European Member States and reflects the car safety standards harmonized by the United Nations [28].

2.1.3 Japanese statistics and extensive study

Another more detailed study about the effectiveness of ESC was conducted by Toyota Japan [3]. Although this study is relatively older than the ones discussed in the previous two sections; the way it was carried on by makes it still interesting. In this study they tend to analyze the causes of the fatal accidents and measure the percentage of these accidents that was caused by the loss of stability.

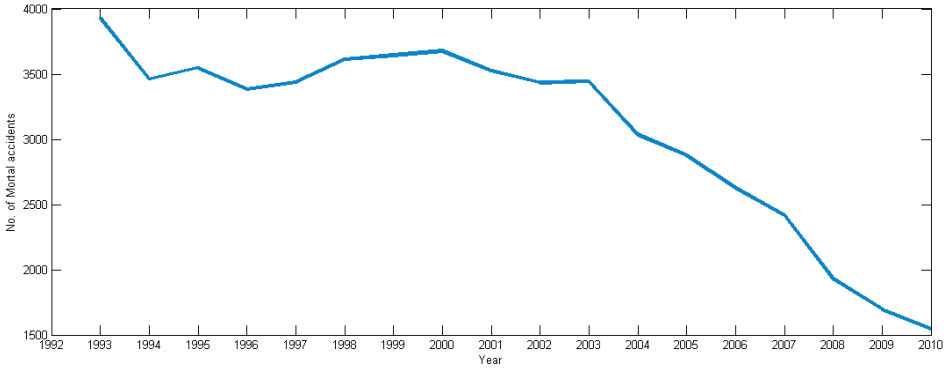

Figure 2.1: Number of mortal accidents in Spain [2]

Basing their data on the Japanese statistics of traffic accidents, vehicles with ESC showed approximately a 35% reduction in single car accidents and a 30% reduction for head-on collisions with other automobiles. While in more severe accidents, this result would increase to approximately 50% and 40% reductions. Furthermore, analysis showed that VSC may reduce more accidents in higher speed ranges where vehicle dynamics play a greater part.

The study states that from all the serious accidents that takes place in Japan, 20% of them are due to the loss of stability. Where 65% of them are caused due to car skidding. From these accidents that are caused by skidding, 25% of them is caused by inadequate steering maneuver and 20% due to the change of road conditions, see figure 2.2. All these percentages could be eliminated by a vehicle stability control system.

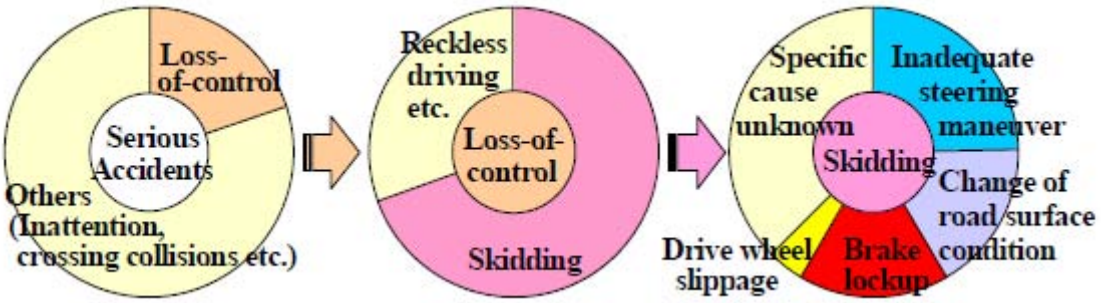

Figure 2.2: Breakdown of Serious Accidents [3]

2.2 Research challenges

As suggested from the previous sections ESC seems to yield exceptional results and has a noticeable impact on the reduction of the number of accidents and road victims. But is this enough? have we reached a perfect control system that cannot be improved?

According to Bruton et al.[29], the confirmation of the efficiency of ESC, is inconclusive, but promising. Which demands more extensive research and analysis of these systems to be carried out, as these safety systems are increasingly becoming standard fittings in modern vehicles.

And hither starts the presented thesis, to try to offer an improvement of the available systems by integrating other chassis control systems to work in parallel with a DSC system, to achieve improved safety of the vehicle's ride. The integrated control system presented in this work is designed and tested using Matlab and Simulink simulation software, and hence the next section is dedicated to describe the importance of simulation in such systems.

2.3 Role of Simulation in the development of Active Vehicle Dynamics Control systems

Active Vehicle Dynamics Control systems are highly considered to be safety critical systems; such that, any malfunction or failure of these systems may result in serious accidents or severe damage. Hence, the testing phase of the design process, although its a crucial phase, it is not an easy task and usually it's costly and time consuming. Furthermore, these systems are designed to improve the stability of the vehicle as it approaches its handling limits. And therefore, these systems should be tested at these sever situations, which may lead to fatal crashes in case of any error. Moreover, the tuning of such controllers needs lots of data of different vehicle maneuvers at different road conditions, and certainly these data on its turn is influenced with human error which makes it less accurate and/or less repeatable.

Therefore, the simulation can play a highly important role in the design and testing phases, especially when introducing new controlling concepts or controlling algorithms. Since testing on a simulation is much faster and easier than a lab test, because a simulation takes much less time than a field test.

And as the simulation would always be an approximation to the real situation, the simulation quality is highly affected by the quality of the vehicle model used in the simulation. Such that, a high quality model with a high number of degrees of freedom would provide a more substantive simulation than another simpler model.

Furthermore, simulations offer high flexibility to redesign the control system or re-adapt it from one vehicle model to the other. For example, while changing a suspension in the testing vehicle would require removing the actual suspension and installing the new one and consequently re-instrumenting the vehicle. In a simulation, this could be simply achieved by mainly changing the spring and damper curves in the used vehicle model.

So to help reduce the project costs and development time, an excellent procedure would be using a simulation to design the controller and tune it, then the verification phase would be done using field tests [30].

Chapter 3

Literature Review

This chapter aims to briefly review the extensive state of the art of the different technologies used to improve the vehicle lateral stability. The chapter starts by briefly explaining the basic concepts of vehicles lateral dynamics that are necessary for the further explanation of this chapter. Afterward, it reviews the published work on active chassis control systems, first by discussing the different types of standalone controllers divided by their effect on tire forces. Afterward, the integration approaches of different controllers are discussed along with reviewing the published work that used these techniques. Finally, the chapter explains the used integration technology.

3.1 Vehicle Cornering Dynamics

NB This section is dedicated to review the old well known basic concepts of vehicles lateral dynamics. And therefore, it provides a summary of the explanation provided in the books [5, 31, 6, 32, 33] and the university lecture notes [4, 34].

Vehicle handling is a loosely used expression that refers to the responsiveness of a vehicle to the driver input. The cornering behavior of the vehicle is considered an important measurement of that handling. So that handling characteristics considers the relationship between both the driver and the vehicle; where the driver is the intelligence, the observer and controller, and the vehicle is the system that creates the maneuver force; this system is considered as a "closed-loop" system, figure 3.1. But since it's very difficult to characterize the driver, the vehicle is characterized alone as an "open-loop" system

which is the vehicle response to the steering input or more accurately "directional response". Usually the directional response or the open-loop response is measured by the understeer gradient under steady-state conditions or even quasi-steady-state conditions.

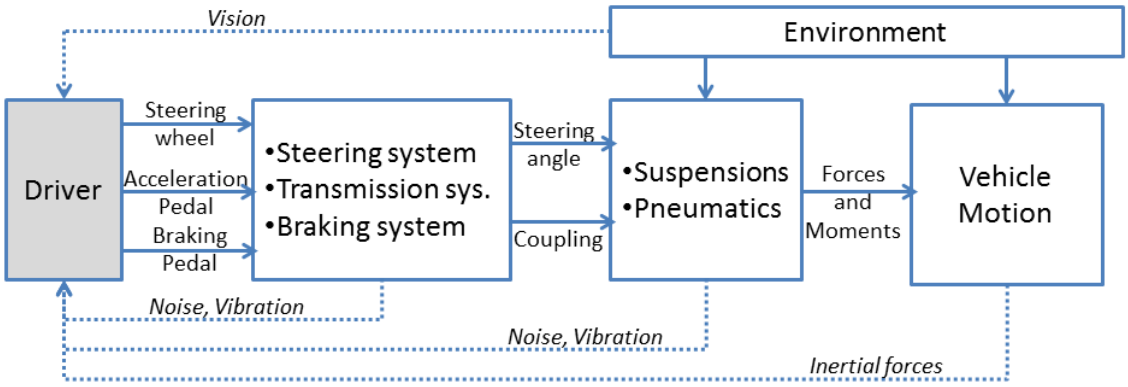

Figure 3.1: Driver-vehicle interaction as a closed-loop relation [4]

This section will start by making a brief explanation of the role of tires on the cornering performance of the vehicle. Afterward, a simplified vehicle model is explained, this model will be further used to explain the cornering behavior of the vehicle. Consequently, the cornering dynamics of a vehicle turning on both low speed and high speed are explained; to show the difference between both situations and to highlight the need of control systems to makeup for the vehicle instabilities generated by the vehicle cornering characteristics. Then the oversteering and understeering behaviors of the vehicles are explained, and the environmental disturbances that accentuate these behaviors are mentioned. Finally the control variables that indicates a good measurement of the vehicle's instability are reviewed, while showing the mathematical relation between them and between the previously discussed equations. These control variables are the mostly used ones in the literature that will be reviewed in the next section and also the control variables used in the presented control systems.

3.1.1 Tire mechanics

The point of contact between the vehicle and the ground are the wheels and therefore the tire mechanics play a very important role in negotiating the desired maneuvers since they represent the transmission of all the vehicle components efforts to the ground. The field of tire mechanics is a very ample

field and lots of research have been dedicated to it and still more research is contributed day after day. Therefore, this section will only present a summary of the related aspects to of the tire mechanics to the lateral vehicle dynamics.

When a lateral force is applied to a tire, the contact patch of this tire is deformed and it develops a lateral force opposing to this applied force. If the same scenario happens while the tire is in action (rolling), the tire moves forward with an angle α with respect to its direction, due to the generated opposing lateral force, this angle is called the slip angle, see figure 3.2. This side-slip angle is a result of the flexible character of the rubber tire that allows it to keep heading to its intended direction while having a lateral motion. This angle has a substantial effect on the vehicle dynamics and stability, and could be a cause or a consequence of the lateral forces. For example, a lateral force due to gust would lead to a side-slip of the tire and hence reaction forces under the tire. Also steering the steering wheel, leads to a side-slip in the tire that would produce lateral forces to turn the vehicle.

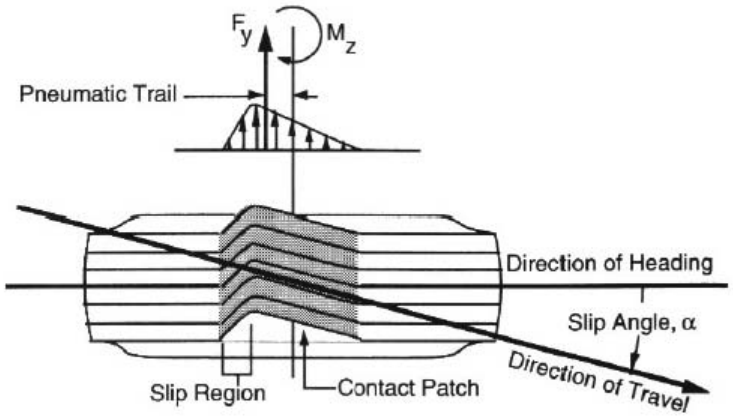

Figure 3.2: Representation of the simplified bicycle model [5]

Another important aspect of a vehicle negotiating a curve is the body roll movement and consequently the lateral load transfer, see figure 3.3. Such that, the lateral force decreases as the vertical load increases, and this is known as the load sensitivity phenomenon. Furthermore the friction coefficient of the tires μ, that describes the amount of the friction between the tire and the road, is defined as the ratio of the lateral force to the applied vertical load:

$$\mu = {}^{F_y}/_{F_z} \tag{3.1}$$

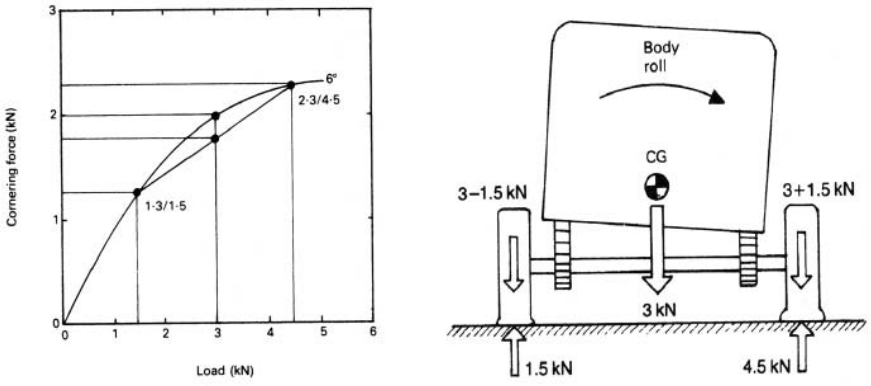

Figure 3.3: Relation between the lateral force with respect to the lateral load transfer [5]

The lateral force generated by the wheel F_y is known as the "cornering force". This force increases proportionally with the slip angle and at low slip angles ($\leq 5°$) the relationship between both is linear, and can be described as:

$$F_y = C_\alpha \alpha \tag{3.2}$$

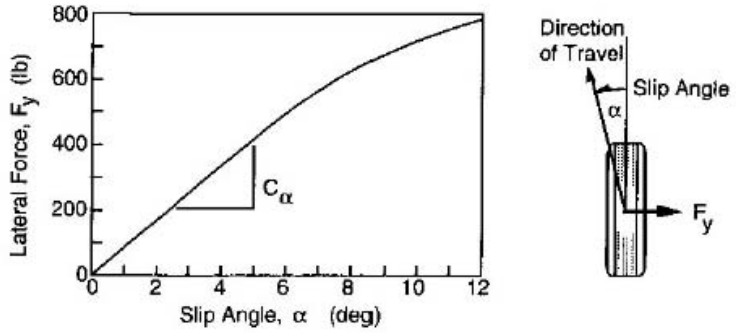

Figure 3.4: Cornering stifness of the tire [5]

C_α is known as the "cornering stiffness", and is defined as the slope of the curve for F_y with α, see figure 3.4. The cornering stiffness is dependent on the tire properties; such as, the tire size, its type, the number of plies, the cord angles, the wheel width and tread; all are significant variables which define the tire characteristics. But above all the tire load and inflation pressure are of a high importance. Nevertheless, the speed does not affect highly the cornering forces produced by the tire. Due to the high sensitivity of the cornering force to the vertical load, the cornering coefficient CC_α is used to describe the tire

cornering properties, and is defined as:

$$CC_\alpha = C_\alpha / F_z \tag{3.3}$$

3.1.2 A Simplified Vehicle Model

To be able to explain the rest of this chapter a simple vehicle model would be helpful to describe the basic concepts of the vehicle lateral dynamics. A good simplification of the vehicle model when the behavior of the left and right front wheels are assumed to be similar is the simple bicycle model, where the two front wheels and the two rear wheels are considered to be on the same track, see figure 3.5. This model has the ability of considering many important properties of the vehicle's dynamics and stability performance under many different conditions. This model is explained here only to help explain the other parts of the current chapter, but will not be further used through the thesis. Instead the work presented by this thesis uses more complex vehicle models and will be explained later in chapter 6.

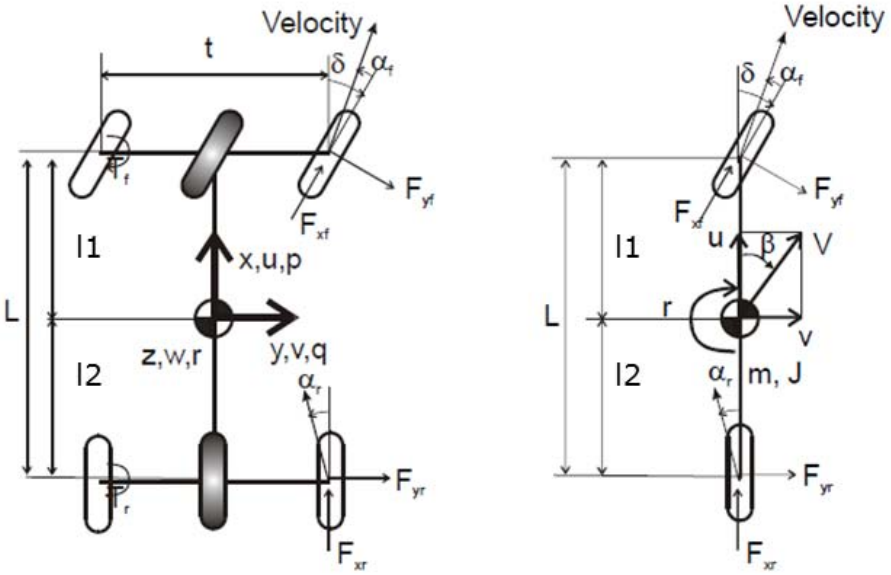

Figure 3.5: Representation of the simplified bicycle model [4]

As could be derived from figure 3.5, the bicycle model is a 2-DOF model that neglects all of the lateral and longitudinal load transfer, the roll p and pitch q motion and the aerodynamics effects and the tires remains in linear

regime. It considers a constant forward velocity $V = u = constant$ and no compliance effect of the suspensions and of the body.

The assumption of the linear regime is considered to be valid if the lateral acceleration remains below 0.4 g, small steering and slip angles, smooth floor to neglect the suspension. The degrees of freedom of this model could be described by the lateral velocity v and the yaw speed r, that could be described by the following equations of motion:

$$m(\dot{v} + V_x r) = F_{yf}\cos(\delta) + F_{yr} - F_{xf}\sin(\delta) \tag{3.4}$$

$$J_{zz}\dot{r} = l_1 F_{yf}\cos(\delta) - l_2 F_{yr} + l_1 F_{xf}\sin(\delta) \tag{3.5}$$

where F_{xf}, F_{yf} and F_{yr} are the respective tire forces and are to be obtained from a tire model, later in section 6.2.3 the Dugoff tire model shall be explained.

Other parameters that describes this model as seen in the diagram could be explained as, vehicle mass m, the steering angle δ and the inertia about the z axis J_{zz}. The dimensions t, L, $l1$, $l2$ are describe to be the wheel-track, the wheel-base, the distance between the front axle and the COG and the distance between the rear axle and the COG, respectively. And finally the front and rear tires slip angles α_f and α_r.

3.1.3 Low-Speed Turning

To be able to understand the vehicle cornering dynamics, analyzing the low-speed turning would be the first step. At low speed, a maneuver for parking for example, the centrifugal accelerations are negligible and the tires does not need to develop lateral forces and the turning is done by the wheel rolling without a slip angle and the vehicle is intended to make a turn as the one illustrated in figure 3.6, where the center of the turn lies on the projection of the rear axle.

Similarly, the perpendicular line that passes through the center of each of the front wheels should pass through the center point of the turn or else the front tires would fight each other during the turn. Therefore the optimal turning angles on the front wheels are designed; such that, they can describe the geometry seen in figure 3.6, where δ_e and δ_i describes the steering angles of external and internal wheels according to the turn, and could be calculated

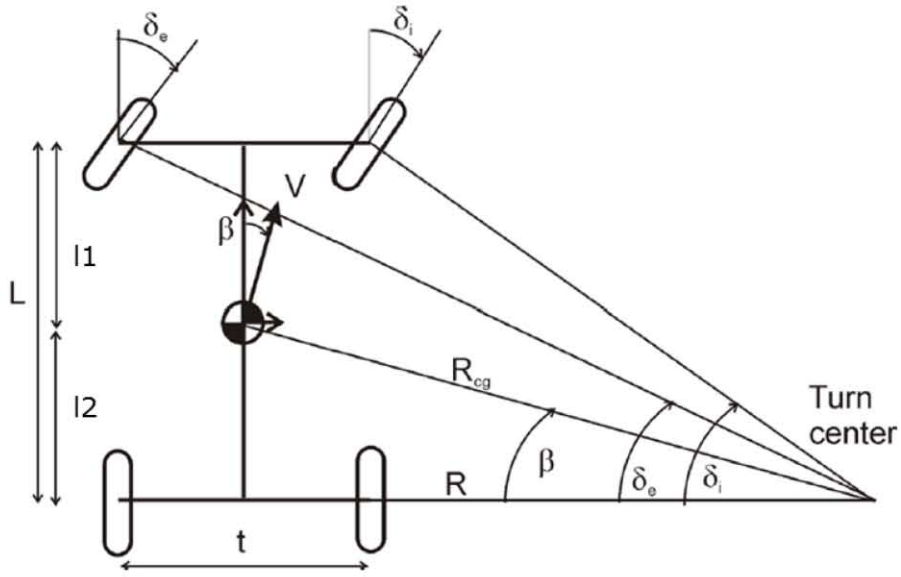

Figure 3.6: Geometry of a turning vehicle at a low speed [4]

as:

$$\tan \delta_i = \frac{L}{(R - t/2)} \tag{3.6}$$

$$\tan \delta_e = \frac{L}{(R + t/2)} \tag{3.7}$$

and therefore the Ackerman-Jeantaud condition would be,

$$\cot \delta_e - \cot \delta_i = \frac{t}{L} \tag{3.8}$$

Corollary:

$$\delta_e \leq \delta_i \tag{3.9}$$

Or could be simplified to our bicycle model, see figure 3.7, where the front steering angle known by Ackerman can be written as:

$$\tan \delta = \frac{L}{R} \tag{3.10}$$

where the Ackerman Geometry is a term often used to describe the exact geometry of the front wheels. It imposes a geometric arrangement of linkages to help the wheels negotiate their intended maneuver by adjusting the angles of both the right and left sides. These angles mainly depend on the wheelbase L and the negotiated turning angle R. This geometry helps reduce the front

tire wear and affects the centering torques of the steering system providing the driver with a natural feel in the feedback through the steering wheel.

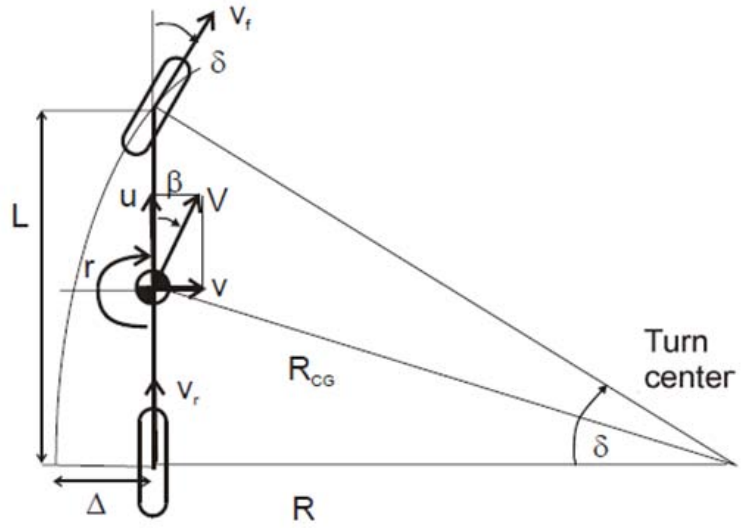

Figure 3.7: Bicycle model turning at low speed [4]

Other equations describing this model could be described as follows. The curvature radius at the COG could be written as:

$$R_{COG} = \sqrt{{l_2}^2 + R^2} = \sqrt{{l_2}^2 + L^2 \cot^2 \delta} \tag{3.11}$$

$$R_{COG} \approx R\sqrt{1 + {l_2}^2/R^2} \approx R\left(1 + {l_2}^2/R^2\right) \approx R \tag{3.12}$$

and the relation between the turning curve and the steering angle could be written as:

$$R_{COG} \approx R \approx L \cot \delta \approx \frac{L}{\delta} \tag{3.13}$$

$$L \approx \delta R \tag{3.14}$$

The side-slip angle β of the vehicle's COG, that defines the angle between the vehicles intended direction and its actual velocity vector, could be written as:

$$\beta = \arctan\left(\frac{l_2}{R}\right) = \arcsin\left(\frac{l_2}{R_{COG}}\right) = \arcsin\left(\frac{l_2}{\sqrt{R^2 + {l_2}^2}}\right) \tag{3.15}$$

$$\beta = \frac{\delta l_2}{L} \tag{3.16}$$

3.1.4 High-Speed Turning

At high speed, the tires need to develop lateral forces to keep up with the lateral accelerations. But the tires can develop lateral forces *if and only if* they are subjected to a side-slip angle as they roll. Due to the motion kinematics the center of the turn gets displaced to be located at the intersection of the normal forces that are perpendicular on the velocity vectors under the tires, see figure 3.8.

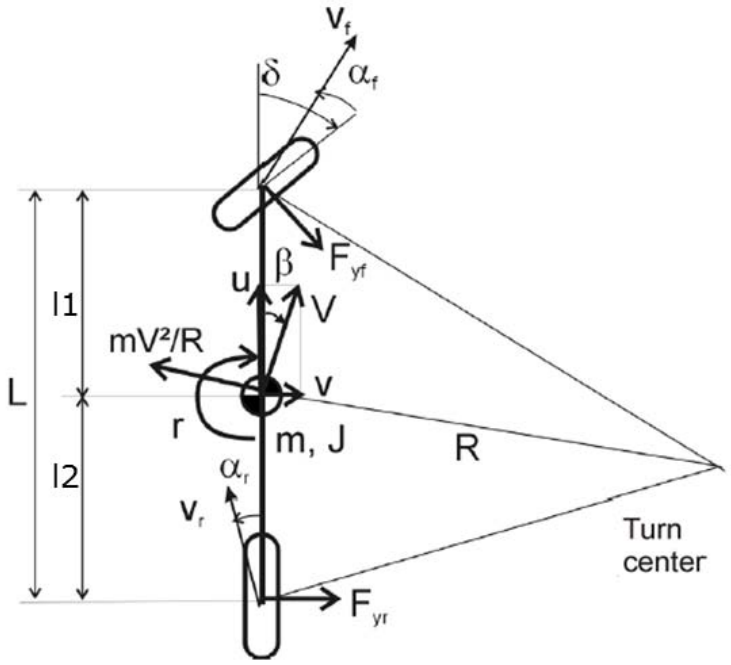

Figure 3.8: Bicycle model turning at high speed [4]

At high speed, the cornering equations differ due to the presence of lateral acceleration. To counteract the lateral acceleration, the tires must develop lateral forces, and slip angles will be present at each wheel. The steady-state cornering equations are derived from the application of Newton's Second Law along with the equation describing the vehicles geometry in the turn while taking into account the slip angle conditions of the tires. At high speeds the radius of the turn is much bigger than the wheelbase of the vehicle, therefore, we can still assume the tire slip angles to be relatively small, and the difference between δ_e and δ_i to be negligible. Therefore the bicycle model would still be functional to explain further this section.

As the vehicle travels forward with a speed V, the sum of the forces in the

lateral direction from the tires must be equal to the mass times the centripetal acceleration:

$$\sum F_y = \sum F_{yf} + \sum F_{yr} = m\frac{V^2}{R} \tag{3.17}$$

Also, for the vehicle to be in a moment equilibrium about its COG, the sum of the moments from the front and rear lateral forces must be equal to zero.

$$F_{yf}l_1 - F_{yr}l_2 = 0 \tag{3.18}$$

Solving equations 3.17 and 3.18 simultaneously we get:

$$F_{yf} = \frac{l_2}{L}m\frac{V^2}{R} \tag{3.19}$$

$$F_{yr} = \frac{l_1}{L}m\frac{V^2}{R} \tag{3.20}$$

From 3.3, 3.19 and 3.20 we get

$$F_{yf} = C_{\alpha f}\alpha_f = \frac{l_2}{L}m\frac{V^2}{R} \tag{3.21}$$

$$F_{yr} = C_{\alpha r}\alpha_r = \frac{l_1}{L}m\frac{V^2}{R} \tag{3.22}$$

ans therefore the Gratzmüller equality could be deducted:

$$\frac{\alpha_f}{\alpha_r} = \frac{l_2 C_{\alpha r}}{l_1 C_{\alpha f}} \tag{3.23}$$

As for the velocity under both the front and rear wheels could be described as:

$$u_r = u \approx V \tag{3.24}$$

$$v_r = v - l_2 r \tag{3.25}$$

where r is the yaw velocity of the vehicle at its COG. This compatibility of velocity gives the slip angle α_r under the rear wheels:

$$\tan\alpha_r = \frac{-v_r}{u_r} = \frac{-v + l_2 r}{V} \tag{3.26}$$

$$V = rR \tag{3.27}$$

$$\alpha_r = -\beta + \frac{l_2}{R} \tag{3.28}$$

with the previous assumption of relatively small angles. Simillarly the velocity under the front wheels are described as:

$$u_f = u \approx V \tag{3.29}$$

$$v_f = v - l_1 r \tag{3.30}$$

and the front slip angle α_f could also be written as:

$$\tan(\delta - \alpha_f) = \frac{-v_f}{u_f} = \frac{v + l_1 r}{V} \tag{3.31}$$

$$\delta - \alpha_f = \beta + \frac{l_1}{R} \tag{3.32}$$

As for the steering angle, since at high speed turning it is affected by the front and rear wheels slip angles, it could be rewritten now as:

$$\delta = \frac{L}{R} + \alpha_f - \alpha_r \tag{3.33}$$

or as a function of the velocity and cornering stiffness C_α of the wheels sets as:

$$\delta = \frac{L}{R} + \left(\frac{ml_2}{C_{\alpha f}L} - \frac{ml_1}{C_{\alpha r}L}\right)\frac{V^2}{R} \tag{3.34}$$

$$\delta = \frac{L}{R} + \left(\frac{W_f}{C_{\alpha f}} - \frac{W_r}{C_{\alpha r}}\right)\frac{V^2}{gR} \tag{3.35}$$

where W represents the weight.

3.1.5 Oversteering and Understeering

These two expressions be extensively used through out this thesis, since the main objectives of the thesis is to correct these undesired vehicle behaviors. Figure 3.9 shows a vehicle intending to make the same trajectory while enduring oversteering, understeering and the neutral desired performance.

A vehicle could have a general oversteering or understeering tendency due to its design and the cornering stiffness C_α of the wheels sets. Back to equation

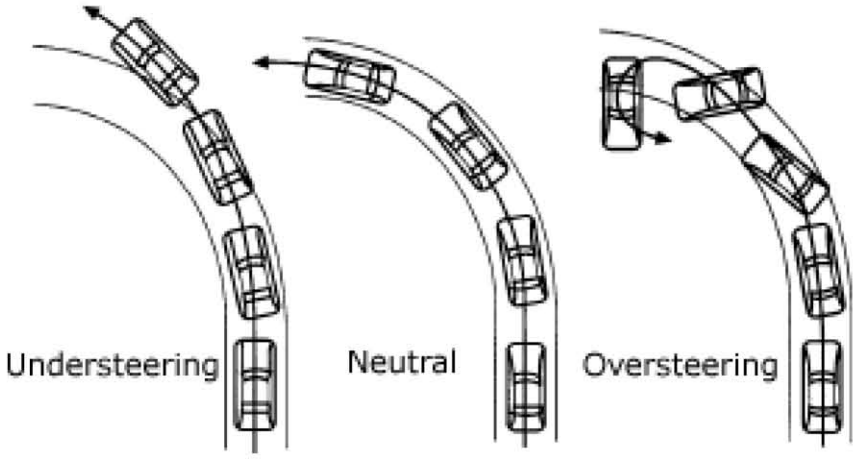

Figure 3.9: Neutral-, over- and under-steering conditions [6]

3.34 the steering angle is expressed in terms of centrifugal acceleration:

$$\delta = \frac{L}{R} + \left(\frac{ml_2}{C_{\alpha f} L} - \frac{ml_1}{C_{\alpha r} L} \right) \frac{V^2}{R} \tag{3.36}$$

where the part $\left(\frac{ml_2}{C_{\alpha f} L} - \frac{ml_1}{C_{\alpha r} L} \right)$ is called K and defined as the understeer gradient, and the steering equation could now be rewritten as:

$$\delta = \frac{L}{R} + K \frac{V^2}{R} \tag{3.37}$$

This steering gradient determines the vehicle's behavior as Neutral-, over- or under-steering tendency. A summary of this behaviors from [4] can be seen in the list below:

- If K=0, the vehicle is said to be of a neutralsteer:
  $K = 0 \Leftrightarrow l_2 C_{\alpha r} = l_1 C_{\alpha f}$
  The front and rear wheels sets have the same directional ability.

- If $K > 0$, the vehicle is of understeer:
  $K > 0 \Leftrightarrow l_2 C_{\alpha r} > l_1 C_{\alpha f}$
  Larger directional factor of the rear wheels.

- If $K < 0$, the vehicle is oversteer:
  $K < 0 \Leftrightarrow l_2 C_{\alpha r} < l_1 C_{\alpha f}$
  Larger directional factor of the front wheels.

The total speed of the vehicle plays a very important role in revealing the effect of the vehicle's steering behavior. Figure 3.10 shows the effect of the speed on the steering behavior on a constant-radius turn, till the vehicle reaches its critical or characteristic speed. As seen from the figure, in a neutral-steering vehicle simply the Ackerman angle is need to be applied. But in the case of an understeering one, the steering angle increases with the square of the vehicle speed, reaching twice the initial angle till it reaches the characteristic speed. And therefore requires a steering angle that is twice as big as the Ackerman angle:

$$\delta = {}^{2L}/_{R} \tag{3.38}$$

$$V_{car} = \sqrt{\frac{L}{K}} \tag{3.39}$$

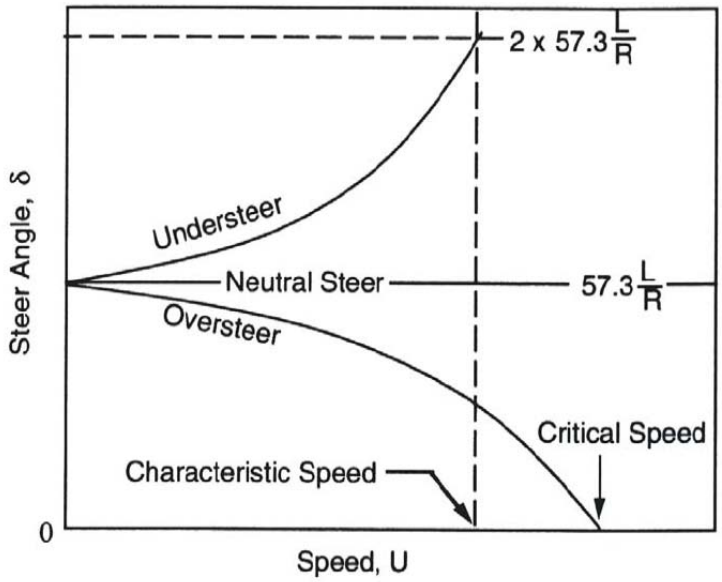

Figure 3.10: Speed effect on the steering angle [5]

While in the case of an oversteering vehicle, the steer angle decreases with the square of the speed and becomes zero at the critical speed above which the vehicle becomes unstable and hardly controllable:

$$\delta = 0 \tag{3.40}$$

$$V_{critical} = \sqrt{\frac{L}{|K|}} \tag{3.41}$$

It is worth mentioning that lateral load transfer, when a wheel or more looses traction, split-μ situations and low friction slippery road would affect greatly the understeer gradient K and consequently the car stability performance.

3.1.6 Dominant control parameters

The parameters R, α_f, α_r, $C_{\alpha f}$ and $C_{\alpha r}$ play a very important role in determining the state of stability of the vehicle. Nevertheless, these variables are very hard (if not impossible) to measure so that a controller could try to improve the performance of the given vehicle. Yet, there exists other three parameters that are measurable through sensors and observers, that gives a great indication to the stability of the vehicles. These three parameters are the lateral acceleration, the yaw rate and the side-slip angle of the vehicle body. This section will review the importance of these parameters that will be later referred to in the next section of the literature review and will be further used in the presented controller.

3.1.6.1 Lateral acceleration

The main purpose of steering a vehicle is to produce a lateral acceleration and hence the turning equation can be used to examine the vehicle performance from this perspective. Equation 3.37 can be rewritten in terms of the lateral acceleration a_y as:

$$\delta = \frac{L}{R} + K a_y \tag{3.42}$$

So the lateral acceleration gain could be represented through this ratio:

$$\frac{a_y}{\delta} = \frac{\frac{V^2}{L}}{1 + \frac{KV^2}{L}} \tag{3.43}$$

Such that when K is zero (neutral steer), the lateral acceleration gain is determined only by the numerator. Therefore it becomes directly proportional to square the speed. While when K becomes positive (understeer), the gain is diminished as the denominator's second term increases, since it will always be

less than that of a neutral steer. Last but not least, when K becomes negative (oversteer), the second term in the denominator subtracts from 1, and therefore will increase the lateral acceleration gain. This makes the magnitude of the term dependent on the square of the speed, and goes approaches 1 as the speed reaches the critical speed. Thus, the critical speed in equation 3.41 corresponds to the denominator approaching zero (infinite gain) in equation 3.43.

3.1.6.2 Yaw rate

The second aim of steering is to change the vehicle's heading angle through developing a yaw velocity (yaw rate) r which is defined as the rate of rotation in heading angle and could be calculated from equation 3.27 as:

$$r = \frac{V}{R} \tag{3.44}$$

Substituting once more in 3.42 to get the yaw rate ratio with the steering, we get:

$$\frac{r}{\delta} = \frac{\frac{V}{L}}{1 + \frac{KV^2}{L}} \tag{3.45}$$

This ratio represents a "gain" that is proportional to the velocity of a neutral-steering vehicle. Figure 3.11 shows the relation between the yaw velocity and the vehicle speed at each of neutral-, over- and under-steering vehicles. From the yaw rate gain equation and the graph it can be deduced that a neutral vehicle would have a yaw velocity that is proportional to the steering angle, while in an under-steering vehicle its yaw velocity will increase with its speed until the characteristic velocity afterward it begins to decrease again. And therefore the characteristic velocity means the speed at which the vehicle is most responsive in yaw. Finally in an oversteering vehicle, the yaw rates approaches infinity at the vehicles critical speed and for that reason the vehicle becomes unstable and highly uncontrolable for the driver.

3.1.6.3 Side-slip angle

As the vehicle negotiates a slow turn, the lateral acceleration is almost negligible and the rear wheels almost makes the same trajectory as the front ones, but as the vehicle turns faster the lateral acceleration significantly in-

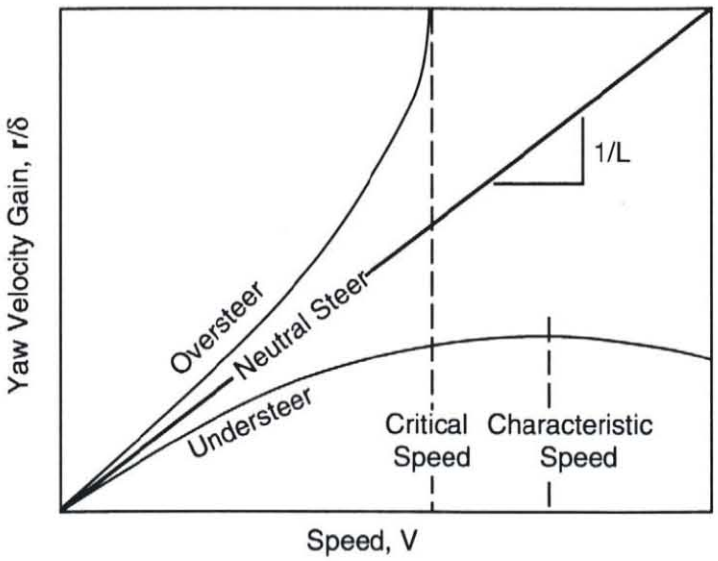

Figure 3.11: The relation between the yaw velocity and the speed [5]

creases and the rear of the vehicle must drift outward to develop the necessary slip angles on the rear tires. Hence the side-slip angle β, as explained before is the angle between the longitudinal axis and the vehicle's velocity vector V at the COG:

$$\beta = \frac{v_{COG}}{u_{COG}} \tag{3.46}$$

Figure 3.12 shows a vehicle negotiating a curve at low speed at this case the side-slip angle is of a positive magnitude relative to the vehicle steering angle. But at high speed the slip angle on the rear wheels causes the side-slip angle at the COG to become negative as in figure 3.13.

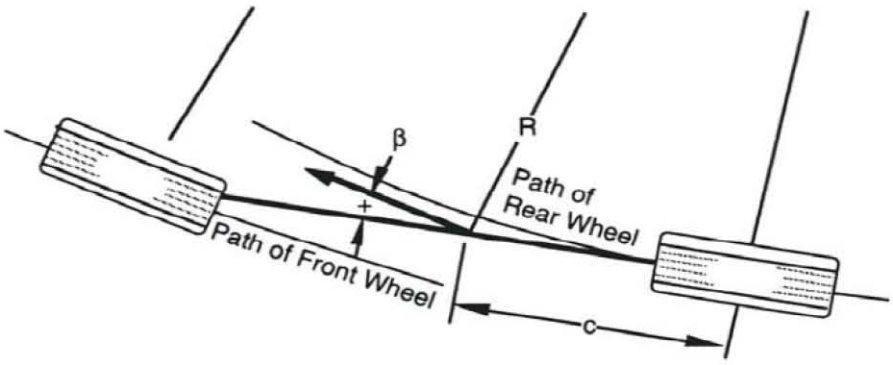

Figure 3.12: Side-slip angle of a low speed turning maneuver [5]

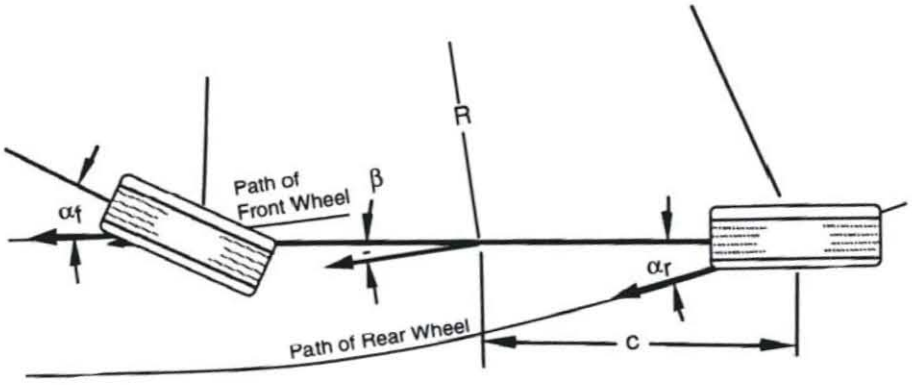

Figure 3.13: Side-slip angle of a high speed turning maneuver [5]

The calculation of the side-slip angle could be calculated from equations 3.29 and 3.32 as:

$$\beta = \frac{l_2 r}{V} - \alpha_r = \delta - \alpha_f - \frac{l_1 r}{V} \tag{3.47}$$

or as a function of velocity as:

$$\beta = \frac{l_2}{R} + -\frac{W_r}{C_{\alpha r}} \frac{V^2}{gR} \tag{3.48}$$

Such that it becomes zero when the vehicle satisfies this condition independent of R:

$$V_{\beta=0} = \sqrt{l_2 g \frac{C_{\alpha r}}{W_r}} \tag{3.49}$$

3.2 Standalone Chassis Control

Nowadays, modern vehicles contains numerous Electronic Control Units (ECUs) used to improve the comfort, safety, fuel consumption and even for providing extra luxurious services for the driver. Although, these ECUs could affect significantly the price of the automobile [17], they became one of the principal choices when buying a new car. Many of these standalone controllers have been designed with the purpose of active control of vehicle handling, to increase the passenger's safety and comfort during the ride. These systems are the focus of the presented thesis and will be reviewed extensively in the next sections. Some of these ECUs are categorized as standalone controllers; such that, they work on their own without being a part of a controlling set or being

connected to other ECUs.

This section is dedicated to the discussion of the various types of standalone vehicle handling and stability control systems that exists in the literature. It categorizes these systems into steering-based active control systems that actively steers the front wheels or rear wheels or both together. Then it discusses the Dynamic Stability Control (DSC) systems (also referred to as Direct Yaw moment Control (DYC) systems) that controls the longitudinal acceleration/deceleration of separate wheels to create a corrective yaw moment about the vehicle's vertical axis. Afterward, this section reviews the suspension-based handling systems. Finally, it ends by concluding the discussed system while justifying the choice of the systems that are integrated in the presented controller.

3.2.1 Steering based active control systems

An Active Steering (AS) system has a great influence on regulating the lateral behavior of the vehicle, through regulating the wheels steering angles [35]. Considered as the first active chassis control system, the Active Rear Steering (ARS) started to attract research interest in the early 1980's [36, 37], shortly followed by the introduction on of Active Four Wheel Steering (A4S) in the late eighties [38]. AS systems have an important role in enhancing the steerability and the cornering dynamics of the vehicles as they can directly control the tire slip angles that play an important role in the lateral tire forces [32, 39, 40].

Lately, a considerable attention is being projected on the Active Front Steering (AFS), specifically after BMW announced using them in 2003 [19] and their effective introduction in the 5 series by 2004 [9, 41]. In academia as well, between the three discussed systems, recently the most commonly used is the AFS [35]. Also, it's the only AS used in this thesis. Nevertheless, a brief review of the three systems will be discussed to show the pros and cons of each. And to conclude a discussion of the choosing decision accompanied by a comparative study is presented in section 3.2.1.4.

3.2.1.1 Active Rear Steering (ARS)

After the introduction of these systems in the early 80s, the ARS systems started to attract a lot of academic and manufacturers attention, they first

appeared in the Honda Prelude in 1987. ARS systems are designed for different control objectives, some are designed to decrease the side-slip angle of the vehicle and others try to neutralize the handling of the vehicle or even follow a dynamic vehicle model behavior. Also the controlling input have varied between models that depends on the longitudinal speed of the vehicle [42, 43] or the steering wheel angle [44, 45] or the turning speed of the steer wheel angle [46]. And basically worked on synchronizing or inverting the front and the rear wheel angles depending on the control input.

Yet these systems were mainly concerned about the side-slip angle while ignoring the yaw rate desired value, and hence were not effective at external disturbance circumstances like in the presence of crosswind. To compensate for this problem more research was dedicated to ARS control using yaw rate some of which could be seen in [47, 48, 49, 50, 51].

Later, in [52] a fuzzy logic controller have been tried to control an ARS system. Yet the lack of feedback in the control as it requires special types of sensors that are difficult to implement in practical use [51], along with the doubt of the effectivness of a control method that uses only one control input to control two states led to the decrease of research interest on ARS [9].

Lately ARS haven't been receiving the same attention since they don't replace the AFS functionality. Instead another system known as A4S is used, that combines between both the of the AFS and ARS systems. Later in this chapter, the A4S systems will be reviewed, where A4S are not exactly the same as Four Wheel Steering (4WS) which some times may refer to ARS; such that, the term 4WS doesn't specify that all the four wheels are actively steered.

3.2.1.2 Active Front Steering (AFS)

AFS has been lately introduced to the vehicle market [53, 54]; yet by 2013, it is claimed to be the most commonly used Active Steering (AS) approach [35]. It was first announced to be used by BMW in 2003 [19] and was released in the BMW 5 series by 2004 [9, 41]. This system mainly consists of a power assisted steering rack and pinion steering gear, a double planetary gear system, steering column, an electric actuating motor and finally the hand steering wheel [41, 53], see figure 3.14.

Other AFS systems use Steer-By-Wire (SBW) where the mechanical linking system between the steering wheel and the front wheels is removed and

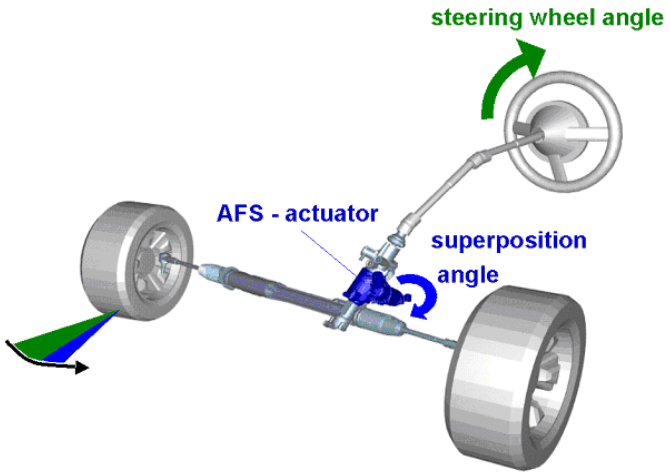

Figure 3.14: Mechatronic Active Front Steering system [7]

therefore the front wheel angles are controlled by an ECU through sensors on the steering wheel and electric motors (actuators) on the front wheels [32]. And although the first SBW prototype were almost built 11 years ago, no production car has been released to the market till the date. That's because till now the mechanical systems are much more reliable than the electronic ones, and a SBW car would need even a license to circulate in some countries. Yet, Nissan is announcing the release of the first SBW production car in 2014 on the Infiniti Q50 model [55]. Figure 3.15 shows the mechanism of three types of steering systems, where 3.15a shows a typical hydraulic operated steering system, 3.15b shows a power assisted Active Front Steering where the extra electronic components works beside the usual hydraulic ones and finally 3.15c shows the Steer-By-Wire system that replaces all the mechanical components by electric ones.

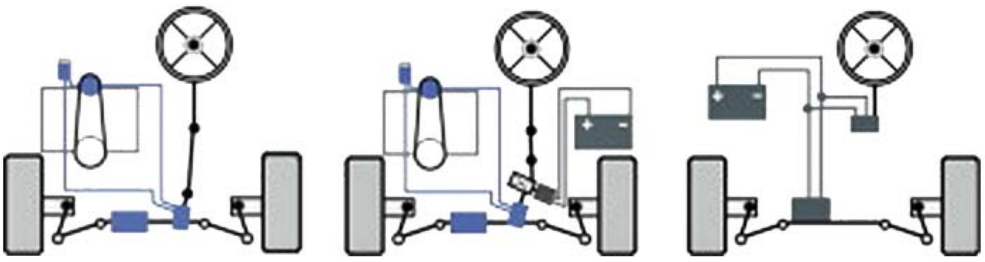

(a) Typical hydraulic power steering system (b) Power assisted AFS (c) Steer-By-Wire system

Figure 3.15: Different types of steering systems [8]

Academia as well had its share of research about this AS, from 1992 to 1996 various simulations of AFS controllers have been proposed [56, 57, 58, 59] yet these systems lacked robustness [9]. Concurrently, more work has been presented in [60, 61, 62, 63, 64] that have used simulations and road tests for verification, yet more test cases were needed to verify its effectives.

More research have followed [65, 66, 67, 68] and the robustness of the presented AFS have increased considerably to achieve its two principal functions. However, as the handling limit of the vehicle approaches AFS does not demonstrate sufficient effectiveness to handle the vehicle stability so as to eliminate the ESP.

3.2.1.3 Active Four Wheel Steering (A4S)

These are systems where both the front and rear wheel axes are steered actively and could be considered a combination of the two previously discussed ASs. A4S are completely different from Four Wheel Steering (4WS), where the later doesn't entail the use of Active Steering in all the for wheels. Instead, 4WS mostly refer to ARS where all the wheels could be steered without the need of the front axle to be steered actively as well.

A4S systems aims to resolve the conceptual control problem of the first two ASs; such that, they aimed to control two control inputs (yaw rate and side-slip angle) by only one control output. Nevertheless, to achieve the desirable response two control outputs are needed to control two inputs [69, 70].

The concept was first proposed in the late 80's through a virtual vehicle model that used feedforward and feedback compensation to control actively both the front and rear steering angles [38, 71]. Basing on the same technique of feedforward and feedback compensation, more studies have followed [72, 73] yet they had the same robustness problem faced by the ARS.

A more prospect study was demonstrated in [74], which used a SBW technique that intended to solve the robustness problem in [73] and basing its work on the ARS presented in [48] while solving the major understeer problem faced by the later. Yet, more forward speed variation tests were missing to conclude the robustness of this model.

A more recent study [54] have also used the feedforward and feedback compensation techniques. Yet, the robustness problem of ARS systems under the crosswind and split-μ effects were not addressed.

Very recent studies show seemingly prosperous results using sliding mode control [75, 76], where the first have even showed effectiveness with the presence of crosswind. Other recent studies have even tested the robustness of A4S using hardware in the loop systems in the presence of crosswind [77]. Nevertheless, this topic remains under research as it needs more verification before it's effective implementation. And therefore could be found in very limited models of modern high-end cars like the Infiniti G sport model [78].

3.2.1.4 Discussion

Junjie He [9] presented a comparative study between both AFS and ARS through simulation. The simulation model used is an 8-DOF Non-Linear Vehicle Model (NLVM) that uses a 2-DOF bicycle model as a reference model to calculate the desired yaw rate angle needed to be achieved by the vehicle. In this study multiple simulations were realized at different handling conditions to study the effectiveness of each of the standalone AS control systems. The comparison held between both systems aims to compare their ability of desired yaw rate tracking to generate the required corrective yaw moment on the vehicle.

The results of this study shows that the AFS was able to produce an equal amount of positive yaw and negative yaw moment (positive and negative in terms of the steering direction) during non to mild lateral acceleration. While at moderate lateral acceleration situations, the negative yaw moment produced was bigger than the positive one. And since this steering process can considerably decrease the side-slip angle that consequently will affect the lateral force at the front axle creating a large change in the yaw moment. But when the vehicle approached the handling limits, both the achieved positive and negative yaw moments were small. The study suggests that this behavior is due to the fact that at the handling limit, the steering angle of the front wheels are usually large and therefore the front axle reaches its saturation point where relatively small changes in the steering angle. As a result, the tire slip angle shall have a very little effect on the lateral forces. Figure 3.16a shows the results obtained by the AFS system presented in that study; where the x, y and z axes presents the corrective steering angle, the lateral acceleration and the yaw moment respectively.

Consequently the results of the ARS is shown in figure 3.16b, where

although this system showed a similar performance as the AFS at mild lateral acceleration; when the vehicle approached the handling limits the positive yaw moment was even larger than the negative one. The study explains this behavior to be due to the fact that at the handling limit the tire slip angle of the rear wheels are large as well and consequently their lateral tire forces approaches its maximum. Hence, by steering the rear wheels in the opposite direction of the front ones the slip angle and the lateral forces of the rear wheels can be reduced considerably. Nevertheless, due to the saturation of the lateral tire forces at the rear axle, the slip angle of these tires can not be increased to produce the negative yaw moment by simply increasing the rear wheel angle.

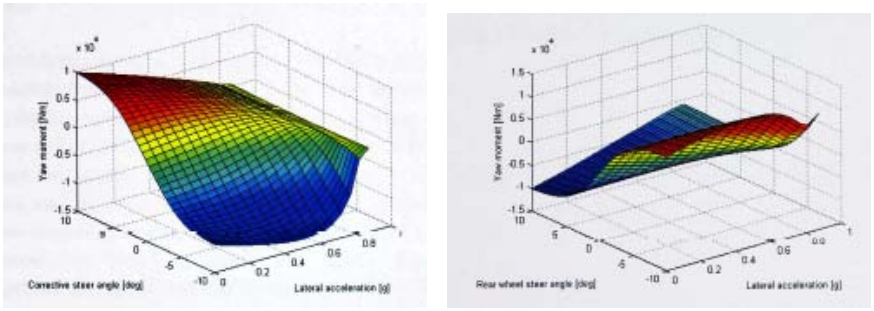

(a) Corrective yaw moment generated by AFS

(b) Corrective yaw moment generated by ARS

Figure 3.16: Corrective yaw moment results from [9]

The study concludes that the previous comparison shows that both AFS and ARS improves the vehicle steerability response before the vehicle reaches its handling limits. But as the vehicle gets closer to that zone, although the ARS is more powerful in generating positive yaw moment when instability happens ARS is not fully capable of correcting the situation, especially because of its low negative yaw moment generation capability. On the other hand, AFS showed more effectiveness in the negative yaw moment generation especially at relatively small steering wheel input. Nevertheless, both AS systems fail to follow the desired side-slip behavior of the vehicle and are not sufficiently effective as the vehicle approaches the handling limit.

With the guidance of the results obtained from the previous study, besides the fact that rear wheel steering systems requires the presence of extra mechanisms either hydraulic or electric actuators to steer the rear wheels and hence increases the complexity of the vehicle mechanics and accordingly raises its price [6]. The choice have been made to only choose Active Front Steering

to achieve the desired yaw rate behavior of the vehicle. While for regulating the vehicle's side-slip behavior a DSC is proposed, this new subsystem should be also responsible of improving the vehicle's behavior as it approaches the handling limit. Consequently, we will review the available DSCs and the criteria of choosing the other subsystem.

3.2.2 Dynamic Stability Control (DSC)

AS systems become less effective in controlling the stability of the vehicle as the vehicle approaches its handling limits due to the tires saturation. Therefore, the need emerged for another system that is able to generate a contra yaw moment especially at the handling limits. Hence, an alternative approach of using a differential longitudinal force between the left and right sides of the vehicle producing this necessary yaw moment to bring the vehicle back on track was proposed [10, 32, 40, 70], see figure 3.17. And from here came the name of Direct Yaw moment Control (DYC) systems, as they directly control the yaw moment of the vehicle.

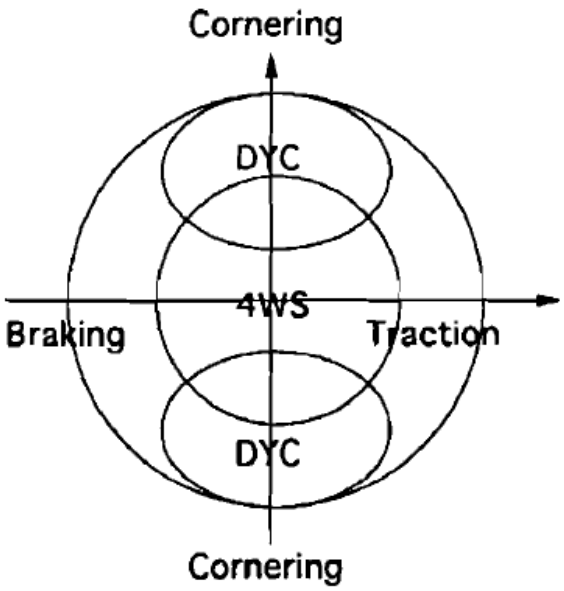

Figure 3.17: Effective zones of steering systems and DYC systems [10]

There are two ways to generate this differential longitudinal force, either by braking asymmetric wheels or providing them with a different engine torque. The two DSC systems that uses this technique are known as Brake-based

and Driveline-based DSC respectively, and will be discussed in the next two sections.

3.2.2.1 Brake-based DSC

The brake-based DSC, also known as, Vehicle Stability Control (VSC) or Electronic Stability Program (ESP) or Electronic Stability Control (ESC) is considered one of the most widely used vehicle stability control systems. According to the driving situation it applies brakes to individual or asymetric wheels to create a yaw moment torque about the vehicle's vertical axis. This torque opposes the undesired generated torque that is an effect of the oversteering or understeering behavior. Therefore, this controller intends to decelerate the vehicle slip to bring it back to a neutral steering performance that conforms with the driver's expectations, see figures 3.18 and 3.19.

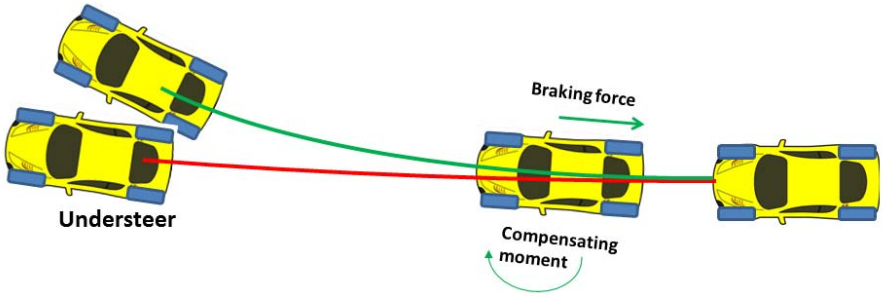

Figure 3.18: Contra yaw moment to adjust an understeering situation

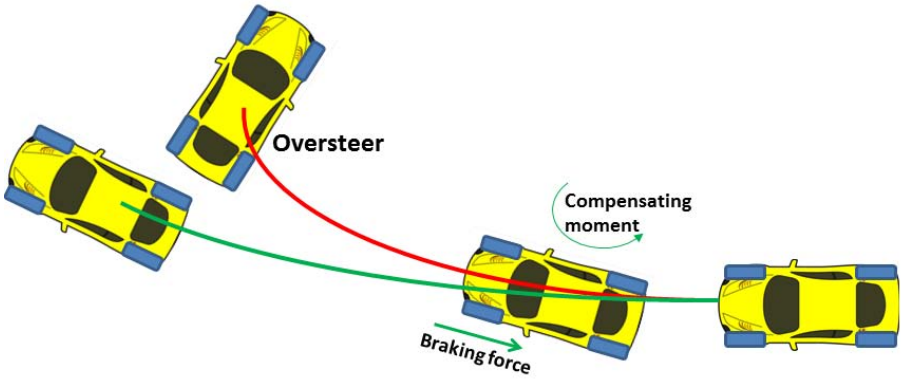

Figure 3.19: Contra yaw moment to adjust an oversteering situation

These systems have a great advantage over its other competitors, that they need very little hardware on their own and can share their sensors and

actuators with the normal ABS system that is installed in almost all the modern vehicles nowaday. Therefore this system doesn't imply neither an extra high cost nor further mechanical complexity. Furthermore, these systems are considered to be sufficiently developed in practical development and in academia.

In academia, for example various researches have investigated the use of different control variables. Some researches aimed to control the yaw rate of the vehicle like in [79, 80]. Others have tried to control the side-slip angle of the vehicle [81, 82, 83, 84] or even a combination of the side-slip angle and its angular velocity [85, 86, 87]. Some research have even tried to control both the yaw rate and the side-slip angle like in [88, 89, 90].

3.2.2.2 Driveline-based DSC

The driveline-based Dynamic Stability Control works on a very similar concept as that of the brake-based DSC. It also intends to generate a contra yaw moment about the vehicle's vertical axis to bring back the vehicle to its desired course. But this time by redistributing the torque between the vehicle's wheels, or in other words, instead of braking separate wheels it transmits less engine torque to separate wheels. The driveline-based DSC acts either on making a difference between the front/rear or left/right torque distribution. To generate a difference between the front/rear torque distribution a Four Wheel Drive (4WD) hardware is needed. While for the left/right torque distribution there are four mechanisms to produce this torque split: controlled Limited Slip Differential (LSD), control using braking, control using driving torque and torque bypass [9, 19]. In the left/right torque splitting control a considerable corrective yaw moment is generated due to the difference in the generated longitudinal force and have shown to be more effective than that of the front/rear distribution [91].

Some examples of the commercial systems that uses active vehicle yaw control using torque management between the front/rear axes are the Nissan V-TCS, the Haldex LSC, the BMW xDrive, the Bosch CCC. As for the front/rear systems that act on demand there exists the GKN TMD, the Dana Dynamic Trak and the Ricardo. Last but not least, examples of those systems that acts on the left/right torque splitting are the Honda SH-AWD and the Mitsubishi AYC [92].

3.2.2.3 Discussion

DYC systems have proved its effectiveness in controlling the vehicle stability by correcting the vehicle performance and bringing it back to its intended course. Both the driveline-based and the brake-based DYC use the same principles in handling the vehicle control. Yet to create the corrective yaw moment, one uses the variation in the engine transfered torque to the wheels and the other uses the brakes to brake separate wheels. Both methods have their advantages and disadvantages. For example, the brake-based DYC is effective in both of the linear/nonlinear operational region, yet its use in non-severe situations is not desirable since it brakes the wheels and therefore affects the vehicle's longitudinal velocity [40]. This characteristic could transmit a feeling of uncontrollability especially in situations when the driver wishes to increase the speed [93].

On the other hand, the driveline-based technique doesn't deteriorate the speed, but it is not as effective as the brake-based technique as the vehicle approaches the handling limit [94]. That's due to the fact that the driving torque depends mainly on the engine capacity and the driving situation, furthermore, the driving torque usually has a lower limit than that of the braking torque. Therefore, the available corrective yaw moment generated by the driveline-based system is considerably small in comparison to that generated by the brake-based system [9]. Also, the driveline-based DYC systems require extra hardware to operate, while the brake-based share their sensors and actuators with that of the ABS, which makes the brake-based systems less costly, also it imposes less hardware complexity and is more accessible.

Therefore in the presented work, the only applied DYC system is the brake-based DYC. And to make up for the disadvantage of unnecessary braking the DYC is combined by an integration control technique with an AFS system that is used to correct the vehicle performance as the vehicle stays in its linear zone and the use of DYC is limited to the necessary situations, as the vehicle approaches its handling limits.

3.2.3 Suspension-based handling systems

These systems aim to control the vertical movement of the wheels through an active control system rather than the passive movement of the normal

suspensions system that is solely determined by the road surface. Such systems are the semi-active suspensions, the fully-active suspensions and the active roll systems. These systems enable the control of the vertical displacement of the tires and to keep the tires perpendicular to the road while negotiating curves. By that it reduces the effect of the lateral load transfer and therefore allows better traction and stability. Also the active/semi-active control they provide aims to improve the ride quality by effectively isolating the suspended mass from the road imperfections.

Fully-active suspension systems are usually hydraulic actuators that could function on its own or with the aid of passive spring and damper components. While the semi-active ones only intent to modify the damping rate of the shock-absorber. These systems uses special dampers, lately the most common of which are the Electro or Magneto Rheological dampers, which uses fluids that changes its viscosity in the presence of an electric or magnetic field. Whilst the active roll systems only aim to control the roll stiffness of the suspension by using either a linear or rotary actuator that affects the roll bar properties. Due to the high cost and high complexity of the fully-active suspensions, there have been more research and commercial interest in the later two systems [19, 95].

Suspension-based handling systems play an important role in affecting the vehicle's roll moment in its steady-state handling by moving the roll moment generated by the vehicle cornering back from the inside of the curve to the outside. As a result of the nonlinear nature of the tires, the lateral force generated on each axis is reduced due to the lateral load transfer. Therefore, as the roll moment increases on the front axis the vehicle will tend to understeer and as it increases on the rear axis the vehicle will tend to oversteer. Furthermore, the rear suspensions are commonly stiffer than the front ones, so that they can reduce the pitch vibration [5, 31]. Therefore the vehicle will tend to have an oversteering behavior. For that reason, the active/semi-active suspensions become advantageous in improving the steady-state handling of the vehicle [96].

Nevertheless, the effect of the Suspension-based handling systems is only effective at high lateral acceleration (above 4 m/s^2) and its effect mainly depends on the longitudinal weight distribution of the vehicle. And therefore at linear circulating these systems shows almost no effect [9, 19, 94].

Despite the fact that, these system will not be further used in this work,

as the presented controller aims to develop a simple and accessible controlling technique that controls the vehicle before the situation gets extremely severe. The description of such systems would serve in the further review of the integrated control systems present in the literature.

3.2.4 Standalone systems discussion

This section has reviewed the different types of standalone controllers that aims to improve the vehicle handling and stability. It started in section 3.2.1 by reviewing the different types of Active Steering systems; AFS, ARS and A4S, and provided a comparative study between the three of them. In that section it was concluded the choice of AFS to control the vehicle handling at low to mid-range situations, due to its hardware simplicity, low cost in comparison to the other AS systems and its effectiveness in the production of the needed corrective yaw moment. While, choosing a DSC system to control the vehicle as it approaches its handling limits as suggested by [19, 97, 40], this comparison is detailed in section 3.2.1.4.

Consequently, section 3.2.2 reviewed the different types of Dynamic Stability Control systems: the driveline-based and the brake-based DSCs. And it concluded the use of only a brake-based DSC due to its higher effectiveness (in contrast to the driveline-based one) at the uncovered zone by the used AS system. Besides its low cost, hardware simplicity and development readiness in comparison to the other DSC system. Nevertheless, to makeup for its unnecessary speed reduction inconvenience, its use will be limited to only necessary control situation, detailed comparison in section 3.2.2.3.

Finally, section 3.2.3 quickly reviewed the suspension-based handling systems, due to the fact that it's out of the scope of the presented integrated control approach. The section justified that, it will not be used due to the limitation of its effectiveness to only extremely high lateral acceleration situations, as it depends mainly on affecting the lateral weight displacement. Yet it was important to review such systems to provide a sufficient background review for the upcoming literature.

Thereafter, the rest of this chapter will be dedicated to review the different integration techniques in the literature and explain the chosen integration technique used by this thesis to integrate the two chosen standalone vehicle handling and stability controllers: the Active Front Steering system and the

brake-based Dynamic Stability Control system.

3.3 Integrated Vehicle Dynamics Control

The previous section discussed the different vehicle stability control systems provided in the literature. Through the previous discussion it was shown that each of these systems has their advantages and disadvantages, or in other words are more effective in some control zones than others. Due to the difference of the characteristics of each system and the vehicle dynamics they intend to control; the use of more than one of these system is recommended to cover the different control zones. Nevertheless, combining these safety critical systems couldn't be done by a simple arithmetic operation; because in this way many problems could occur due to the presence of inherently vehicle dynamics coupling.

The presence of several control systems can generate two main problems. First, since the systems are not inter connected repetition of sensors and actuators could occur increasing the hardware complexity of the vehicle. Also the total vehicle software system will be more complicated due to the number of signals to be coordinated. Second, due to the possible function overlapping between the different control systems can lead to a conflict between the sub-modules or even an overcorrection behavior due to the different control objectives of each module [12].

Thus, a careful integration technique is required to regulate the behavior of each of the integrated controllers. Such an integration should be designed with the aim of adding modularity, scalability and robustness [11]. In addition to solving the two addressed problems; such that, the first could be solved through sharing sensors and actuators, while the other by carefully regulating the control objectives and especially at functional overlapping zones. Such systems are called Integrated Vehicle Dynamics Control (IVDC) or "Integrated chassis control". Figures 3.20 and 3.21 show the difference between the working scheme of different standalone systems and their integration hierarchy, respectively.

IVDC allows the reduction of the controlling systems' complexity and in some cases even reduces the cost since it allows the sharing of sensors and actuators between the different control system modules, therefore could reduce

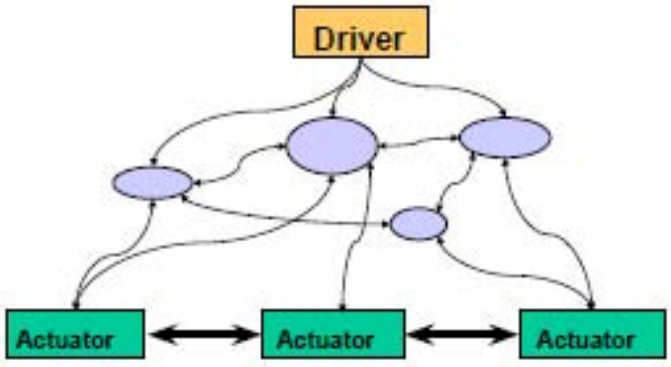

Figure 3.20: Various stand alone controllers [11]

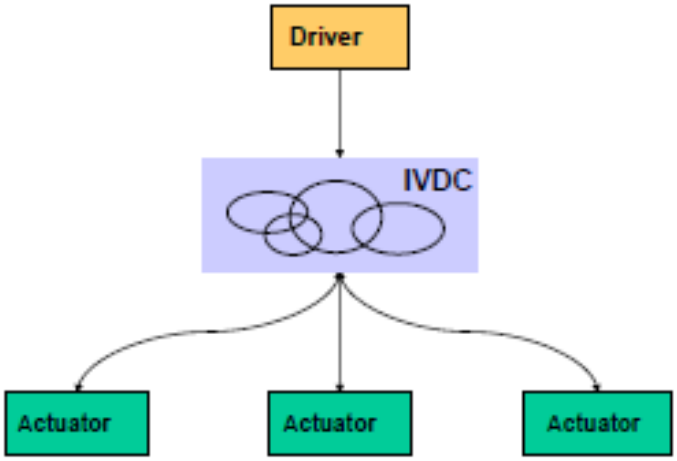

Figure 3.21: Integration of different standalone controllers [11]

their number as well as the vehicle weight. Also this integration allows having a unique calculating processor that handles the different sensors and actuators through only a singular decision maker. Also, it is suggested that this integration could increase the flexibility of the control system design, for example, if the control objective could be broken down into separate tasks, where each of which could be designed separately. Other suggestion is that the careful integration of the different modules could yield a further improved performance than that of a simple combination of the different modules [9, 12, 20], see figure 3.22. Lately IVDC has been a hot research topic [12, 54], the rest of this section will be dedicated to review some of the provided literature about this topic.

Nagai et al. proposed a coordination scheme between steering and braking using a feedforward controller and an optimal state feedback controller. Their

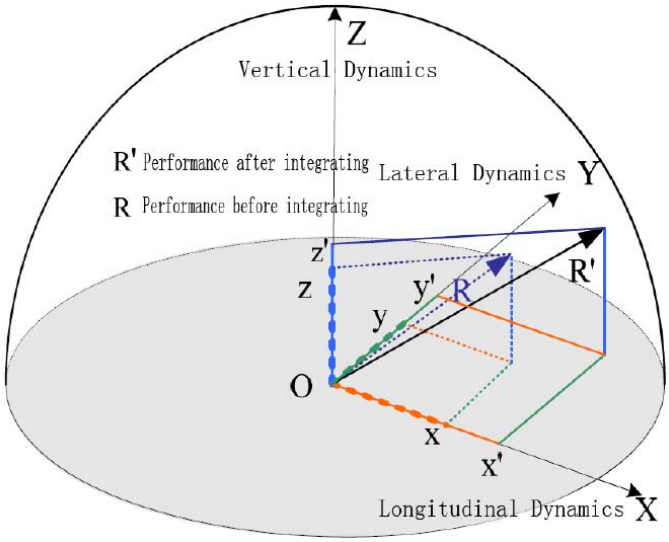

Figure 3.22: Potential benefits of acsIVDC[12]

proposed idea targeted ARS in [10, 98, 99] then AFS in [69]. Where in [69] the proposed model was composed of a steering angle-based feedforward controller and an optimal state feedback controller. But the effectiveness of the presented system was only investigated using a 2-DOF vehicle model.

[100] presented a simple model regulator to coordinate both AFS and braking-based DYC through measuring the yaw rate feedback. In [101], in order to enhance vehicle steerability, lateral stability, and roll stability a yaw rate controller was designed to track the target yaw rate based on sliding mode control theory. [102, 103] presented a fuzzy logic controller that controls the vehicle's yaw rate to improve the vehicle handling and stability through steering and suspension system. While [104] and [105] presented other fuzzy logic controllers that also controls the vehicle's yaw rate through AFS and brake-based DYC. Nevertheless, the effectiveness of these controllers are questionable since theoretically, at least two control inputs are needed to control two output variables to achieve the desired response [69, 70].

A body of work was presented by He et al. [97, 106, 107] that aimed to integrate AS systems with both braking-based and drive-line based DYCs using Sliding Mode Control by controlling both the vehicle's yaw rate and side-slip angle. Other work by Doumiati et al. [35, 40] suggested using Linear Parameter Varying controller synthesized within the **LMI!** (**LMI!**) framework, while warranting robust H∞ performances. This controller controls both AFS and braking-based DYCs through the vehicle's yaw rate and side-slip angle.

Others have used optimal control and linear H∞ control algorithms [108, 109]. In [110], a coordination of active front steering and direct yaw control based on optimal guaranteed cost control theory is presented. Other algorithms based on direct Lyapunov method have been proposed [111]. These controllers have shown promising results in improving the vehicle handling; however, these systems were manly designed and tested on limited number of maneuvers and conditions.

In [70] and [112], a fuzzy logic-based yaw moment and steering controllers were introduced. They controlled the vehicle through adding a correcting value to the vehicle's front braking and front steering angle through evaluating the feedback of both the yaw rate and the side-slip angle. The controllers demonstrated a noticeable improvement in following the control objectives; the desired values of the side-slip angle and yaw rate, in complicated maneuvers. Nevertheless, since fuzzy logic systems are linguistically comprehensive and can deal with high level information, the control system rules were based on experts' knowledge. Which make them fall under the same category like the former reviewed controllers.

Nevertheless, in a safety critical control system where each variation of its input needs an accurate response to guarantee the safety of the passenger, experts' knowledge solely and human-designed systems cannot be reliable [113]. Especially when the system designing conditions and maneuvers are the same as the testing conditions. This makes the reliability and predictability of the system questionable.

Therefore, in this presented work, we intend to replace the expert's knowledge and the human-designed systems with an intelligent automated system that auto-construct the control system without human intervention to match with each modeled vehicle properties. This approach uses an intelligent neural network that learns the optimum control values through an extensive data mining algorithm; and accordingly auto-construct a fuzzy controller that corrects the vehicle stability through AFS and brake-based DYC. The control inputs of this system will be the yaw rate and the side-slip angles like the most effective controllers presented in the literature.

The intelligent system that carries out such a process of auto learning and auto constructing is known as: Adaptive Neuro-Fuzzy Inference System (ANFIS). The ANFIS controller combines the benefits from both: Neural Net-

works and Fuzzy logic; where, the first have the quality of being adaptive and can learn by generalization and pattern recognition, and the latter allows soft and steady performance [114]. This technology will be further explained in the following section.

3.3.1 Main advantages of the proposed approach

The main advantages that the proposed approach presents over similar control systems from the literature could be listed as following. First, the algorithm helps to eliminate the inaccurate human-factor in deciding the control rules, by searching for the best control decisions through iteratively testing the car response on a wide range generic maneuver. Together with the FLC approximation property, the proposed algorithm can guarantee the inclusion of the maneuvers that a car can go through. This aspect is considered very important for such a safety critical system. Because manually designed control system are more prone to errors like uncoverage of certain control zones or approximation of control decisions values, due to the human imprecision.

Secondly, the automated algorithm affords the ability to auto-construct and auto-adapt the control system according to the current characteristics of the model to be controlled without the need of human interference. This feature allows the change of the model characteristics, like the vehicle's suspensions, tires, shape, etc., without the need of redesigning the control model or manually tuning some model variables like in [70, 97, 40].

Last but not least, the algorithm takes into consideration the coordination between the control of AFS and DYC, to eliminate the undesired braking at mild driving situations while being able to control the vehicle as it approaches its handling limits. This problem has been faced in the literature by [97, 110, 40], and others, since both controllers affect each other and have to be coordinated so that they won't contradict each other nor exceed the required control value. Nevertheless, the solutions proposed in these works were either to activate one while deactivating the other, or control both together, or a hybrid between the previous both depending on the control zone (critical or uncritical). Yet, such solutions were manually adapted and hence they are also prone to human imprecision and the need of manual re-adaption as the characteristics of the vehicle changes, as explained above.

3.4 Used integration technology Adaptive Neuro-Fuzzy Inference System (ANFIS)

Inspired by its name Adaptive Neuro-Fuzzy Inference System (ANFIS) systems combines between the two Artificial Intelligence fields: the Artificial Neural Networks and the Fuzzy Logic Control. To be able to explain the characteristics and the working scheme of the ANFIS systems it is essential to discuss its background technologies. Therefore this section will be dedicated to give a brief explanation of these three Artificial Intelligence research topics.

3.5 Artificial Intelligence in Control

In the last two decades, the word Artificial Intelligence (AI) started to be heard more frequently than ever before, not only in the world of science fiction movies and books, but also excessively in the world of engineers and researchers. Therefore, some engineers and researchers decided to get closer to this field and discover what it may offer them of applications and advancements, while others have decide to stick to the classical approaches. Nevertheless, regardless to their decision, both stayed hearing about more advancements of AI related to their fields, and even without being aware, both uses applications and instruments that implement one of the applications of AI.

Artificial Intelligence is one of the youngest sciences yet has achieved fast advancements and a rapid spread influencing almost all other sciences. While math and physics have been out there since the commence of civilizations, the first recognized work in AI dates back to 1943 [13]. This progress calls the attention of many researchers who are keen to exploit the uses of this, young and promising, field in their research.

In this section, we will be reviewing some of the most popular topics in the field which also have relation with the implementation presented in this thesis. In sections 3.6 and 3.7, we will present the topics of Fuzzy Logic Control (FLC) and Artificial Neural Network (ANN), the last section(3.8) will present a new AI field (ANFIS), that combines between the two previous ones advantaging from the benefits of each. This last topic is the one used in the application presented in this thesis. This section is written from the knowledge obtained mainly from [115, 116, 13] and experience obtained through the years

from working in these fields.

3.6 Fuzzy Logic Control

The definition of fuzzy logic in the words of its founder is "Fuzzy logic is determined as a set of mathematical principles for knowledge representation based on degrees of membership rather than on crisp membership of classical binary logic"[117].

3.6.1 Simple explanation from real life examples

Let's define this in lamen terms, the normal English dictionary from Cambridge University defines the word fuzzy as "not clear, without strict edges or having noise". Before explaining the relation between the scientific definition and the simple English definition, let's agree to a point. Life comes in shades of gray not only strictly black neither strictly white, even human expressions and comprehension doesn't necessarily represents the extreme cases. For example, saying that someone is very tall or too short or that the weather is quiet hot or a city is fairly beautiful or that shirt is not very expensive. These expressions are all sliding degrees between two extremes, that humans use daily in their natural language especially when it comes to describing temperature, height, speed, distance, beauty or anything of that sort.

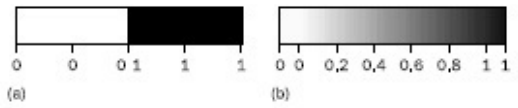

Figure 3.23: Range of logical values in Boolean and fuzzy logic: (a) Boolean logic; (b) multivalued logic[13]

Yet machines and computers don't understand neither human ambiguous language nor their fuzzy world, they only understand "0 or 1", "ON or OFF"...etc. And here comes the role of fuzzy logic to make the translation between both worlds, see figure 3.23. As explained by [13] "fuzzy logic is not logic that is fuzzy, but logic that is used to describe fuzziness. Fuzzy logic is the theory of fuzzy sets, sets that calibrate vagueness. Fuzzy logic is based on the idea that all things admit of degrees".

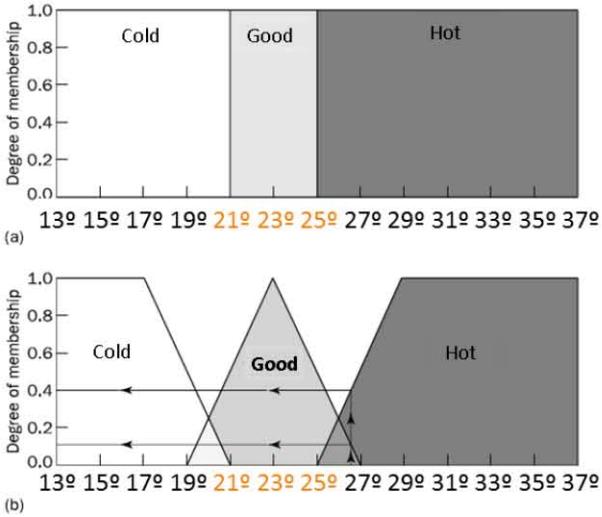

Figure 3.24: Fuzzy Logic Controller block diagram

An example of a real application might facilitate the understanding of this concept. Think of a relatively intelligent air conditioner that should maintain the room at an acceptable temperature, 24°C for example. If this air conditioner uses a typical controller, most probably the controller will limit the accepted room temperature from 21°C to 25°C as shown in figure 3.24(a). But what happens if the temperature of the room was approximately 21°C with a $\pm$ 0.5 variation. Then each time the temp reaches 20.8°C, for example, the air conditioner will start working then when it reaches 21°C it will stop working, going between an on and off and on and off. Such a performance abuses the motors or the controlled system.

If that same air conditioner would get a fuzzy controller, the fuzzy controller may have three fuzzy sets specifying the ranges of the acceptable, hot and cold temperatures. Then have an overlapping between their sliding ranges, where at each point of the temperature range the air conditioner is controlled to give an intermediate value of power; not only an on or off as the basic controller discussed above. Figure 3.24(b), shows an example of a possible FLC used to control such a system. Where, the room temperature is around 27°C, the air conditioner is ordered to work with only 40% of its capacity.

3.6.2 Technical details

The fuzzy logic controllers in general mainly have four main modules,as shown in figure 3.25, are:

1. Fuzzifier
    - Inputs: A single value that is being recorded from the sensors.
    - Outputs: The degree of membership value of this reading to the available fuzzy sets.
2. Rule base
    - Sets of rule available to the FLS.
3. Inference Engine
    - Inputs: A set of rule from the rule base and the degree of membership values that are the output of the fuzzifier.
    - Outputs: The rules that are being fired with their firing strength and the corresponding output.
4. Defuzzifier
    - Inputs: The outputs from the inference engine
    - Outputs: Single value for the final output.

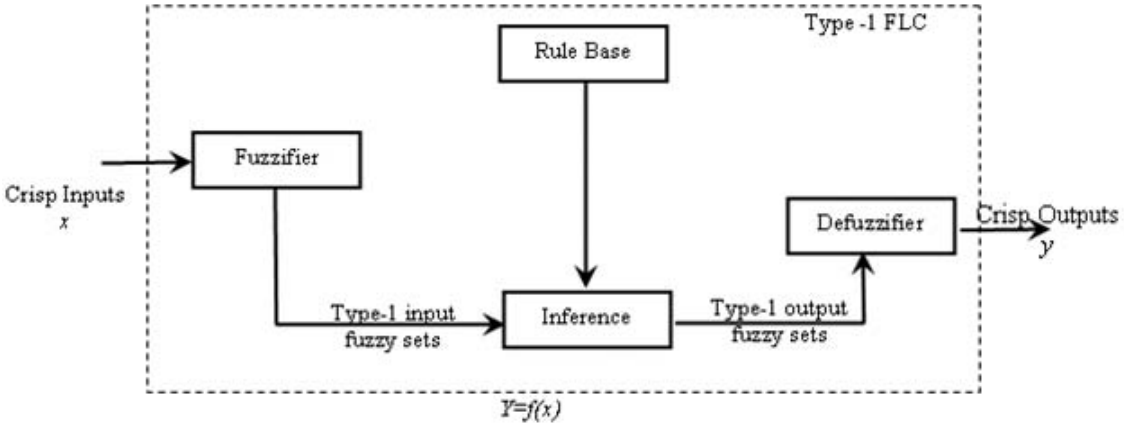

Figure 3.25: Fuzzy Logic Controller block diagram

To calculate the final output yielded by the controller these steps are to be followed:

1. Get the membership value for each given input

2. Get the firing strength of each fired rule in the rule base.
3. Get the outputs of the fired rules.
4. Get one final defuzzified output

3.7 Artificial Neural Networks

Lately, the most advanced Artificial Intelligence techniques and topics were aiming to mimic the Natural Intelligence. Either by mimicking biologically inspired life; like multi agents researches mimicking ants' life for example or genetic algorithms mimicking the evolution theory and how genes mutate and reproduce. Table 3.1 shows some examples on biologically inspired computing and their biological counterparts, listed in [118].

Biologically inspired computing	**Biological counterparts**
Genetic algorithms	Evolution
Biodegradability prediction	Biodegradation
Cellular automata	Life
Emergent systems	Ants, termites, bees, wasps
Neural Networks	The human brain
Artificial Life	Life
Artificial Immune Systems	Immune Systems
Rendering (in computer graphics)	Patterning and rendering of animal skins, bird feathers, mollusk shells and bacterial colonies
Lindenmayer systems	Plant structures
Communication networks and protocols	Epidemiology and the spread of disease
Membrane computers	Intra-membrane molecular processes in the living cell
Excitable media	Forest fires, the Mexican wave, Heart conditions, etc
Sensors Networks	Animal or Human Body

Table 3.1: Some examples on biologically inspired computing and their biological counterparts

One of the best examples on biologically inspired artificial intelligent techniques is Artificial Neural Networks (ANN). So let's begin by explaining

the natural neural networks that exists in the human brain to gain an understanding of the underlying concept of this advanced technique. In this chapter, we will try to explain the fundamental concepts of Neural Networks and the concepts that lies beneath the used types of networks and Learning algorithms used in our study.

3.7.1 Natural Neural Networks

The Nervous System: The human nervous system, as defined by [119], can be broken down into three stages that may be represented in a block diagram form as shown in figure 3.26, where:

- The receptors collect information from the environment - e.g. photons on the retina.
- The effectors generate interactions with the environment - e.g. activate muscles.
- The flow of information/activation is represented by arrows - feedforward and feedback.

Our primarily concern in this system is the neural network in the middle.

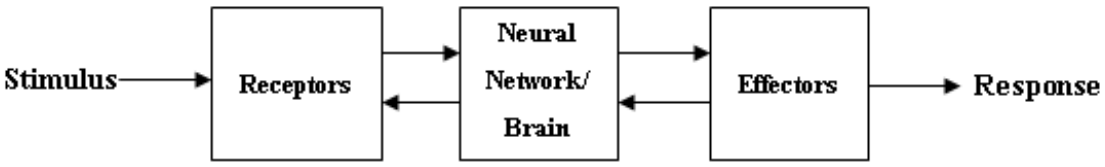

Figure 3.26: Neural Network communication block diagram

Biological Neural System A human brain consists of about 1011 hundred billions computing elements called neurons [116], that communicate through synaptic connections. Each neuron has about 10,000 synapses.

The brain contains both large scale and small scale anatomical structures and different functions take place at higher and lower levels [119]. There is a hierarchy of interwoven levels of organization (illustrated as well in figure 3.27):

1. Molecules and Ions

2. Synapses
3. Neuronal microcircuits
4. Dendritic trees
5. Neurons
6. Local circuits
7. Inter-regional circuits
8. Central nervous system

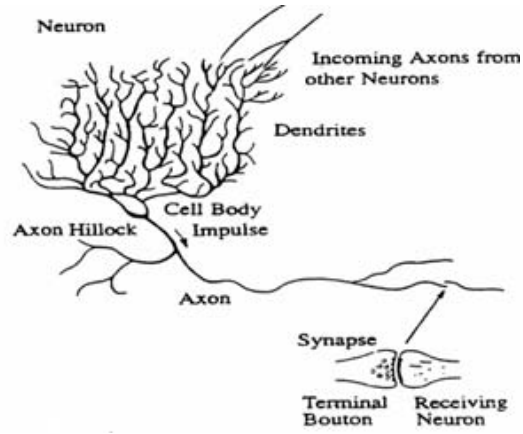

Figure 3.27: Detailed diagram of a brain neuron

Although how brains work is not known exactly [120], science knows certain things about it. For example, that it is resilient to a certain amount of damage, in addition to the continual loss human suffer as they get older. There have been reports of objects being passed all the way through the brain with only slight impairment to the persons mental capability.

Computational perspective From a computational point of view we also know that the fundamental processing unit of the brain is a neuron, where:

- A neuron consists of a cell body, or soma, that contains a nucleus.
- Each neuron has a number of dendrites which receive connections from other neurons.

- Neurons also have an axon which goes out from the neuron and eventually splits into a number of strands to make a connection to other neurons.

- The point at which neurons join other neurons is called a synapse.

- A neuron may connect to as many as 100,000 other neurons.

Signals move from neuron to neuron via electrochemical reactions. The synapses release a chemical transmitter which enters the dendrite. This raises or lowers the electrical potential of the cell body. The soma sums the inputs it receives and once a threshold level is reached an electrical impulse is sent down the axon; often known as firing. These impulses eventually reach synapses and the cycle continues. Synapses which raise the potential within a cell body are called excitatory. Synapses which lower the potential are called inhibitory. It has been found that the synapses exhibit plasticity. This means that long-term changes in the strengths of the connections can be formed depending on the firing patterns of other neurons. This is thought to be the basis for learning in our brains. But when referring to Artificial Neural Networks (ANNs), it is referred mainly to a module of crude approximations to levels 5 and 6.

Brains versus Computers Although computer scientists and engineers are trying to mimic such a very developed system that through the decades was able to build such a civilization that we are living nowadays- the human brain. Our apparently very intelligent ANNs, are very far away beyond the capabilities of the Natural Neural Networks. Below is a comparison of the brain's capability against that's of the computers as in [119].

- There are approximately 10 billion neurons in the human cortex, compared with 10 of thousands of processors in the most powerful parallel computers.

- Each biological neuron is connected to several thousands of other neurons, similar to the connectivity in powerful parallel computers.

- Lack of processing units can be compensated by speed. The typical operating speeds of biological neurons is measured in milliseconds (10-3 s), while a silicon chip can operate in nanoseconds (10-9 s).

- The human brain is extremely energy efficient, using approximately 10-16 joules per operation per second, whereas the best computers today use around 10-6 joules per operation per second.
- Brains have been evolving for tens of millions of years, computers have been evolving for tens of decades.

3.7.2 Artificial Neural Networks (ANNs)

So let's first give a definition for what is an ANN. According to Simon Haykin [121], a neural network is a massively parallel distributed processor made up of simple (adaptive) processing units, which has a natural propensity for storing experiential knowledge and making it available for use. It resembles the brain in two respects:

1. Knowledge is acquired by the network from its environment through a learning process.
2. Inter-neuron connection strengths, known as synaptic weights, are used to store the acquired knowledge.

Now let's begin talking about the formulation of our neurons and their functions.

The McCulloch-Pitts Neuron (The First Artificial Neuron) McCulloch and Pitts in 1943 produced the first neural network, which was based on their artificial neuron. Although this work was developed in the early forties, many of the principles can still be seen in the neural networks of today [122].

This vastly simplified model of real neurons, showed in figure 3.28, works as follows:

1. A set of synapses (i.e. connections) brings in activations from other neurons.
2. A processing unit sums the inputs, and then applies a non-linear activation function (i.e. squashing/transfer/threshold function).
3. An output line transmits the result to other neurons.

And from here begins the fundamentals of all the concepts of artificial neural networks.

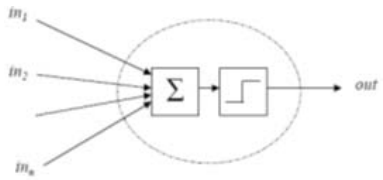

Figure 3.28: The First Artificial Neuron

Neuron Model The most famous neuron model and the one used in this study can be written as follow:

$$y_k = \varphi(\sum_{j=0}^{m} w_{kj}x_j) = \varphi(\sum_{j=0}^{m} w_{kj}x_j + b_k) \tag{3.50}$$

Where b_k the bias, can be treated as a special weight[116]. In figure 3.29, you can see the diagram and graph description of the equation. Where the x_{0-m} are the input neurons to the main neuron, connected to the main neuron through synapses weights represented by the $w_{k(0-m)}$ then all the weights of the connected neurons are summed with the summing function and this value is entered in the activation function $\varphi(\cdot)$ and this represent the output of that current neuron y_k.

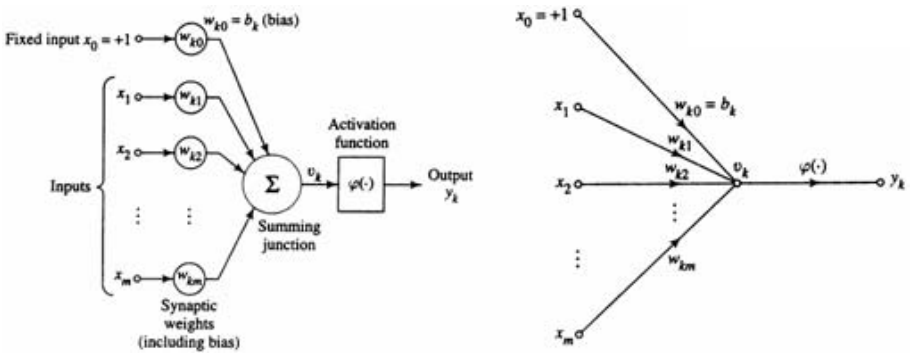

Figure 3.29: Simple ANN model

Feedforward Neural Network The feed forward neural network is the most famous type of neural network and the one used in our proposed study as well. Figure 3.30, shows the diagram representing the feedforward multi layer precepetron neural network and its operation function is represented in equation 3.51, where the term multi layer precepetron refers to the existence of one or more hidden layers. Feedforward neural networks have a number of

hidden layers that connects the input neurons to the output neurons, where the input neurons are the receptors of our data from and the output neurons give us the final output of the network. The number of input neurons output neurons and hidden layers are subjected to the type of application and the structure of data.

$$y_k = \varphi(\sum_{i=0}^{n} w_{ki} h_i) = \varphi(\sum_{i=0}^{n} w_{ki} \varphi^h(\sum_{j=0}^{m} w_{ij}^h x_j)) \tag{3.51}$$

where $h_0 = x_0 = 1$.

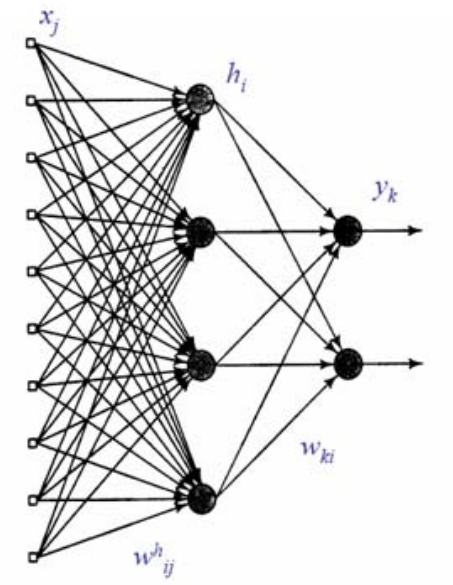

Figure 3.30: Feedforward Neural Network

3.7.3 Learning in Neural Networks

The learning in the neural network is very similar to how the human brain learns. According to the Hebbian's postulate, simply when two neurons on either size of a synapses are activated asynchronously, then that synapse is selectively weakened or eliminated otherwise the synapses is strengthened, in our artificial network the weight of the connection is increased or decreased [116]. And as the weight of each connection increase, the influence of its neuron in increased as well (remember that the weight is a multiplication factor). Equation 3.52 represents the mathematical formulation of the Hebbian's learning rule explained above and is illustrated in figure 3.31.

$$\Delta w_{kj}(n) = \eta y_k(n) y_j(n) \tag{3.52}$$

where η is the learning rate.

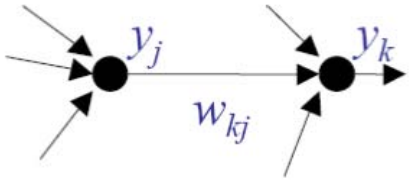

Figure 3.31: Hebbian's learning rule

There are various learning algorithms that are used to train Artificial Neural Networks, one of the most popular and easy to understand is the back-propagation learning algorithm. A hybrid of this algorithm with another forward path that uses the least-squares learning technique, is the learning algorithm used by the ANFIS system used in this project and explained in more details in 3.8.

Below is a quick explanation of how this algorithm works, while a detailed illustration of its equations is listed in appendix A.

The Back Propagation Learning Algorithm Operating on our previously explained feedforward neural network the algorithm should work as follows:

1. Set the network size (number of hidden neurons), learning rates and other parameters. Initialize the weights (including baises) by setting them to small random values.

2. Present a training data pair (repeated cyclically) and calculate the corresponding network output.

3. Calculate the output error and the local gradient of the output neurons δ_k, and update the output weights.

4. Calculate the local gradient of the hidden weights δ_i^h.

5. Go to step 2, and repeat until the weights stabilizes or the output error is small enough. (or if your stopping condition applied, if there were any)

3.8 ANFIS

Adaptive Neuro-Fuzzy Inference System (ANFIS) systems are a class of adaptive networks that are funcionally equivalent to fuzzy inference systems. In more simple words, they are an advanced artificial intelligence technique that uses Neural Networks to construct automatically a fuzzy logic controller (FLC) for each specific case. In order for the Neural Network to construct the controller, we need to train the network with some data that defines the required performance of the controller. The neural network learns this data through trials and error epochs and with the knowledge it gains from these trials it constructs a FLC that mimics the required performance.

The advantage of using the ANFIS technique is that it combines the benefits from both: Neural Networks and Fuzzy logic, where; the first have the quality of being adaptive and can learn by generalization and pattern recognition, and the latter allows soft and steady performance [114].

ANFIS uses a Takagi-Sugeno[123] fuzzy inference method in contrast with the model from [70] that uses the Mamdani method [124]. Takagi-Sugeno is a more compact and computationally more efficient than the Mamdani system, furthermore, it is more flexible to the use of adaptive techniques. But on the other hand, the Mamdani system is more intuitive and understandable by the human side [13] .

Chapter 4

Objectives

4.1 Problem Statement

As a vehicle negotiates a turning maneuver at high velocity, undesired lateral acceleration makes the vehicle tends to be more instable and less controllable from the driver's point of view. This instability could be translated in an undesired vehicle behavior like understeering or oversteering that may lead the vehicle to leave its intended course or even rollover. Furthermore, statistical studies verify the impact of the lateral vehicle instability in causing severe and fatal accidents. To make up for this problem, various control systems have been proposed to generate a contra action that brings back the vehicle to its desired course.

These standalone systems aim to alter in a way or another the tire forces to produce compensating forces to help maintain the vehicle's lateral control. Each controller presents a different control strategy, some aims to directly affect the tires steering angles, others affect the tire longitudinal forces to create a yaw moment around the vehicle's vertical axis and others affect the vertical load distribution between the tires. Due to the difference of the characteristics of each of these systems their capability of controlling also differs. Without detracting value to any of the systems, some systems are more effective at mild instability situations, others are more effective as the vehicle reaches its handling limits, and others are more effective as the lateral acceleration exceeds a certain value.

For this reason, the use of more than one control system is recommended to profit from the different advantages of the distinct controlling concepts.

Nevertheless, combining more than one stability controller in a vehicle is not an easy task, as it could produce conflicts between the different controllers as well as overlapping of the different control objectives. Also a simple combination could lead to a further hardware and software complexity due to the possible repetition of sensors and actuators and hence their signal connecting cables and systems.

Hence Integrated Vehicle Dynamics Control (IVDC) systems have been proposed to provide a carefully designed integration to coordinate between the different chassis control systems. This way the control conflicts could be eliminated and the control results could be even further boosted by such a combination. Also the system cost and complexity could be reduced due to the possible sharing of sensors, actuators, cables and control units.

Lately, IVDC has been a hot research topic, and there exists different systems in the literature that have tried controlling different combination of the different standalone systems using a variety of control techniques. Many controllers of which have shown promising results in improving the vehicle handling through testing them on vehicle models.

However, these systems were manly designed and tested on limited number of maneuvers and conditions. Also, they have been tested on the same maneuvers used for their design; hence their reliability and predictability are questionable. Furthermore, a vehicle stability control system is considered to be a safety critical system where any error of it could lead to a fatal damage. While a manually designed controller that is devised through a limited situation testing is prone to errors like uncoverage of certain control zones or approximation of control decisions values, due to the human imprecision.

Moreover, the manual selection of the control margin dedicated to each integrated sub-system doesn't assure the optimal exploitation of the controllers capabilities. Also, since these controllers are human-designed, any variation of the car model characteristics even as small as changing the suspension stiffness will need human intervention for re-calibrating or even re-adjusting the system manually to suit the newly made variation which makes these control systems less portable.

4.2 Objectives

The main objective of this thesis is to make up for the problems faced by the literature and propose a reliable, predictable and portable Integrated Vehicle Dynamics Control that improves the vehicle handling and stability. As well as, efficiently utilizing the available integrated control hardware to cover the different possible control zones, while providing the driver with the needed controllability feeling. To achieve this final goal, a work break-down of objectives needs to be defined:

- Present an Integrated Vehicle Dynamics Control technique that combines between different stand-alone vehicle chassis controllers that compliment the uncovered zones and/or the disadvantages of each other. While considering the chosen controllers, complexity, cost and market availability; to base the study on a realistic and achievable implementation goals
- The Integrated Vehicle Dynamics Control should aim to exploit the maximum advantages of the integrated control systems, to make the best use of the available resources.
- The system design should insure the reliability and predictability of the proposed controller; such that, it should be able to handle all the situations that a driver might go through since it is a safety critical system that can cause fatal accidents if it crashes.
- The system should also be of a high repetitiveness; such that, it could maintain its performance regardless of the possible sensors noise or frequent maneuvers.
- The system should also be portable from one vehicle model to another and easy to be adjusted in the case of the change of the vehicle characteristics; such that, least human intervention would be necessary to achieve this functionality.
- Develop a high quality non-linear full vehicle model with the appropriate Degrees of Freedom and complexity, to study the vehicle cornering dynamics and evaluate the proposed model performance.
- Define the control objectives that the proposed system should follow.

- The model should show an improvement of the vehicle handling and control in comparison to an exact uncontrolled vehicle and another vehicle controlled by a controller from the literature.

Chapter 5

Phases

This chapter reviews the carried out phases of the thesis that makes the presented work comply with the thesis objectives stated in the last chapter. To reach the thesis objectives the work structure have to go through five main phases as shown in figure 5.1 and detailed through out this chapter.

5.1 The Non-Linear Vehicle Model

As mentioned before in section 2.3, mechanical models simulations plays a great role in the facilitation and the cost reduction of the designing process in the automobile industry. Yet the simulation results are of the same quality of the simulated model. In other words, the more degrees of freedom and the more considered aspects of the model, the more realistic its simulation of the vehicle could be. For that reason the first phase was to construct a full car Non-Linear Vehicle Model (NLVM), with 13-Degrees of Freedom (DOF) that comes from the vehicle longitudinal velocity and its lateral velocity; the vehicle yaw, roll and pitch rates; the different four wheels rotational speeds; the vertical motions for sprung mass; and for the unsprung masses at each of the four vehicle extremes.

Since the vehicle wheels play a very important part in the vehicle cornering performance, as discussed in section 3.1. The well-known Dugoff vehicle model [125] was implemented to simulate the vehicle tires behavior. The NLVM will be further discussed is section 6.1.1 and the equations that describes its mechanical components in section 6.2

5.2 Control objectives definition and desired values calculation

As discussed in chapter 3, when the vehicle negotiate a turn on high speed, it becomes less controllable by the traditional approaches. And as the vehicle approaches the physical limit of adhesion it becomes less responsive to the driver steering inputs and its behavior becomes less predictable and nonlinear. At such situations, the correcting control systems prove their importance as they try to keep the vehicle on its designated track [126]. These control systems are built on the concept of evaluating the instability indicating variables and controlling the vehicle to follow the desired values of these variables. And as discussed in section 3.1.6, there are three main dominant control parameters that indicates the vehicle stability situation. They are the lateral stability, the vehicle yaw rate and the vehicle side-slip angle. But since the lateral stability value is already integrated in the later two variables to insure the design simplicity and reduce the system response time.

Between all the presented stand-alone vehicle stability control systems presented in section 3.2, the only two systems chosen to be integrated in the presented Integrated Vehicle Dynamics Control (IVDC) system are the Active Front Steering (AFS) and the brake-based Direct Yaw moment Control (DYC). These two systems were chosen over their other competitors due to their effectiveness in complimentary control zones, their hardware simplicity and their relative economical competence, more details on the made choice can be found in section 3.2.

5.3 Construction of the Adaptive Neuro-Fuzzy Controller

As explained before in section 4.1 and beforehand detailed in section 3.3, there exists vaious IVDC in the literature that aims to improve the vehicle stability. Yet these systems were manly designed and tested on limited number of maneuvers and conditions. Also, they have been tested on the same maneuvers used for their design, hence their reliability and predictability are questionable. And therefore the presented controlling approach aims to replace the human-imprecision by an auto-constructed control systems that is

designed through advanced Artificial Intelligence (AI) techniques, more details about the benefits of this approach is described in section 3.3.1.

To be able to design such an automatically designed control system in a manner that allows it to follow the most optimal control decisions, two steps had to be carried out. First of which, to find the optimal control decisions which is made through an intelligent algorithm. Second, to construct the controller to follow these optimal decisions discovered previously by the algorithm. Below a brief summary of both steps is presented.

5.3.1 Intelligent Algorithm

To automatically construct the IVDC controller information about the vehicle behavior is needed. In previously presented controllers from the literature, this information was obtained from humans, which could be faulty and hence would be very dangerous in such a safety critical control system. For this reason, an automatic data mining algorithm was constructed to search the space of variables for the best control decisions. The algorithm works by fixing one of the two control parameters and starts to vary the other testing its effect on the car performance, then it switches the operation to vary the fixed parameter and fix the previously-varied one to get the best control combination. The best decision is then stored in a database.

The algorithm enters through lots of test cases, from very complicated maneuvering to the easiest one, to secure covering all the maneuvers that a car can get through. Unlike the manually constructed system from the literature, these data are collected extensively and tested one by one to assure the credibility and reliability of the controller. At each test case and time instance, the best control outputs found by the algorithm are stored along with its correspondent sensors input values. These data are then stored in a database that are later used in the learning of the control system. In section 6.3.1, a detailed explanation of how the algorithm works is presented.

5.3.2 Building the controller

Having now a database with the best control decisions, inputs and outputs, we need to construct a controller that mimics these best decisions. Obviously running this algorithm instead of the controller or storing the data set

of a run through all possible values and then referencing it whenever needed would always yield the best control output. Nevertheless such a solution is infeasible in a real time system, especially a vehicle, where the speed of decision taking is very crucial. Here a feasible solution is proposed by Adaptive Neuro-Fuzzy Inference System (ANFIS) where data are obtained through the algorithm, the learning is made offline and then using the generalization and pattern recognition ability of the Artificial Neural Network (ANN), the optimum performance can be learned and a new Fuzzy Logic System (FLS) can be constructed to mimic that optimum performance.

In this study, the controller is built using the MatLab ANFIS toolbox. A more detailed explanation of the learning parameters and the controller performance are explained in section 6.3.2. While more background information about ANFIS, ANNs and FLS are to be found in section 3.4

5.4 Integration of the controller in the car model

Once the ANFIS auto-learning system constructs the new Fuzzy Logic Control from the learned parameters. The controller is ready to be integrated in the vehicle. To do so, the controller is imported as a Simulink block and is connected to the vehicle. Also an observer that provides the controller with the side-slip angle data is constructed from a 3-DOF full vehicle model and is connected to the car sensors and the proposed controller, more details of this integration will be provided in chapter 6. Once the modules are connected to the vehicle, the vehicle becomes ready to be tested on the different testing maneuvers.

5.5 Verification of the presented controller effectiveness

To verify the effectiveness of the presented controller, the testing maneuvers were completely different from the designing maneuvers. Unlike the control systems from the literature that uses the same maneuvers to design the controller as the maneuvers to test the controller, which makes their controllers reliability and predictability questionable. For a fair judgment of the obtained results, the presented controller results were compared to that of a passive

vehicle, another controller from the literature and the designated trajectory. All of the three vehicles were simulated negotiating three different maneuver on two different speeds and a different weather condition.

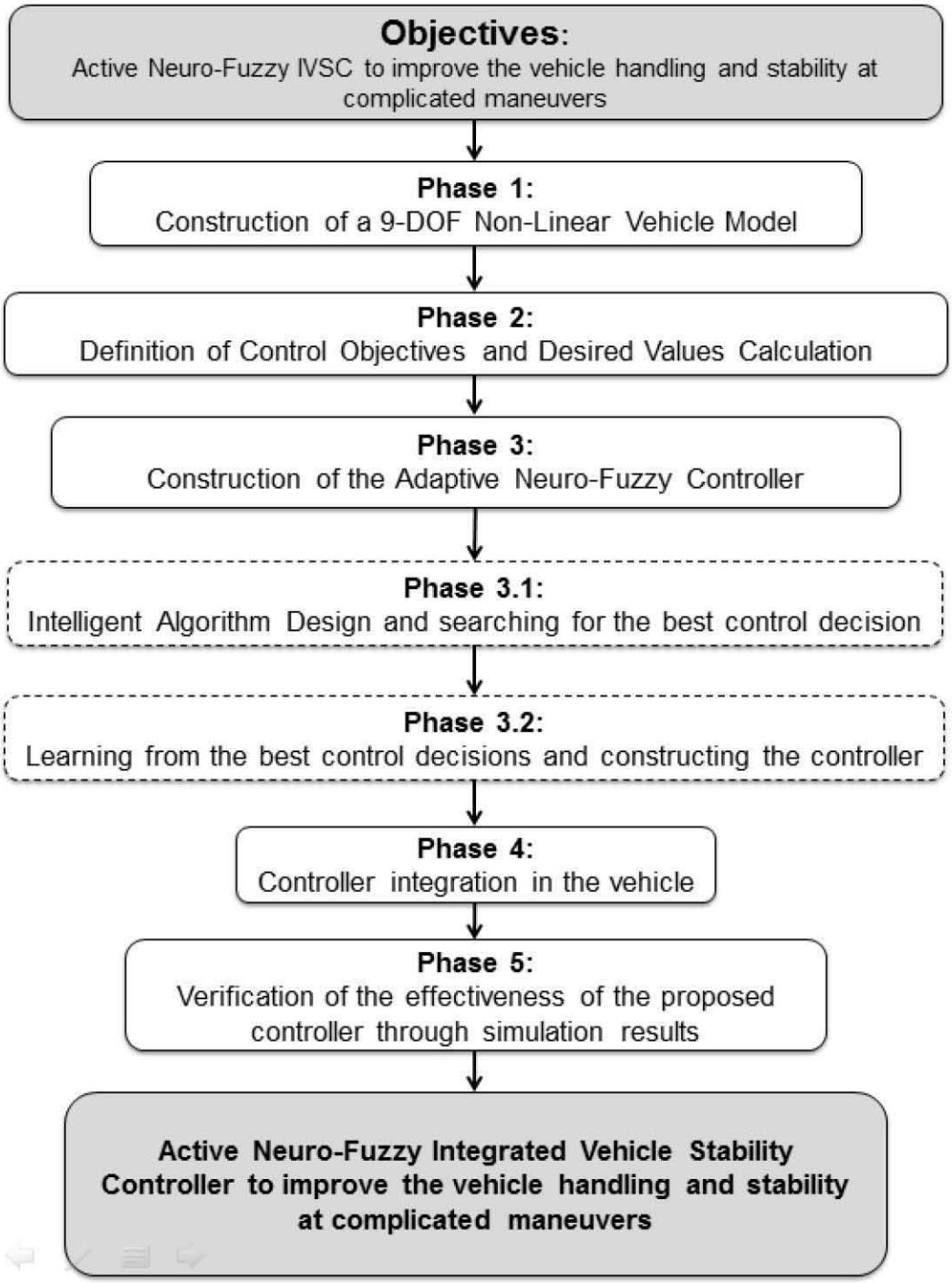

Figure 5.1: Stages of the Ph.D. Thesis Development

Chapter 6

Methodology

This chapter states a detailed description of the proposed system. It starts by describing the different system modules that are used in both the designing and testing phases in section 6.1. That section provides an explanation of how the system is integrated in the car and clarify the data flow between the sensors, actuators, control system and the car. Later section 6.2 explains the vehicle mechanical model used for the simulation process to test the efficiency of the proposed control system. Last but not least, section 6.3 explains the controller designing phases and its operational technique.

6.1 System modules and their interrelation

The system is composed of five main modules, a full vehicle model that simulates the behavior of the car to be controlled. The control system that is used to improve the vehicle stability. A braking force distributor that translates the Moment signal given by the controller to braking forces to break the chosen wheels. An observer that estimates the side-slip angle and pass it as a control input to the controller. And finally a reference model that calculates the desired values of the vehicle's stability indicating variables, in this case the r and the β. These modules and the connection between them is indicated in figure 6.1 and will be detailed in this section.

6.1.1 Full vehicle model

A mathematical Non-Linear Vehicle Model (NLVM) of 13 Degrees of Freedom (DOF) that simulates and evaluates the vehicle response to the con-

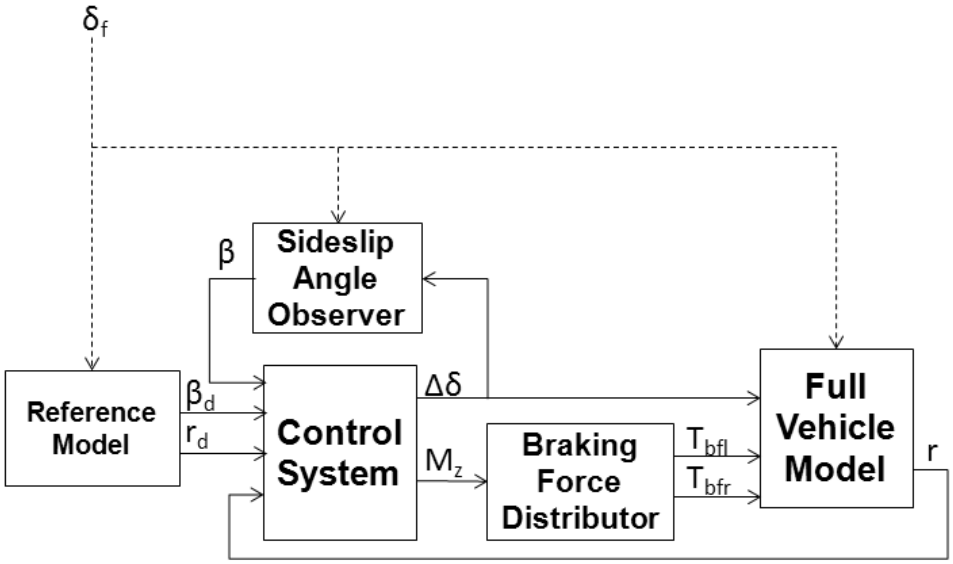

Figure 6.1: Block diagram of the proposed control system

trolled input according to the circulated maneuver. The model was constructed by MatLab Simulink mechanical simulation tool; with the main objective of collecting the data about the performance of a real vehicle and its response to each variation of control entry. Furthermore, this model is used to pre-test the controller performance through simulating bevel maneuvers and testing the effectiveness of its control decisions. The degrees of freedom associated with this model are the longitudinal velocity, U, the lateral velocity, V, the yaw rate, r, the roll rate, p, the pitch rate, $\dot{\theta}$, the wheel rotational speeds, ω_{fl}, ω_{fr}, ω_{rl} and ω_{rr}, and the vertical motions for sprung mass, z_s and for unsprung masses, z_{ufl}, z_{ufr}, z_{url} and z_{urr}.

The equations used to construct this mathematical model comes from well known verified models that are found in the literature to verify the quality of the simulation as discussed in section 2.3. These mechanical models are described in details in sections 6.2.1, 6.2.2 and 6.2.3, that explains the vehicle model, the suspension model and the tire model, respectively.

6.1.2 The control system

Which is the major addition of this presented work, and aims to improve the stability of the vehicle by an integrated control method that controls an Active Front Steering (AFS) system through a steering angle correction signal

$\Delta\delta$ and a brake-based Dynamic Stability Control (DSC) through a direct yaw moment control signal M_z that is then converted into a braking torque, by the 'Braking force distributor'. To judge the stability state of the vehicle so that the controller could output the adequate steering and braking control; three variables are typically used, the lateral acceleration, the yaw rate and the side-slip angle of the vehicle body, explained previously in 3.1.6. Nevertheless, the presented controller uses only the yaw rate r and the side-slip angle β to follow their target values, since the lateral acceleration value is integrated in the previous two. In this way the controller design can be more simple and the response time could be further reduced. For more information about the correcting controllers, like AFS and DSC, please refer to chapter 3.2. While the concept of integrated control, its uses and benefits, could be found in section 3.3.

The selected input signals to the 'control system', the yaw rate can be measured directly by a gyroscope [89, 127], therefore its value is directly taken from the vehicle model. However, the side slip angle can't be measured directly, because as yet the available sensors are optical or GPS based-sensors and are always associated with problems of cost, accuracy, and reliability [128], so the value of the side slip angle is better estimated by an 'observer' [129, 89, 130, 131]. Thus, a three-degrees-of-freedom (3DOF) vehicle model is used to estimate it and is refered to in the block diagram presented in figure 6.1 as the side-slip angle observer.

To construct this controller various Artificial Intelligence (AI) technologies have been used. To obtain a background knowledge about these technologies please refer to section 3.4. Later in section 6.3 the exact control system designing technique will be detailed.

6.1.3 The braking force distributor

This module is a direct model that controls the braking force going to each of the front wheels. Based on the sign of the yaw moment M_z control signal at each instance, this model decides the particular wheel that shall receive the braking torque, such that the wheels don't receive conflicting signals which could lead the vehicle to become unstable.

6.1.4 Sideslip angle observer

This module is a linear simplified 3-DOF full vehicle model, that is used in the estimation of the side-slip angle [132] to substitute the lack of presence of a reliable sensor, as mentioned before. The 3-DOF model could be regarded as a reduced version of the 13-DOF model cited above, where the equations governing the longitudinal, the lateral and the yaw motions in the model are exactly like those of the 13-DOF model. Also, the respective tire forces in the x and y directions are similarly calculated through the Dugoff tire model. A detailed explanation of this model and a description of its guiding equations could be found in section 6.2.4.

6.1.5 The reference model

The driver tries to control the vehicle's stability during normal and moderate cornering from the steerability point of view. Therefore, the reference model reflects the desired relationship between the driver performance and the vehicle stability factors [9]. Hence, the model is designed to generate the desired values of the yaw rate and the side slip angle at each instance, according to the driver's steering wheel angle input and the vehicle speed, while considering a constant forward speed [133, 70, 125]. The desired side slip angle of the vehicle is tried to be maintained as closest as possible to zero [70, 32, 112], since a vehicle slipping to the sides is not a desired behavior.

$$\beta_d \simeq 0 \tag{6.1}$$

On the other hand, while cornering, the yaw rate cannot be assumed as zero. Instead, it has to have a value that depends on the front wheel inclination angle, the forward speed and the vehicle dimensions, and could be calculated as follows [125, 134, 70]:

$$r_d = \frac{U}{l\,(1 + A \cdot U^2)}\delta \tag{6.2}$$

where A is a stability factor taken as 0.005, l is the wheel base, and U is the longitudinal velocity.

6.2 Mechanical Models

In this section the mechanical models used to realize the simulation are described. Sections 6.2.1, 6.2.2 and 6.2.3 are together used to simulate the full Non-Linear Vehicle Model mentioned before. While section 6.2.4 explains how to get the 3-DOF vehicle model that's used to estimate the side-slip angle. In table 6.1 the naming and the values of the used constants can be found.

6.2.1 Full vehicle model

The full vehicle model includes both lateral and longitudinal dynamics, as well as the non-linearity in the vehicle model and a suspension model [102]. The degrees of freedom associated with this model are the longitudinal velocity, U, the lateral velocity, V, the yaw rate, r, the roll rate, p, the pitch rate, $\dot{\theta}$, the wheel rotational speeds, ω_{fl}, ω_{fr}, ω_{rl} and ω_{rr}, and the vertical motions for unsprung masses, z_{ufl}, z_{ufr}, z_{url} and z_{urr}, and for sprung mass, z_s. The equations of motion for the full vehicle model are derived from figure 6.2.

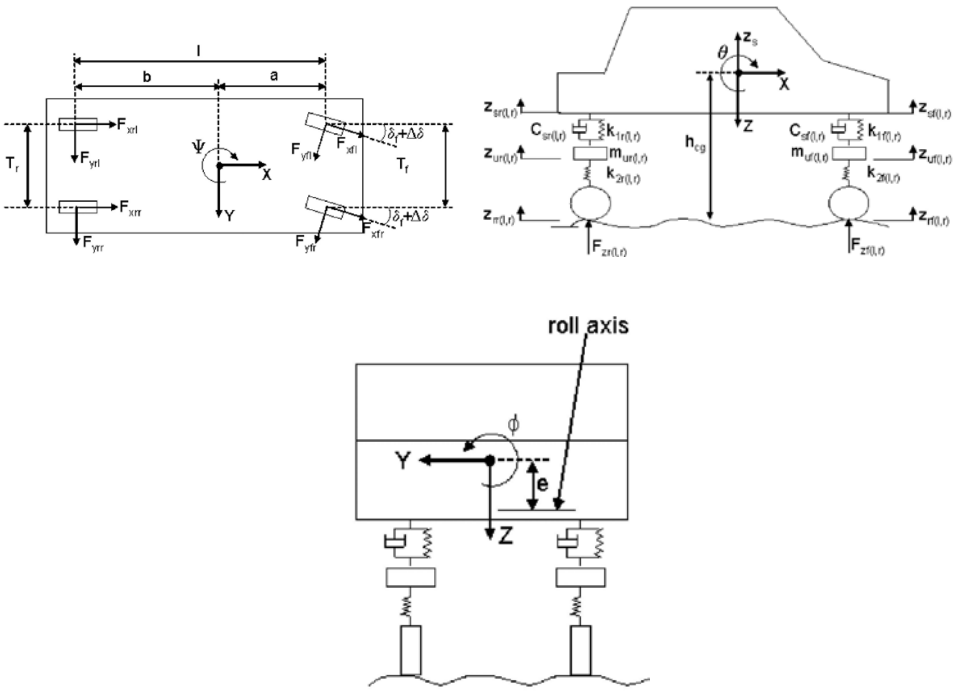

Figure 6.2: Parameter definition of the full vehicle model

where the longitudinal motion is represented by:

$$m \cdot \dot{U} = m \cdot V \cdot r + F_{xfl} + F_{xfr} + F_{xrl} + F_{xrr} \tag{6.3}$$

the lateral motion by:

$$m \cdot \dot{V} = -m \cdot U \cdot r - m_s \cdot e \cdot \dot{p} + F_{yfl} + F_{yfr} + F_{yrl} + F_{yrr} \tag{6.4}$$

the yaw motion by:

$$\begin{aligned} I_{zzs} \cdot \dot{r} = I_{xxs} \cdot \dot{p} + a(F_{yfl} + F_{yfr}) - b(F_{yrl} + F_{yrr}) \\ + \frac{T_f}{2}(F_{xfl} - F_{xfr}) + \frac{T_r}{2}(F_{xrl} - F_{xrr}) \end{aligned} \tag{6.5}$$

the roll motion by:

$$\begin{aligned} I_{xxs} \cdot \dot{p} = -m_s \cdot e \cdot \dot{V} - m_s \cdot e \cdot U \cdot r + I_{xzs} \cdot \dot{r} + m_s \cdot g \cdot e \cdot \phi \\ - \frac{T_f}{2}(F_{1fl} - F_{1fr}) - \frac{T_f}{2}(F_{1rl} - F_{1rr}) - K_\phi \cdot \phi - C_\phi \cdot \dot{\phi} \end{aligned} \tag{6.6}$$

where,

$$\dot{\phi} = p \tag{6.7}$$

and finally the pitch motion by:

$$I_{yys} \cdot \ddot{\theta} = a(F_{1fl} + F_{1fr}) - b(F_{1rl} + F_{1rr}) \tag{6.8}$$

The four wheels rotational motion is represented by:

$$I_w \cdot \dot{\omega}_i = T_i - R_w.F_{xi} \tag{6.9}$$

where i = fl, fr, rl and rr and T_i is the difference between the driving torque, T_d, and the braking torque, T_b, as follows:

$$T_i = T_{d_i} - T_{b_i} \tag{6.10}$$

The terms F_{xi} and F_{yi} represent the respective tire forces in the x and y directions, that can be related to the tractive and the lateral tire forces, denoted by F_{ti} and F_{si} respectively, and will be calculated later from the tire

model:

$$F_{xi} = F_{ti} \cdot \cos\delta_i - F_{si} \cdot sin\delta_i \tag{6.11}$$

$$F_{yi} = F_{ti} \cdot sin\delta_i + F_{si} \cdot \cos\delta_i \tag{6.12}$$

where δ_i is the steering angle including the roll steering, and is calculated by:

$$\delta_{fl} = \delta_{fr} = \delta_f + \Delta\delta_c + \phi \cdot K_{rsf} \tag{6.13}$$

$$\delta_{rl} = \delta_{rr} = \phi \cdot K_{rsr} \tag{6.14}$$

The presented full car model as well includes a quasi-static lateral and longitudinal load transfer. Thus, the normal load equation for each wheel can be expressed as:

$$F_{zi} = \left(m_{ui} + \frac{m_s b}{2l}\right) g - \frac{\left(\dot{U} - V \cdot r\right) h_{cg}}{g \cdot l} - F_{2i} \tag{6.15}$$

where i = fl and fr

$$F_{zi} = \left(m_{ui} + \frac{m_s a}{2l}\right) g + \frac{\left(\dot{U} - V \cdot r\right) h_{cg}}{g \cdot l} - F_{2i} \tag{6.16}$$

where i = rl and rr

The transformations from vehicle model to the global coordinates are given by:

$$\dot{X} = U \cdot \cos\psi - V \cdot sin\psi \tag{6.17}$$

$$\dot{Y} = -U \cdot sin\psi - V \cdot \cos\psi \tag{6.18}$$

where ψ is the yaw angle.

6.2.2 Suspension Model

The sprung mass is modeled by:

$$m_s \cdot \ddot{z}_s = -F_{1fl} - F_{1fr} - F_{1rl} - F_{1rr} \tag{6.19}$$

where

$$F_{1fl} = k_{1fl}(z_{sfl} - z_{ufl}) + c_{sfl}(\dot{z}_{sfl} - \dot{z}_{ufl}) - \frac{K_{af}}{T_f}\left(\phi - \frac{(z_{ufl} - z_{ufr})}{T_f}\right) \tag{6.20}$$

$$F_{1fr} = k_{1fr}(z_{sfr} - z_{ufr}) + c_{sfr}(\dot{z}_{sfr} - \dot{z}_{ufr}) + \frac{K_{af}}{T_f}\left(\phi - \frac{(z_{ufl} - z_{ufr})}{T_f}\right) \tag{6.21}$$

$$F_{1rl} = k_{1rl}(z_{srl} - z_{url}) + c_{srl}(\dot{z}_{srr} - \dot{z}_{url}) - \frac{K_{ar}}{T_r}\left(\phi - \frac{(z_{url} - z_{urr})}{T_r}\right) \tag{6.22}$$

$$F_{1rr} = k_{1rr}(z_{srr} - z_{urr}) + c_{srr}(\dot{z}_{srr} - \dot{z}_{urr}) + \frac{K_{ar}}{T_r}\left(\phi - \frac{(z_{url} - z_{urr})}{T_r}\right) \tag{6.23}$$

and

$$z_{sfl} = z_s - a \cdot \theta + \frac{T_f}{2} \cdot \phi \tag{6.24}$$

$$z_{sfr} = z_s - a \cdot \theta - \frac{T_f}{2} \cdot \phi \tag{6.25}$$

$$z_{srl} = z_s + b \cdot \theta + \frac{T_r}{2} \cdot \phi \tag{6.26}$$

$$z_{srr} = z_s + b \cdot \theta - \frac{T_r}{2} \cdot \phi \tag{6.27}$$

and the unsprung mass is modeled by:

$$m_{ui} \cdot \ddot{z}_{ui} = F_{1i} - F_{2i} \tag{6.28}$$

where i = fl, fr, rl and rr.

$$F_{2i} = k_{2i}(z_{ri} - z_{ui}) \tag{6.29}$$

6.2.3 Tire Model

In this work, the Dugoff model [125] is used to simulate the lateral and longitudinal forces generated by the tires. The Dugoff model was chosen due to its low requirement of computational effort and because it is a function of physical parameters. According to the full vehicle model, each wheel has an independent slip angle and hence can be represented as follows:

$$\alpha_{fl} = \delta_{fl} - \arctan\left(\frac{V + a \cdot r}{U - 1/2 \cdot T_f \cdot r}\right) \tag{6.30}$$

$$\alpha_{fr} = \delta_{fr} - \arctan\left(\frac{V + a \cdot r}{U + 1/2 \cdot T_f \cdot r}\right) \tag{6.31}$$

$$\alpha_{rl} = \delta_{rl} - \arctan\left(\frac{b \cdot r - V}{U - 1/2 \cdot T_r \cdot r}\right) \tag{6.32}$$

$$\alpha_{rr} = \delta_{rr} - \arctan\left(\frac{b \cdot r - V}{U + 1/2 \cdot T_r \cdot r}\right) \tag{6.33}$$

and the longitudinal wheel slip can be defined as:

$$S_i = \left|\frac{R \cdot \omega_i - u_i}{u_i}\right| \tag{6.34}$$

where the ω_i is the wheel rotational speed and the u_i is the velocity component in the wheel plane, given by:

$$u_{fl} = \left(U + \frac{T_f \cdot r}{2}\right)\cos\delta_{fl} + (V + a \cdot r)sin\delta_{fl} \tag{6.35}$$

$$u_{fr} = \left(U - \frac{T_f \cdot r}{2}\right)\cos\delta_{fr} + (V + a \cdot r)sin\delta_{fr} \tag{6.36}$$

$$u_{rl} = \left(U + \frac{T_r \cdot r}{2}\right)\cos\delta_{rl} - (b \cdot r - V)sin\delta_{rl} \tag{6.37}$$

$$u_{rr} = \left(U - \frac{T_r \cdot r}{2}\right)\cos\delta_{rr} - (b \cdot r - V)sin\delta_{rr} \tag{6.38}$$

Neglecting the self-aligning moment, the tractive and the side tire forces, are determined by:

$$\lambda = \frac{\mu \cdot F_{zi}\left[1 - \varepsilon_r \cdot u_i\sqrt{S_i^2 + \tan^2\alpha_i}\right](1 - S_i)}{2\sqrt{C_i^2 \cdot S_i^2 + C_\alpha^2 \cdot \tan^2\alpha_i}} \tag{6.39}$$

$$f(\lambda) = \begin{cases} \lambda(2-\lambda) & \lambda < 1 \\ 1 & \lambda \geq 1 \end{cases} \tag{6.40}$$

$$F_{si} = \frac{C_\alpha \cdot \tan \alpha_i}{1 - S_i} f(\lambda) \tag{6.41}$$

$$F_{ti} = \frac{C_i \cdot S_i}{1 - S_i} f(\lambda) \tag{6.42}$$

6.2.4 3-DOF Vehicle Model

This is a simple and linear full vehicle model with only 3-DOF, and is solely used for the estimation of the side-slip angle. This model could be described as a reduced version of the full vehicle model explained above and could be described by figure 6.3.

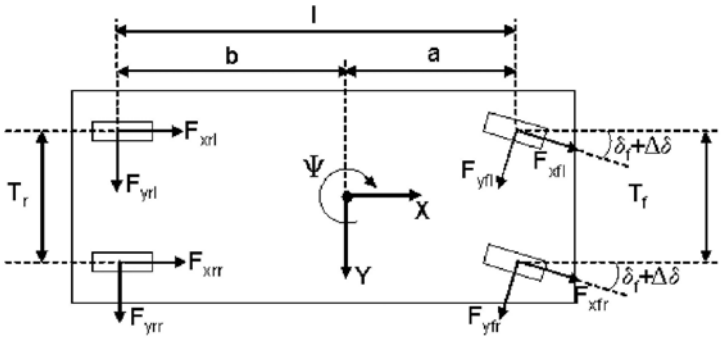

Figure 6.3: Parameter definition of the 3-DOF model

The equations governing the longitudinal, the lateral and the yaw motions of the vehicle model can be expressed as follows [132]:

$$m \cdot \dot{U} = m \cdot V \cdot r + F_{xfl} + F_{xfr} + F_{xrl} + F_{xrr} \tag{6.43}$$

$$m \cdot \dot{V} = -m \cdot U \cdot r - m_s \cdot e \cdot \dot{p} + F_{yfl} + F_{yfr} + F_{yrl} + F_{yrr} \tag{6.44}$$

$$\begin{aligned} I_{zzs} \cdot \dot{r} = I_{xxs} \cdot \dot{p} + a(F_{yfl} + F_{yfr}) - b(F_{yrl} + F_{yrr}) \\ + \frac{T_f}{2}(F_{xfl} - F_{xfr}) + \frac{T_r}{2}(F_{xrl} - F_{xrr}) \end{aligned} \tag{6.45}$$

and the respective tire forces in the x and y directions, F_{xi} and F_{yi}, can be obtained from equations:

$$F_{xi} = F_{ti} \cdot \cos \delta_i - F_{si} \cdot sin\delta_i \tag{6.46}$$

$$F_{yi} = F_{ti} \cdot sin\delta_i + F_{si} \cdot \cos\delta_i \tag{6.47}$$

Where F_{xi} and F_{yi} represent the respective tire forces in the x and y directions, that can be related to the tractive and the lateral tire forces, denoted by F_{ti} and F_{si} respectively,that can be similarly calculated from the Dugoff tire model explained before in section 6.2.3.
The side-slip value of this model can be easily calculated as:

$$\beta = \tan^{-1}\frac{V}{U} \tag{6.48}$$

Var	Information and value
a	distance of the center of gravity from the front axle = 1 m
A	stability factor = 0.005
b	distance of the center of gravity from the rear axle = 1.454 m
C_i	longitudinal stiffness of one tire = 52.526 kN/unit slip
C_{sfj}	left/right front suspension damping constant = 1.57 kN.s/m
C_{srj}	left/right rear suspension damping constant = 1.76 kN.s/m
C_α	cornering stiffness of one tire = 29 kN/rad
C_ϕ	roll axis torsional damping = 3511.6 N.m/rad.s
E	distance of the sprung mass center of gravity from the roll axes = 0.4572 m
g	gravity = 9.81 m/s^2
h_{cg}	height of the sprung mass center of gravity = 0.533 m
I_w	wheel moment of inertia = 2.1 $kg.m^2$
I_{xxs}	vehicle inertia moment about the roll axis = 489.9 $kg.m^2$
I_{yys}	vehicle inertia moment about the pitch axis = 1058.4 $kg.m^2$
I_{zzs}	vehicle inertia moment about the yaw axis = 1627 $kg.m^2$
k_{1fj}	left/right front suspension spring stiffness = 20.6 kN/m
k_{1rj}	left/right rear suspension spring stiffness = 15.2 kN/m
k_{2fj}	left/right front tire spring stiffness = 138 kN/m
k_{2rj}	left/right rear tire spring stiffness = 138 kN/m
k_{af}	front anti-roll bar stiffness = 6.695 kN m/rad
k_{ar}	rear anti-roll bar stiffness = 6.695 kN m/rad
k_{rsf}	front roll steer coefficient = 0.2 rad/rad
k_{rsr}	rear roll steer coefficient = 0.2 rad/rad
k_ϕ	roll axis torsional stiffness = 66185.8 N.m/rad
m	vehicle total mass = 1298 kg
m_s	vehicle sprung mass = 1167.5 kg
m_{ufj}	left/right front unsprung mass = 26.5 kg
m_{urj}	left/right rear unsprung mass = 24.4 kg
R_w	wheel radius = 0.305 m
T_f	front track width = 0.718 m
T_r	rear track width = 0.718 m
ε_r	road adhesion reduction factor = 0.015 s/m
μ	nominal friction coefficient between tire and ground = 0.9 and 0.5

Table 6.1: Vehicle's parameters

6.3 Control System

The proposed control system needs to be constructed on different phases. As discussed before, we intend to replace the expert's knowledge-based control system by an intelligent auto-generated self-tested system, to avoid the human-error. So, the first phase is running the automated algorithm, which on its turn generates the data, chooses the best answer for a set of conditions and finally stores them in a database. The logic behind the algorithm, its implementation and the characteristics of the database that the algorithm generates are discussed in section 6.3.1. Afterward, section 6.3.2 presents a discussion of the Artificial Neural Network (ANN) used to learn from the automatically generated database, by finding correlations among these data in a data mining fashion. Also, the auto constructed Fuzzy Logic Control (FLC) based on the learned correlations, is explained at this point. Finally, section 6.3.3 provides a brief explanation of the system in its operational phase, relating to the modules interrelation from section 6.1.

6.3.1 Automated Data Generation Algorithm

To be able to construct the ANFIS control system, a generous random sample of optimum control values is needed. These control values are then used by the neural network to auto-construct the fuzzy-based controller, such that the new controller would mimic the behavior of the learned values. Nevertheless, in a problem like the one addressed in this paper, this needed data cannot be generated from experimental data, due to the safety criticality of the test and the absence of an instantaneous evaluator that decides the best control decision made at each instance. For these reasons, an algorithm was proposed to search for the optimal values by directly testing the vehicle mathematical model simultaneously, while searching the space of variables.

To achieve this, at first the designed algorithm replaces the 'control system', described in figure 6.1, such that it takes as input the yaw rate r and the side-slip angle β values, both the current and the desired. Accordingly, it tries to guess the best values for the steering correction $\Delta\delta$ and the yaw moment M_z by increasing/decreasing one while fixing the value of the other, and evaluating the input errors that are calculated as:
e(β) = β - β_d

e(r) = r - r_d
where β_d and r_d are calculated by the 'reference model' see figure 6.1 and through equations 6.1 and 6.2, respectively.
The algorithm runs this procedure various times along the training maneuver, choosing equally distributed time slices. At each slice of which the situation is frozen to be studied by the algorithm and to find a control decision for it. Once a control decision is chosen, the algorithm store it as a quadruple of {e(β), e(r), M_z, $\Delta\delta$} in a database for later use. The maneuver used in the data generation of the proposed system was a slowly increasing curve initiating from zero, and the frozen instances studied by the algorithm where 10,000 instance for each curve.

The algorithm is an offline learning algorithm, so the algorithm complexity only affects the pre-learning phase and not the real-time response. Nevertheless, to speed up the training phase and minimize the algorithm search space, since the controller from [70] showed good results. Therefore, that controller decision value was taken as the initial value, that from which the search task begins. To guarantee that the results from [70] won't delimit the new results, experiments on random time samples have been made comparing the results from the algorithm when its search initiating at zero and when it initiates from the other controller values and both were found to be equal.

A simplified summarization of the algorithm can be explained as follows. Initially, the algorithm fixes the M_z and starts to vary the $\Delta\delta$ and testing its effect on the car performance, then it switches the operation to vary the M_z while fixing the $\Delta\delta$ till the best control combination is found. The variation of the $\Delta\delta$ before that of M_z helps to avoid the use of M_z whenever possible so that the drawback of ESC in reducing the car longitudinal speed is averted. The best control decision of each driving situation is then stored in a database.

The state diagram of the presented algorithm is shown in 6.4, where its six states are carried out on each of the 10,000 time-slices mentioned above. Where lots of test cases has been put to experiment, from very complicated maneuvers to the easiest ones, to secure covering all the maneuvers that a car can get through. These six states are described as:
At each time instance do the following:

1. • Get the fuzzy controller decision {err(β), err(r), $\Delta\delta$, M_z} and store it as a reference and as the best-so-far values.

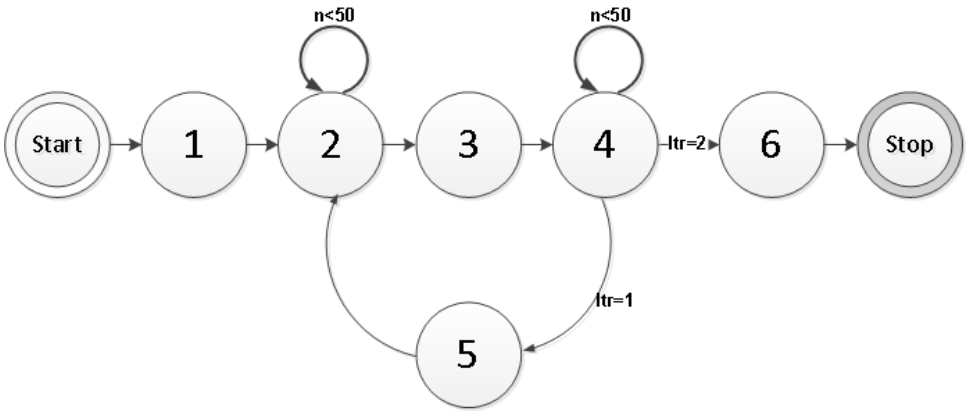

Figure 6.4: Algorithm's state diagram

- Set the new M_z and $\Delta\delta$ values to the fuzzy controller reference values.
- Set Itr to 1.

2.
- If Itr is 1, THEN set Var to $\Delta\delta$, ELSE set Var to M_z
- Increase the Var value and test the car response.
- If the yielded values of err(β) and err(r) were lower than the best-so-far values.
  - THEN: Set best-so-far values to the new yielded values.

3.
- Reset M_z and $\Delta\delta$ values (Var) to reference -to avoid repetition.
- Reset n to 0.

4.
- Decrease the Var value and test the car response.
- If the yielded values of err(β) and err(r) were lower than the best-so-far values.
  - THEN: Set best-so-far values to the new yielded values.

5.
- Reset M_z and $\Delta\delta$ values (Var) to reference.
- Reset n to 0.
- Set Itr to 2

6.
- Store best-so-far 4-tuple values {err(β), err(r), $\Delta\delta$, M_z} in the database of the best control decisions.

Figure 6.5 shows a detailed flow chart of the algorithm steps. The stopping condition referred to in this figure, is the condition that prevents the searching algorithm from entering in an infinite loop as well as it tries to minimize the search space and prevent the algorithm from getting stuck in a local minimum. The stopping condition applies the follows:

- If new e(β) and e(r) are worse than the best e(β) and e(r), allow searching in this direction for only n-more steps as it remains worse, if the performance didn't change until this step, then stop searching in this direction.
- If new e(β) and e(r) are equal to the best e(β) and e(r), allow searching in this direction for only n-more steps as it remains equal, if the performance didn't change until this step, then stop searching in this direction.
- Each time the given direction yields a better performance, it resets the n counter.

In the results presented in this thesis, the n-value was considered as 50 steps. The algorithm as well supports a feature, that gives different weights to each of the evaluation parameters.

In this manner, unlike the manually constructed system from [70], this automated algorithm allows to collect extensive data about the behavior of the vehicle model to assure the credibility and reliability of the controller. For this reason, the more the generic the maneuver could be and the more time slices that are studied, the more the collected data can describe the system behavior accurately. At this point, all the collected data are stored in the previously mentioned database, which will be used by the ANFIS in the learning of the control system to construct a control system that mimics the behavior described by these data, as it will be explained in section 6.3.2.

This algorithm seems to be propitious in controlling various nonlinear controllers due to its generic method and its capabilities to generate offline training data and learn from it without a previous knowledge of the system behavior. Such that, by only knowing the required control inputs and its range of input values, along with the expected control outputs and an error function, the algorithm can then build up a control system with minimal human interference. For instance, the algorithm was tested on a semi-active suspension system, the aim of this study was to improve the safety and the riding

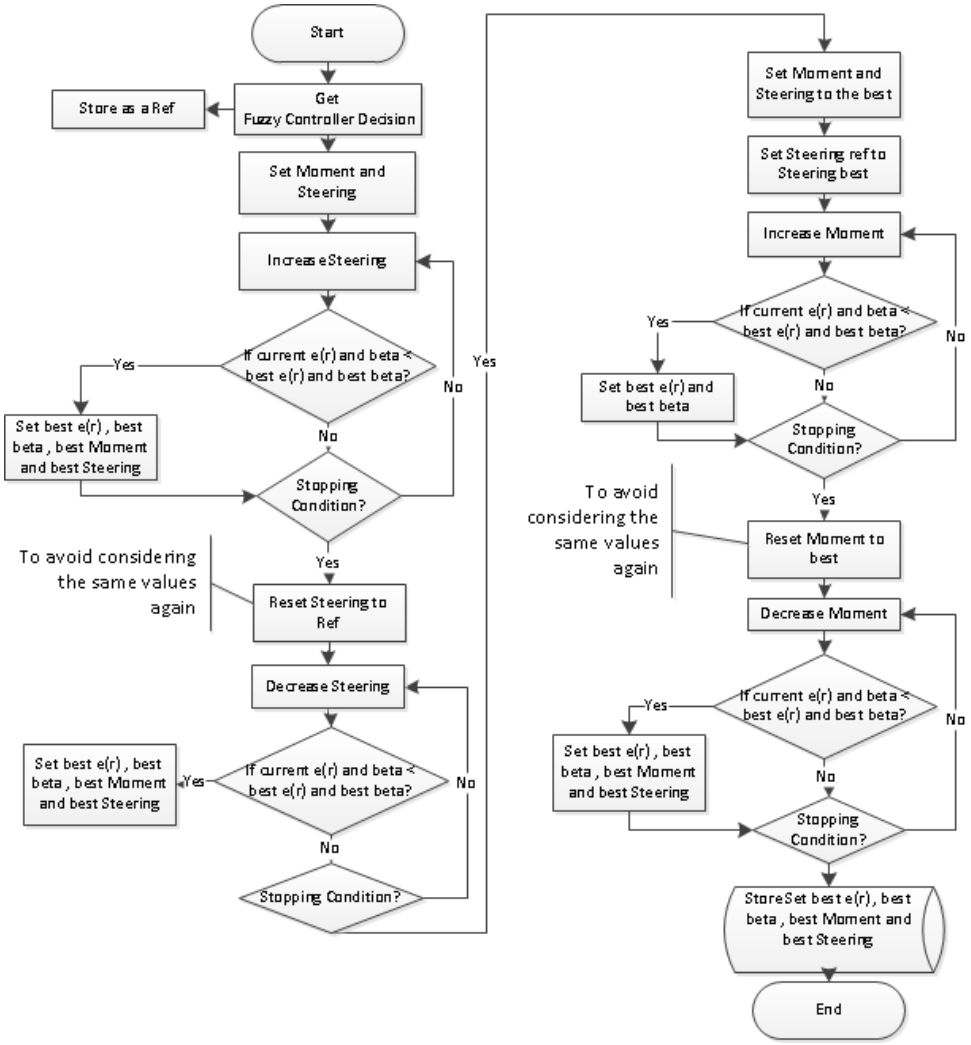

Figure 6.5: Algorithm's flow chart

comfort of passenger vehicles to assure a better riding experience [135]. In that study, the algorithm was meant to find the optimum controlling force f_a that gives the minimum possible values of the vertical acceleration of the sprung mass, the suspension's deflection and the tire's deflection. Simulation results showed a noticeable improvement made by the proposed controller in comparison to the uncontrolled suspension and another controller from [14]. A detailed explanation of this model will be later described in chapter 8.

6.3.2 The ANFIS controller

Once the learning data is ready, we can introduce the database to the Artificial Neural Networks (ANNs) to construct the Fuzzy Logic Control (FLC).

The technology that facilitates this process is called Adaptive Neuro-Fuzzy Inference System (ANFIS) [136]. ANFIS provides a type of ANNs that can learn from a given Inference System, in this case the database constructed in section 6.3.1, and with a minimal human help it can choose the suitable ANN parameters, and hence can automatically construct a FLC that is able to perform like the learned data. The use of ANFIS also allows to benefit from the learning and auto-adaption of an ANN with its ability of generalization, pattern recognition and noise avoidance. While profiting from the smooth controlling performance, fast decision making, efficiency in energy consumption and simplicity of integration provided by the FLC [114, 113]. Detailed explanation of these techniques is provided in section 3.4.

In the presented work, we used the MATLAB ANFIS toolbox to train the ANN and construct the FLC controller. The database that was used to train the ANN contained 10,000 quadruple sets, all collected by the previously explained algorithm. These data were then divided in 3 groups, estimation, validation and testing in the ratio of 2:1:1 respectively, such that each 4 consecutive quadruple sets would be distributed on the three mentioned groups to assure the inclusion of the different system behavior in each group. The network then was trained cycle by cycle on the training data and its performance was checked on the validation set, while the testing set is to prevent the learning algorithm to fall in a global minima, by a technique known as the "early stopping" and is integrated in the MATLAB's ANFIS library.

Unlike the FLC presented in [70] that uses the Mamdani's fuzzy inference method [124], ANFIS uses a Takagi-Sugeno (TS) fuzzy inference method [123]. TS is a more compact and computationally more efficient than the Mamdani system, furthermore, it is more flexible to the use of adaptive techniques. But on the other hand, the Mamdani system is more intuitive and understandable by the human side [113], yet this point will not affect the proposed approach since it only needs minimal human intervention.

The used ANFIS library only generates single-output control systems for efficiency reasons. Therefore a small change was made to the control system design, it is now divided into two FLCs with the same pair of input signals, one FLC is to control the M_z while the other is for controlling the $\Delta\delta$, see figure 6.6. To adapt the data to form two control systems the quadruples from the database are divided into triple sets of $\{e(\beta), e(r), \Delta\delta\}$ and $\{e(\beta), e(r), M_z\}$ to

construct the Steering FLC and the Moment FLC, respectively. Nevertheless, this division doesn't affect the integration approach, since the data-generation and the learning phases were realized as a two-inputs two-outputs process.

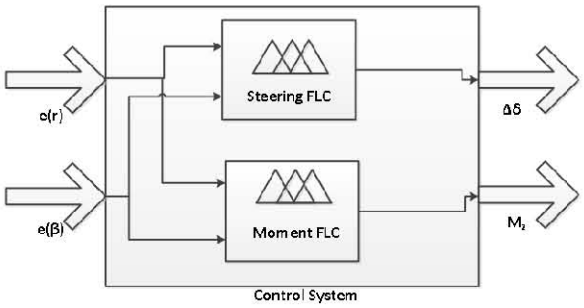

Figure 6.6: The two FLCs that makes up the new control system

Before the ANN is used, a clustering algorithm is applied on the data to help divide it into subsets of approximate behavior. We have used the clustering option provided by the MATLAB ANFIS library that uses the clustering method in deciding the initial characteristics of the FLCs before they are tuned by the ANN. The clustering method used on the Steering data sets was adjusted to have a range of influence of 0.2, a squash factor of 1.25 an accept ratio of 0.1 and a reject ratio of 0.015, more details on the used functions and the effect of these values can be found in [137].

This run yielded the construction of a 30 Gaussian input MFs, 15 MFs for each of the two inputs, 15 rule and 15 constant output MFs. Consequently, the ANN used to tune this FLC had 30 neurons in the input layer, divided by half between the two inputs and each neuron is associated to one of the input MFs; 15 neurons in the hidden layer, each of which corresponds to one of the rules; and 15 neurons in the output layer, to match the 15 output MFs, see figures . The neural networks used to construct the steering and moment controllers are illustrated in figures 6.7 and 6.8, respectively.

The ANN was then trained for 20 epochs by a hybrid training method with zero error tolerance. The performance of the tuned Steering FLC on the training data can be seen in figure 6.9, where the black 'o's are the testing data that the system should follow and the gray '*'s are the output of the control system. Similarly, the clustering method was applied on the Yaw Moment data sets, with a range of influence of 0.1, a squash factor of 1.25 an accept ratio of 0.1 and a reject ratio of 0.015. The run yielded the construction of a 64 Gaussian input MFs, 32 MFs for each input, 32 rule and 32 constant output

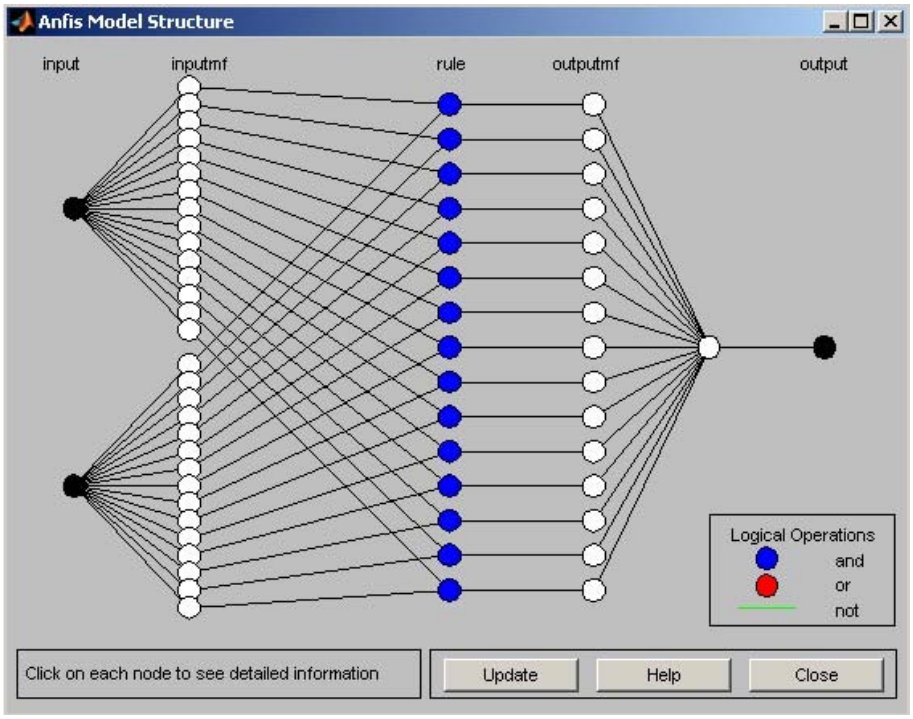

Figure 6.7: ANN model structure to construct the steering controller

MFs. Also the number of neurons in the constructed ANN matched the number of MFs in the same way like the previous ANN, and the ANN was trained for 20 epochs by a hybrid training method with zero error tolerance, as well. The performance of the tuned Moment FLC on the training data is also shown in figure 6.10. Also figures 6.11 and 6.12 show the surface representation of the moment and steering controllers output. Where $input1$ refers to the yaw rate $e(r)$ input and $input2$ refers to the side-slip angle $e(\beta)$ input and the $output$ refers to the steering correction $\Delta\delta$ or the yaw momen correction M_z, respectively.

The selection of the parameters of the clustering algorithm and the training method of the ANN was based on trial and error since it depends mainly on the characteristics of the training data, also the parameter of the clustering algorithm had to be chosen carefully as not to construct excessive number of MFs, because the greatest the number of the membership functions the higher the complexity of the system. Finally, the number of training epochs was chosen by the aid of the early stopping algorithm to prevent the ANN from over-learning and hence falling in a global minima.

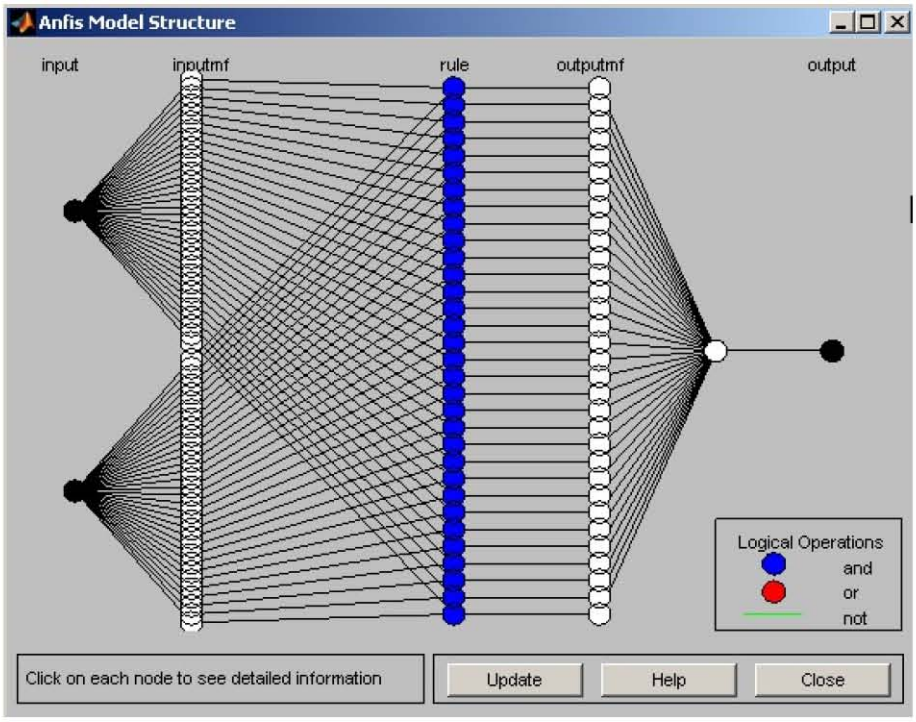

Figure 6.8: ANN model structure to construct the moment controller

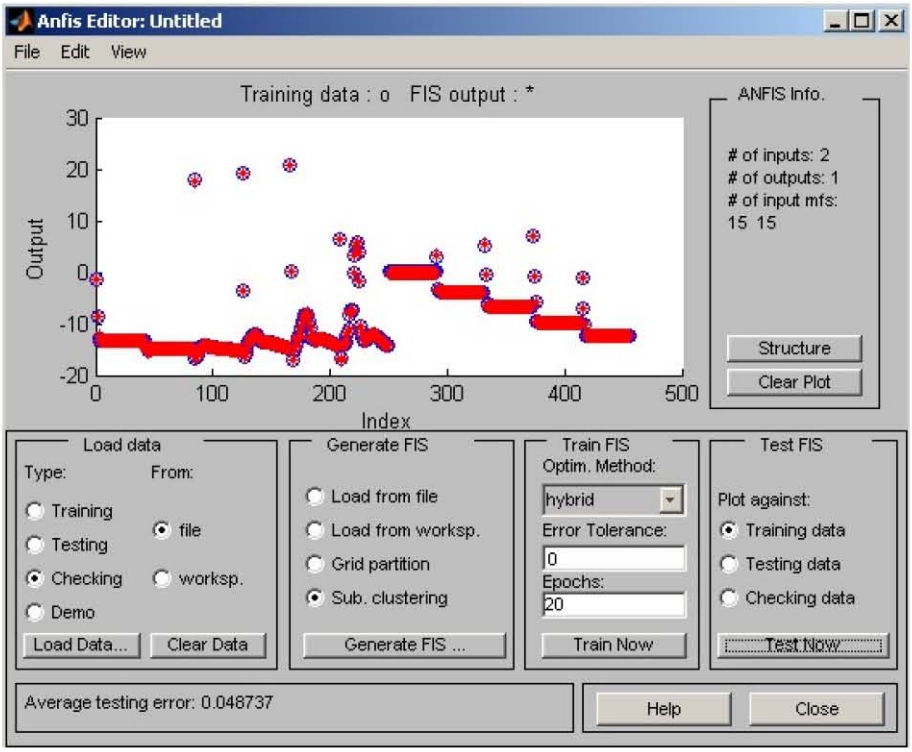

Figure 6.9: Performance of the steering controller after learning the data sets

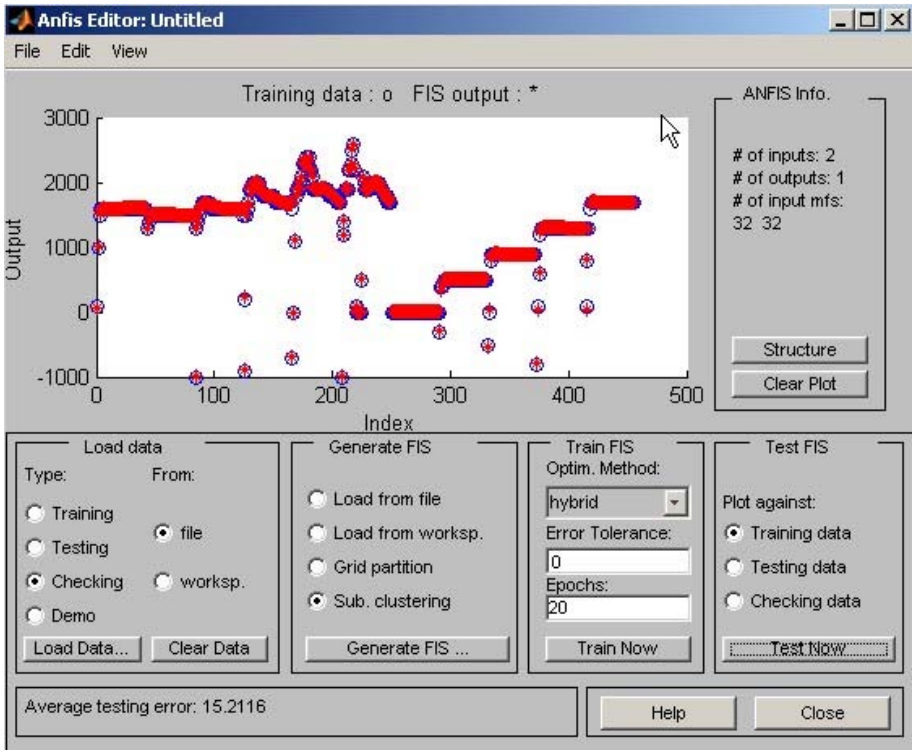

Figure 6.10: Performance of the moment controller after learning the data sets

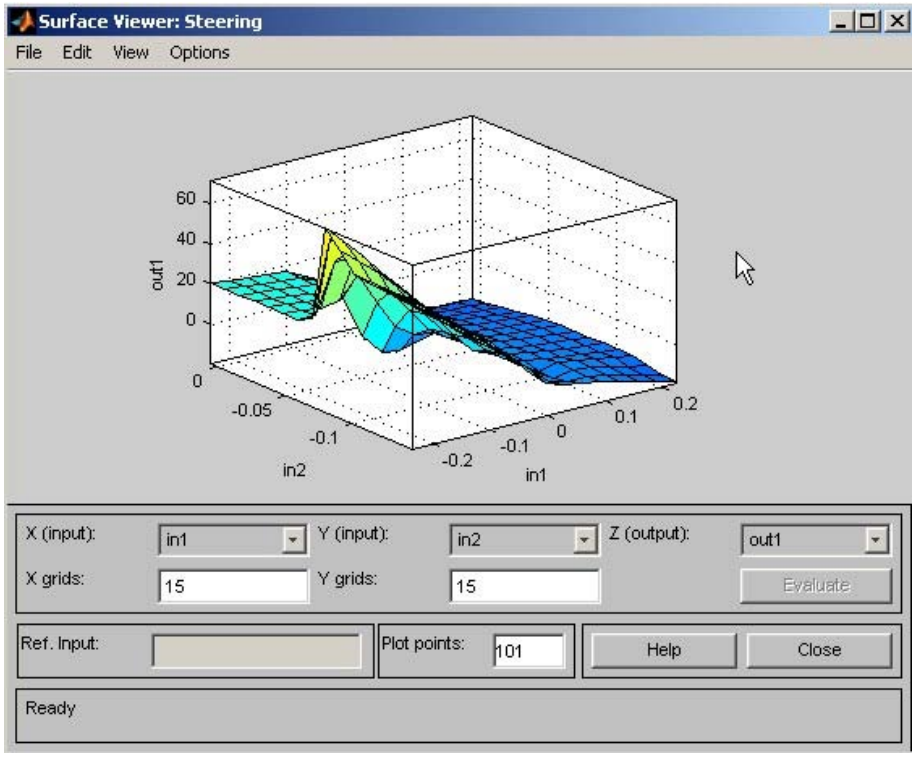

Figure 6.11: Surface representation of the steering controller output

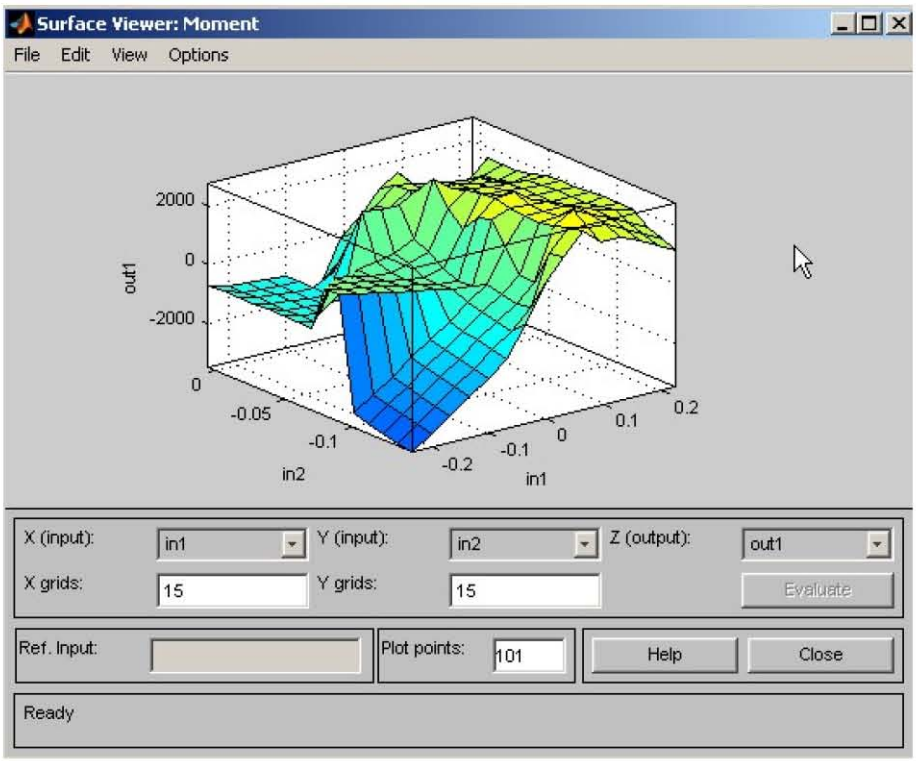

Figure 6.12: Surface representation of the moment controller output

6.3.3 Operational mode

After constructing the FLCs, they are both placed in the 'Control System' from Figure6.1, such that, both FLCs are connected to the two input lines and the output of each is connected to one of the output lines, as shown in Figure6.6. To simulate the results of the proposed model, the mechanical models were implemented using MATLAB SIMULINK simulation software, as seen i n figure 6.13

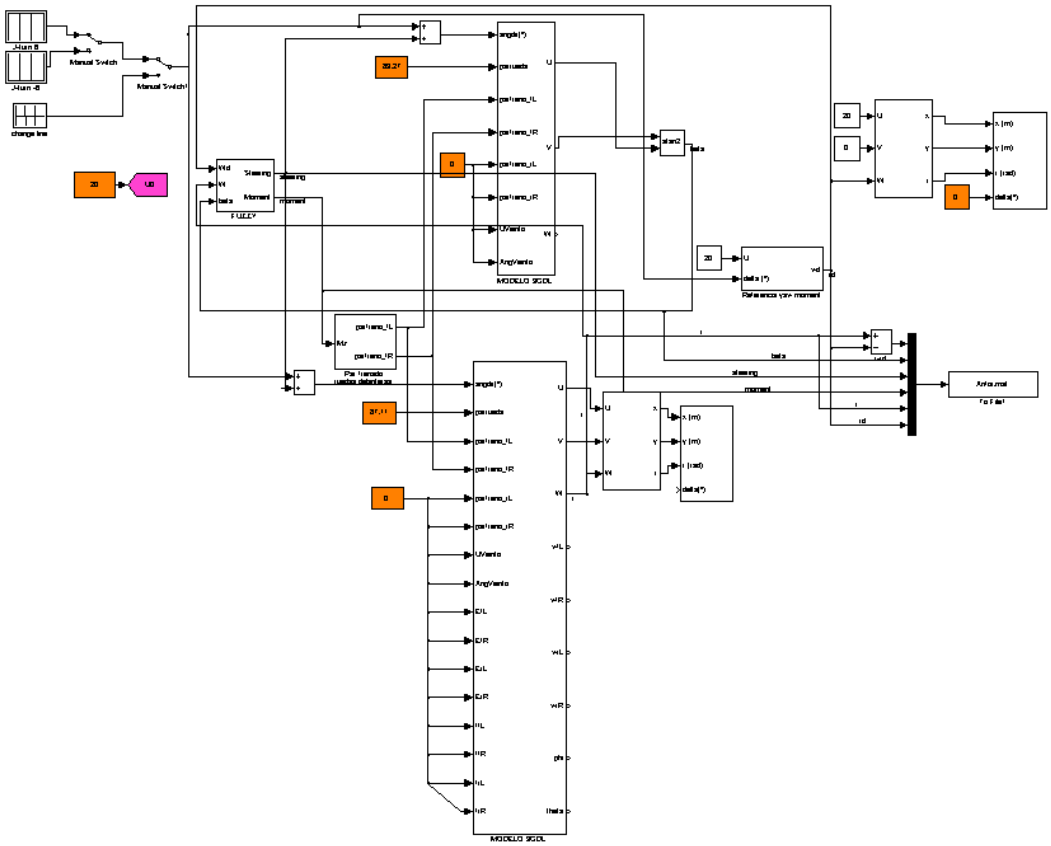

Figure 6.13: Simulink model overview

Obviously running the proposed algorithm in real-time instead of the controller, or storing the database yielded by an offline run of the algorithm and then retrieving it with a search algorithm whenever needed would also yield the same control output. Nevertheless, such solutions are infeasible in a real-time system, especially in a vehicle, where the speed of decision taking is very crucial. This is due to, that the two mentioned solutions would require entering in recursive procedures till they find the right control decision, especially the option of running the algorithm online since it needs to enter

through the vehicle models calculations. While, FLC would only go through a direct three-step calculation of: "Fuzzification", "Decision calculation" and "Defuzzification" providing a quick online response, more details about the FLC calculation can be found in [123]. Furthermore, from the point of space complexity, the solution of storing a database of 10,000 quadruples would need a much bigger space than that required by the FLC to store its MFs and rules, and hence the FLC will generate less complexity at the time of implementing the controller on a real vehicle embedded system. For these reasons, the ANFIS system proves to be a good solution for the given program as it has the ability to convert the big database into a relatively-compact FLC controller.

Chapter 7

Integrated controller results

This chapter presents the simulation results of the integrated vehicle dynamics controller presented in chapter 6. As mentioned before to simulate the results of the proposed model, the vehicle mechanical models were implemented using MATLAB SIMULINK simulation software. The values that define the simulated vehicle characteristics are to be found in table 6.1. The presented algorithm was written in MATLAB m-code and the ANFIS, the ANN and the FLCs were constructed through the MATLAB libraries.

To simulate the proposed controller efficiency various maneuvers where carried out, these maneuvers are the most widely used in the literature to judge the efficiency of the lateral stability controllers. At the beginning the controller is tested in dry weather with a tire-road friction coefficient $\mu = 0.9$, in section 7.1, while negotiating three different maneuvers; a J-turn, a change lane and a consecutive double change lane. The curves described by each of the maneuvers are considered as severe curves especially at the testing speeds, that are 20 m/s and 30 m/s, in other words, 72 and 108 km/h respectively. Afterward, the controller is tested in a more complicated weather condition, in section 7.2, which is in a snowy weather that reduces the tire-grip and the friction coefficient decreases to $\mu = 0.5$. In this road condition the system is tested on the same maneuvers mentioned above but only on a velocity of 20 m/s.

An extremely important aspect of the proposed controller is that the system training maneuvers are completely different from the testing maneuvers, which proves the generic property of the control system. The training maneuver was a steering wheel turn starting at zero and gradually increasing,

while the testing was carried on the maneuvers mentioned above.

For the clarity of the results demonstration, each test case is presented as a comparison between three identical vehicle models one with the presented ANFIS control system deployed in it, the second is controlled by an FLC controller presented in [70] and the third is a passive vehicle without any control systems. The trajectories made by the three vehicles are then compared against a devised line that simulates the desired trajectory.

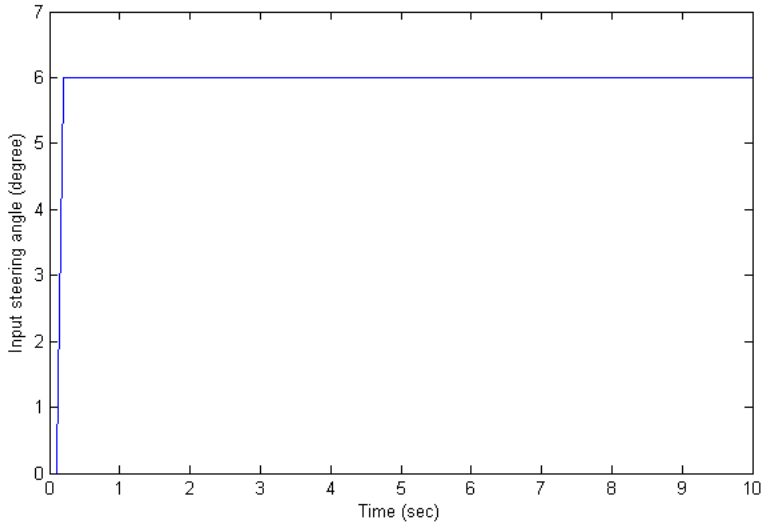

Figure 7.1: Steering input of the J-turn maneuver

This desired trajectory is obtained by substituting the desired values in the variables of these equations:

$$\dot{X} = U \cdot \cos\psi - V \cdot sin\psi \tag{7.1}$$

$$\dot{Y} = -U \cdot sin\psi - V \cdot \cos\psi \tag{7.2}$$

These equations allow to get a transformation of the desired vehicle movements in the global coordinates. Where U, the longitudinal velocity, is fixed to the target speed value (20 or 30 m/s in this case), V, the lateral velocity, is fixed to zero and ψ, the yaw angle, is given as the integration of the desired yaw rate calculated in equation 6.2. The other vehicles trajectories are also simulated using the same equations with the only difference of that the variables are substituted with the real-time values given by the mathematical model of each vehicle, see section 6.2. Finally, the control signals decided by

the ANFIS-controller and the FUZZY-controller for each of the trajectories are shown.

The results of each of the described maneuvers will be discussed along the chapter. Furthermore, an overall discussion of the obtained results will be presented in section 7.3 and Root Mean Squared Deviation (RMSD) comparing tables are provided in appendix B.

7.1 Dry road conditions

In this section the four trajectories of the Anfis-controlled vehicle, the FLC-controlled vehicle, the passive vehicle and the reference values will be studied. Through evaluating the vehicles performance on the J-turn maneuver, the change lane maneuver and the double change lane maneuver described in figures 7.1, 7.2 and 7.3 respectively. The first graph presents an elongated turn of 6° in the front wheels inclination along the simulated time in the x-axis. While the next figure is a two consecutive wheels inclination of 6° in one direction followed by another in the opposite direction that presents a rapid change of the driving lane. The last figure could be described as two changing lanes maneuvers, each in a different direction, such a maneuver is most commonly used to avoid obstacles. In this section all the three maneuvers will be tested with vehicle initial velocities of 20 and 30 m/s. Table 7.1 shows the RMSD values of the three comparative aspects, while tables B.1 and B.2 extend the comparison to the maximum and minimum reached values.

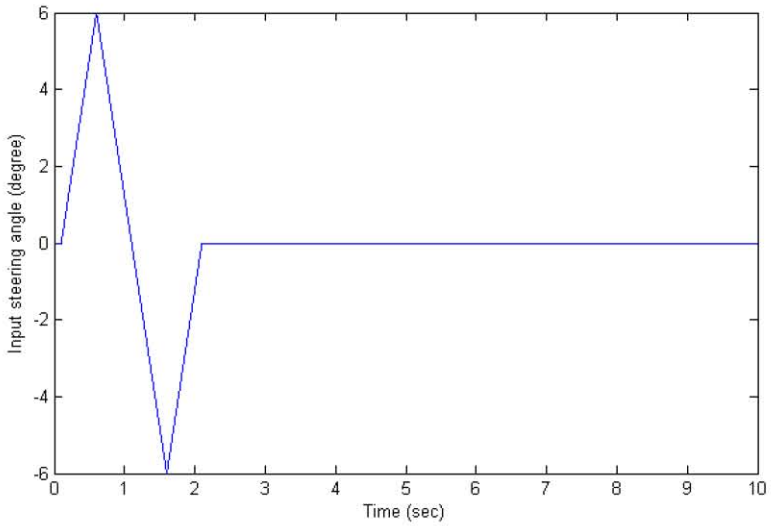

Figure 7.2: Steering input of the change lane maneuver

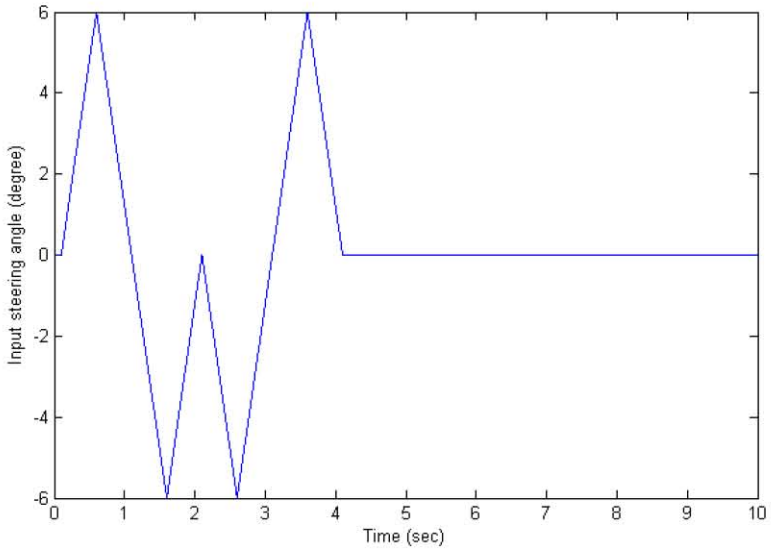

Figure 7.3: Steering input of the double change lane maneuver

7.1.1 J-turn maneuver

Figure 7.4 shows the trajectory made by the three vehicles and the calculated desired path while taking the J-turn maneuver at a speed of 20 m/s. In this figure, as well as in the following ones, the ANFIS-controlled, FUZZY-controlled, the uncontrolled and the desired path are referred to as: ANFIS, Fuzzy, Uncontrolled and Reference, respectively. As seen from figure 7.4, the

Fuzzy Controlled Vehicle (FCV) starts drifting to the right of the reference even more than the ANFIS Controlled Vehicle (ACV) and then to the left with a bigger error than that of the ACV again. Also it draws a shorter trajectory than that drawn by the ACV in the same given time, which means that the FCV brakes more and therefore travels with a slower velocity. This performance is also reflected in the RMSD of the trajectories from the desired path shown in 7.1 and the maximum deviation distance in both the X and Y directions shown in table B.1.

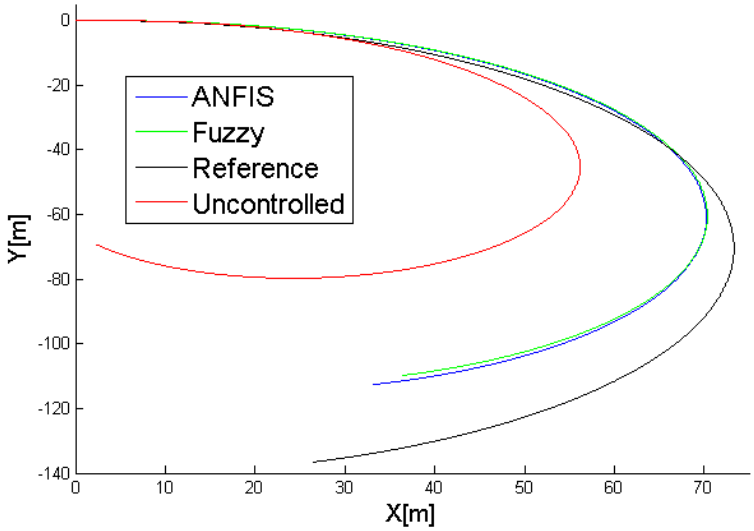

Figure 7.4: J-turn simulation at a speed of 20 m/s

This behavior can be better evaluated by comparing the errors of the yaw rate and Side-slip angle made by both cars, shown in figures 7.5 and 7.6 respectively. As can be seen, the difference between the yaw rate error of each is almost negligible, as shown in the RMSD comparison in tables 7.1 and B.1. Especially as the graph stabilizes after the first second. Yet the Side-slip difference between both explains the instability noticed in the FCV's maneuver, especially in the increase and then the sudden decrease. Due to the fact that the tracked error is accumulative in the way that as the car drifts more, this drifting will affect its previous already drifted position. Hence, a smooth decrease of the error value or a stabilization of it promotes a stable movement while a sudden change promotes instability and discomfort, as shown in figure 7.6.

Figures 7.7 and 7.8, shows the correcting steering signal $\Delta\delta$ and yaw

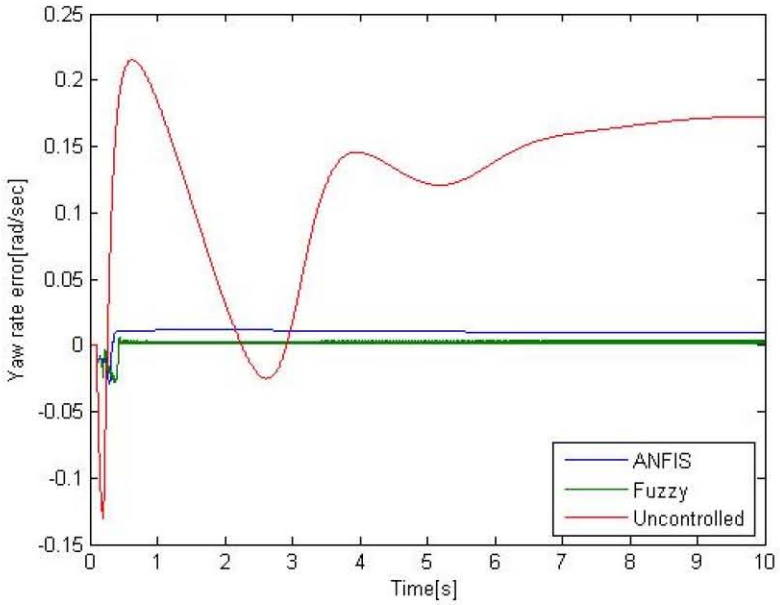

Figure 7.5: J-turn error of yaw rate at 20 m/s

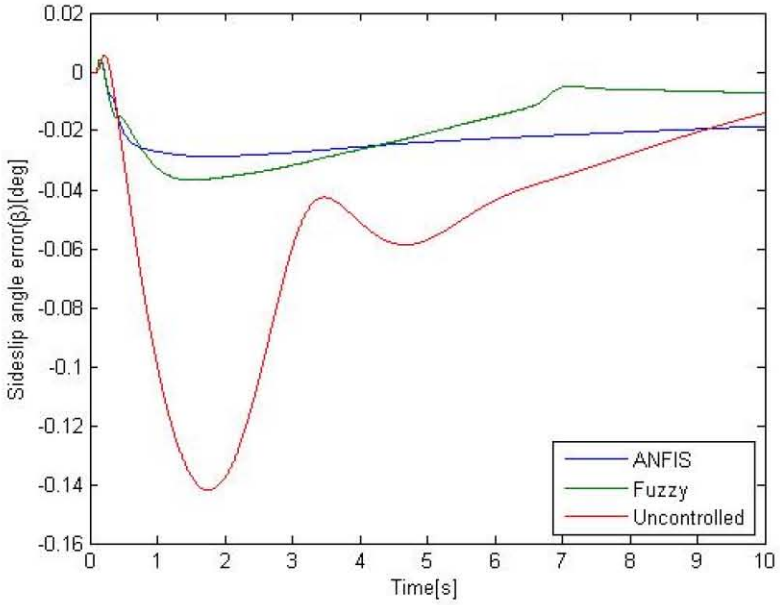

Figure 7.6: J-turn Side-slip angle performance at 20 m/s

moment M_z decisions made by the ANFIS and the Fuzzy controllers through the studied trajectory. The noticed decrease of speed in the drawn trajectory noticed in figure 7.4 was due to the extra use of the braking moment by the FCV rather than the correcting steering signal that is more used by the ACV.

The use of extra braking at situations when it can be avoided, generates a negative feeling to the driver. Which lead to the limiting of the ESP correction to only necessary situations, as discussed in section 3.2.

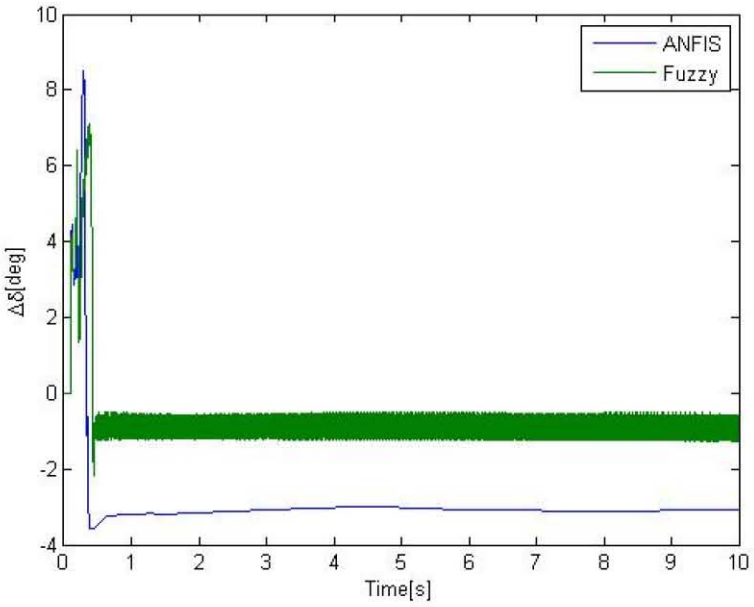

Figure 7.7: J-turn Steering control at 20 m/s

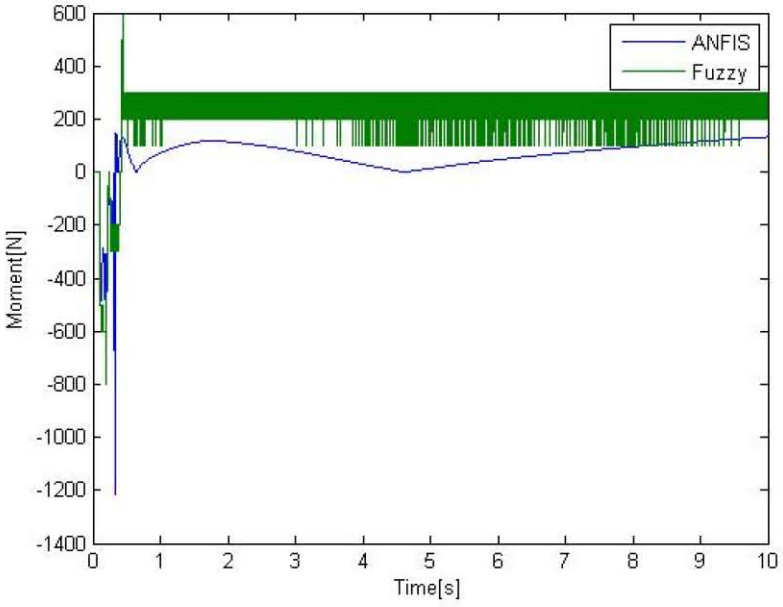

Figure 7.8: J-turn Yaw-Moment control at 20 m/s

This previously noticed behavior can be better seen in a more tricky condition, by increasing the speed to 30 m/s and simulating for 10 more seconds, as shown in figure 7.9, where practically the FCV over-steers and drifts away from its desired trajectory. The yaw rate and the Side-slip angle errors of this maneuver are shown in figures 7.10 and 7.11. Although the yaw rate and the side-slip errors of the FLC seem to stabilize at zero. This stabilizing is a fake indication, because the tires saturate at this point, due to the over-steering, producing a phenomenon known as the "plateau effect" [138]. The decisions made by the ANFIS and the Fuzzy controllers through the examined trajectory are displayed in figure 7.12 for the steering correction output in $\Delta\delta$, and figure 7.13 for the yaw moment control M_z. As could be seen from these two figures, the FLC-based controller almost stopped to emit control signals as its vehicle looses its adhesion. While the ACV vehicle maintained its trajectory and the ANFIS-based controller continued to do its job. In figure 7.13, the ANFIS-based controller chooses a very high yaw moment output, this is due to that this turning maneuver is very delicate and therefore the use of the yaw moment is necessary as the vehicle reaches its adhesion limits.

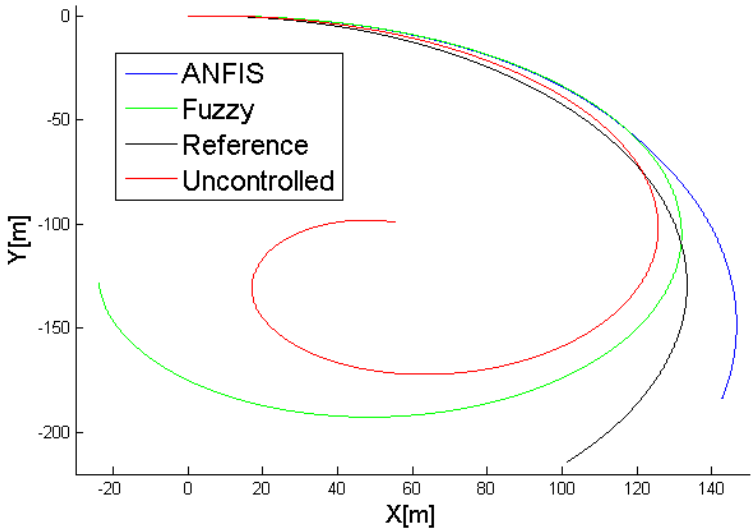

Figure 7.9: J-turn simulation at a speed of 30 m/s

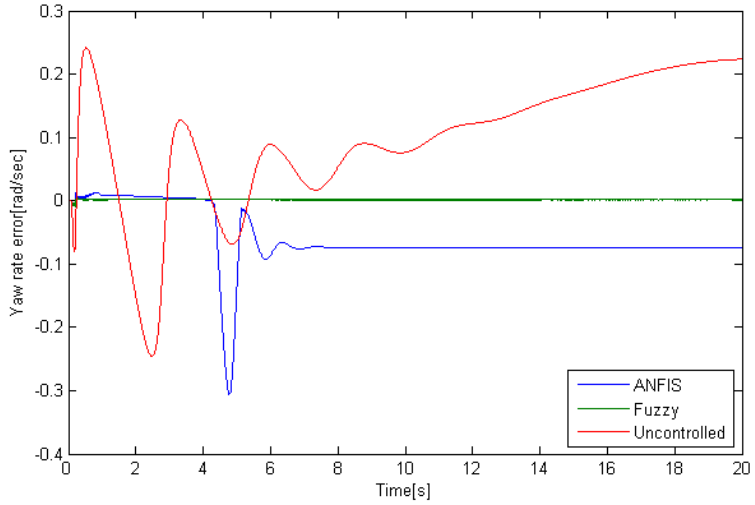

Figure 7.10: J-turn error of yaw rate at 30 m/s

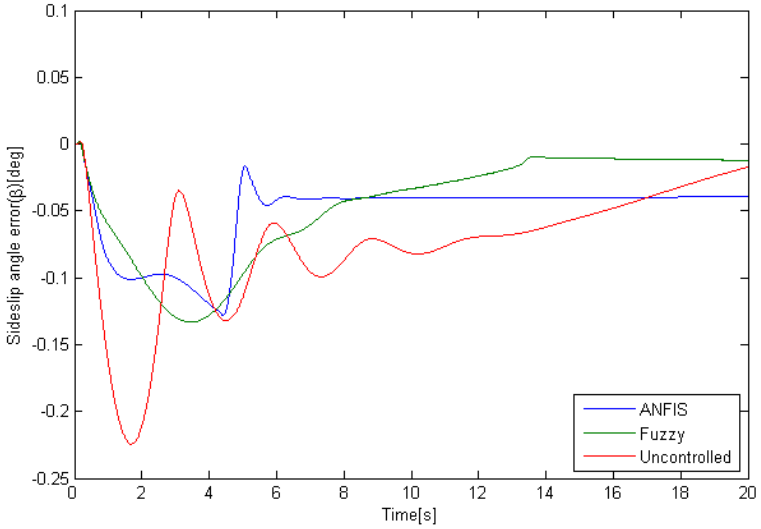

Figure 7.11: J-turn Side-slip angle performance at 30 m/s

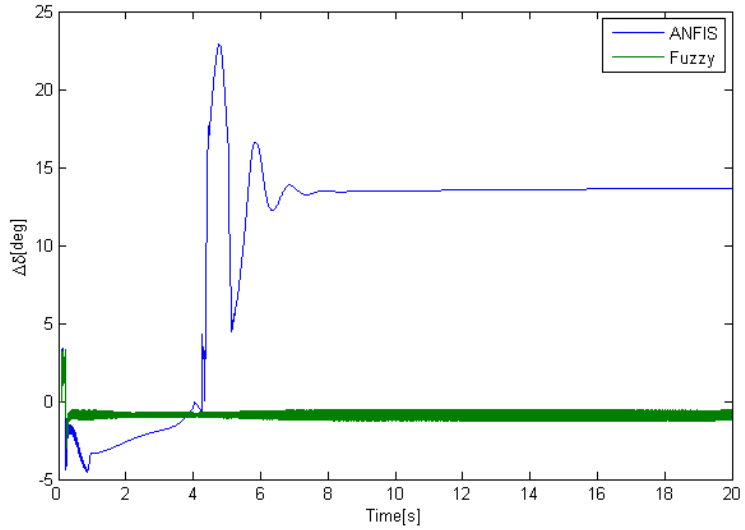

Figure 7.12: J-turn Steering control at 30 m/s

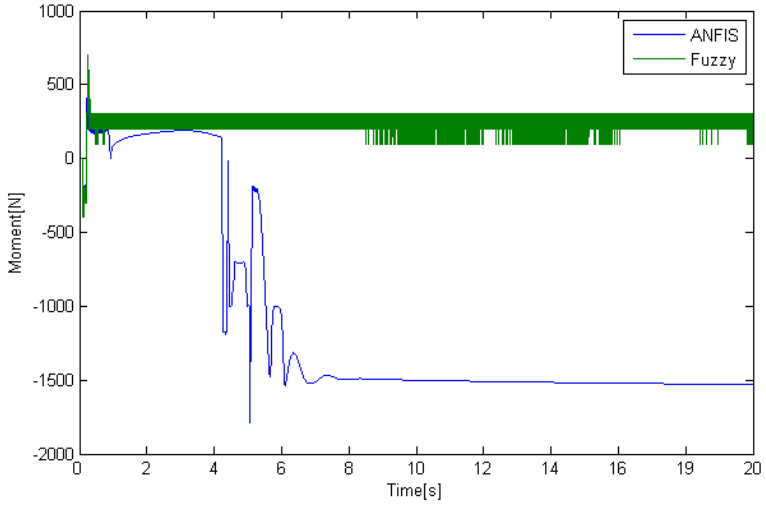

Figure 7.13: J-turn Yaw-Moment control at 30 m/s

7.1.2 Change lane maneuver

The change lane trajectories made by the three vehicles are shown in figures 7.14 and 7.15 for the speeds of 20 m/s and 30 m/s, respectively. As it could be seen from these figures both control systems improves the vehicle handling greatly and prevents the vehicle from entering in an over-steering or an under-steering situations like what happened to the uncontrolled vehicle. Tables 7.1, B.1 and B.2, show that the ACV yielded the best results in following the desired trajectory.

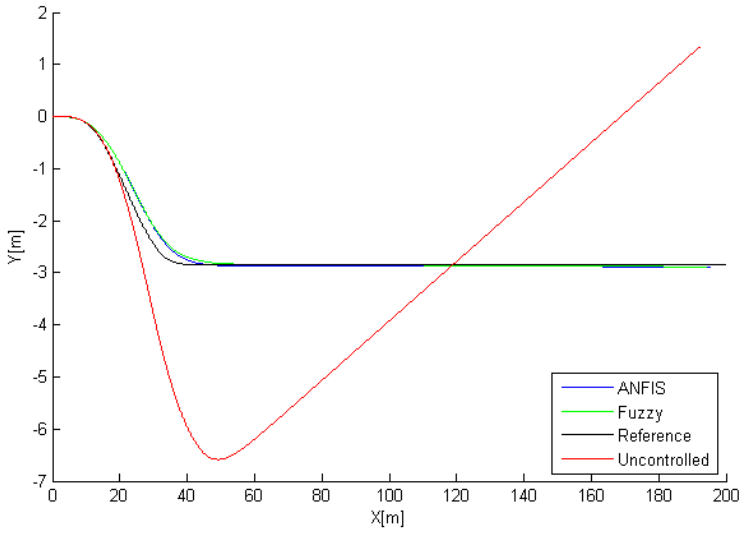

Figure 7.14: Change lane simulation at a speed of 20 m/s

The deviation of their yaw rate from their desired values are demonstrated in figure 7.16 and figure 7.17 and that of the Side-slip angle are in figure 7.18 and figure 7.19. In comparison to the error calculated at the passive vehicle, both of the errors made by the ACV and the FCV are almost negligible, and the difference between them is minute as could be seen in tables 7.1, B.1 and B.2. Except in figure 7.19, that the ACV side-slip angle error is regarded as a bit bigger. But this happens due to the fact that the ANFIS-controller reserves the braking moment only to the necessary situations, which is known to be the most effective Dynamic Stability Control (DSC) system at the limits of adhesion but its excessive braking effect is undesirable for the driver, see section 3.2. Therefore, the ANFIS-controller avoids the M_z use, so as to eliminate this undesired braking effect suffered by the ESP users. For that reason, in figures 7.20 and 7.21 the ANFIS-controller braking moment

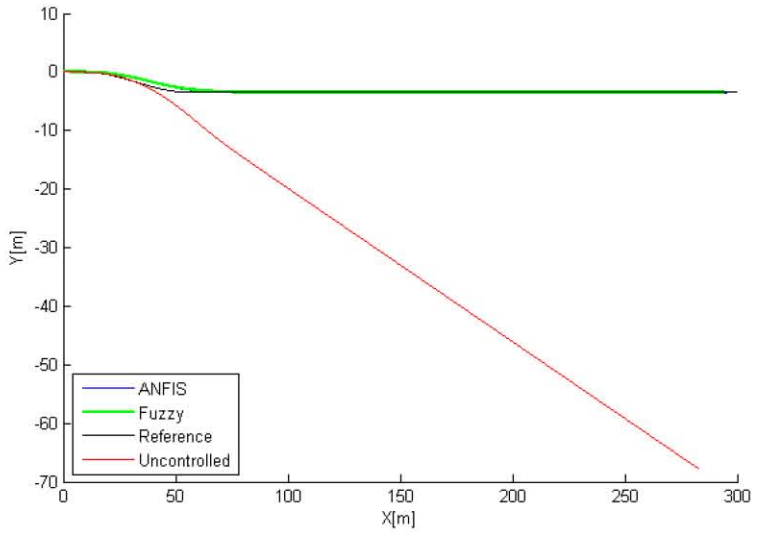

Figure 7.15: Change lane simulation at a speed of 30 m/s

signal is regarded as a punctual signal that is used only when necessary, while the FLC-controller excessively uses this signal even in unessential situations where only the steering correction could be used. On the other hand, figures 7.22 and 7.23 shows that the ANFIS-controller depends highly on the use of the AFS to improve the vehicle stability, and therefore avoid using the brakes as much as possible.

The results of this controlling approach can also be noticed by looking back at the trajectory graphs, figures 7.14 and 7.15. Where a closer look could show that the ACV follows the referenced trajectory more than the FCV. Furthermore, the effect of the speed reduction could be noticed at the extreme right of the graph, where the green line always ends before the blue one, which means that the FCV runs less trajectory than the ACV in the same given time. This speed reduction effect can also be noticed by comparing the maximum X-deviation from the desired path of each of the three vehicles shown in tables B.1 and B.2.

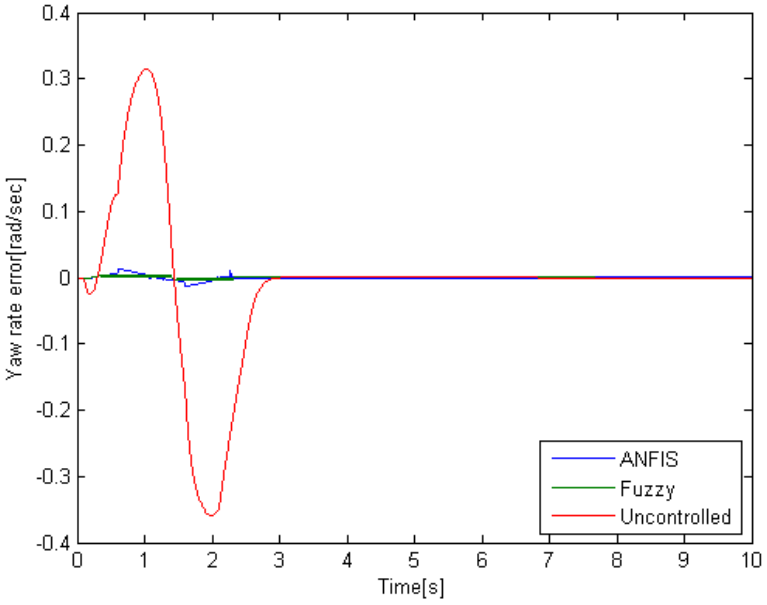

Figure 7.16: Change lane error of yaw rate at 20 m/s

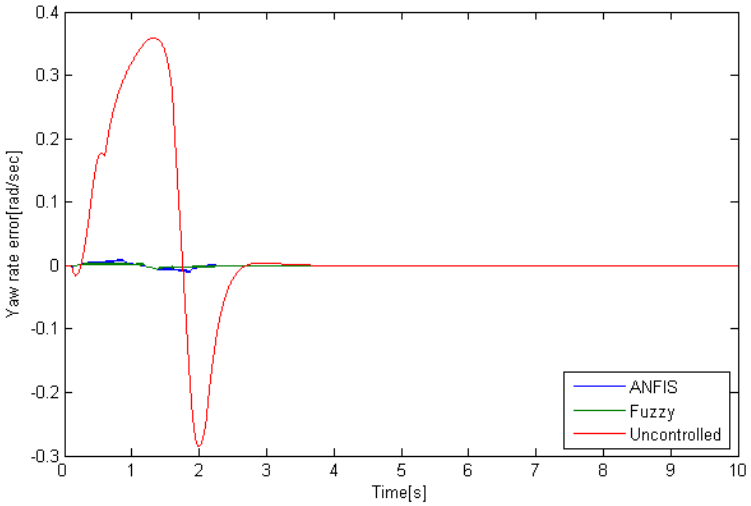

Figure 7.17: Change lane error of yaw rate at 30 m/s

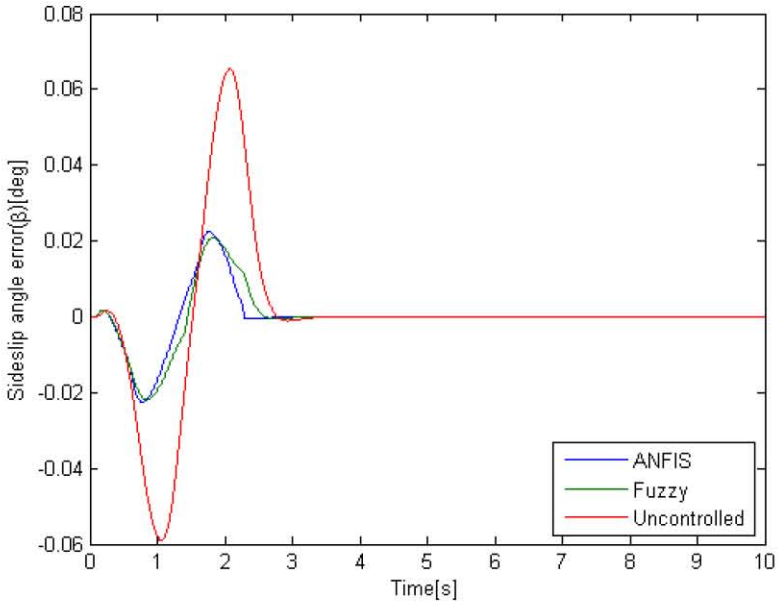

Figure 7.18: Change lane Side-slip angle performance at 20 m/s

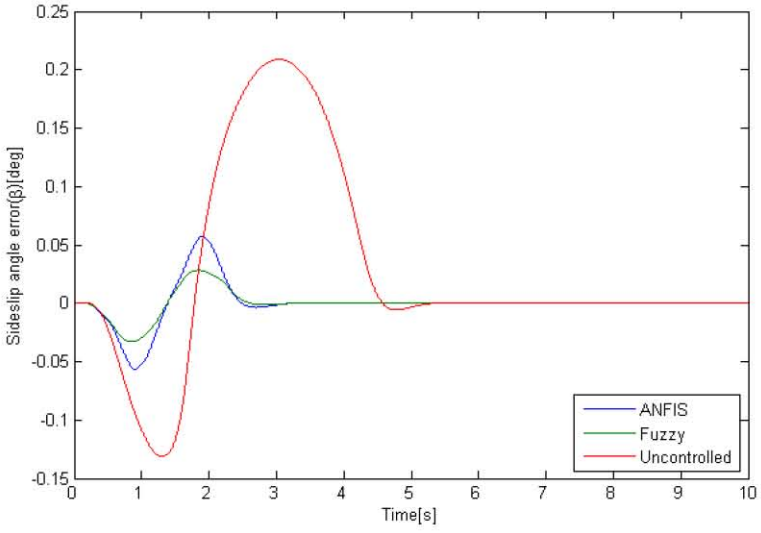

Figure 7.19: Change lane Side-slip angle performance at 30 m/s

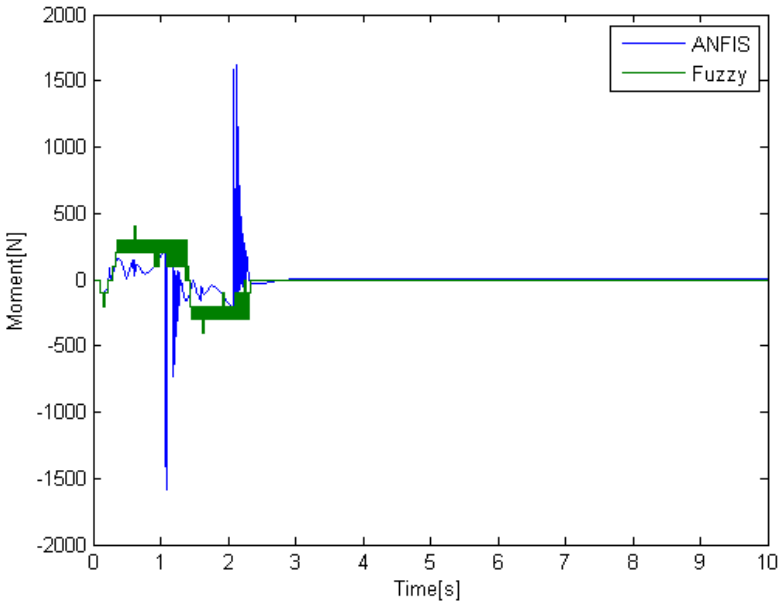

Figure 7.20: Change lane Yaw-Moment control at 20 m/s

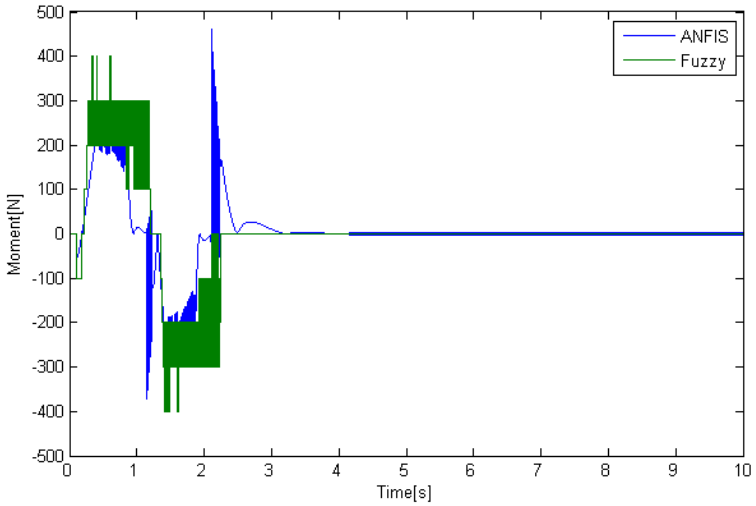

Figure 7.21: Change lane Yaw-Moment control at 30 m/s

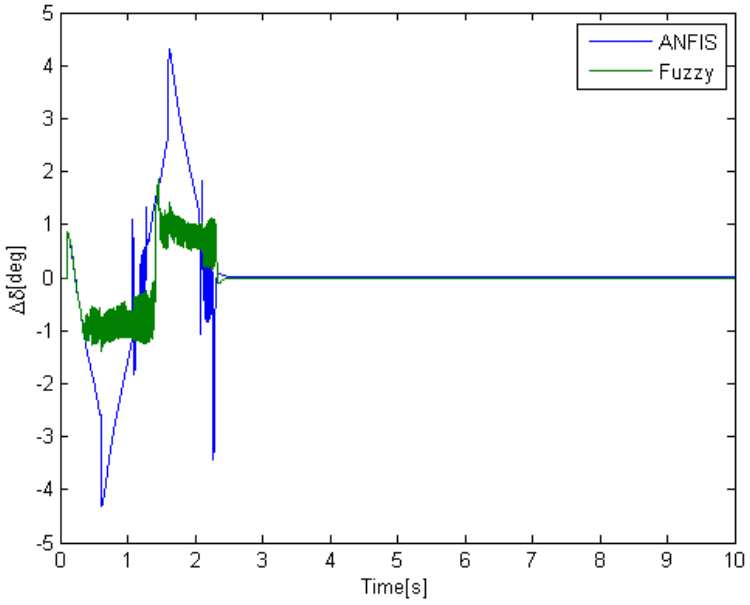

Figure 7.22: Change lane Steering control at 20 m/s

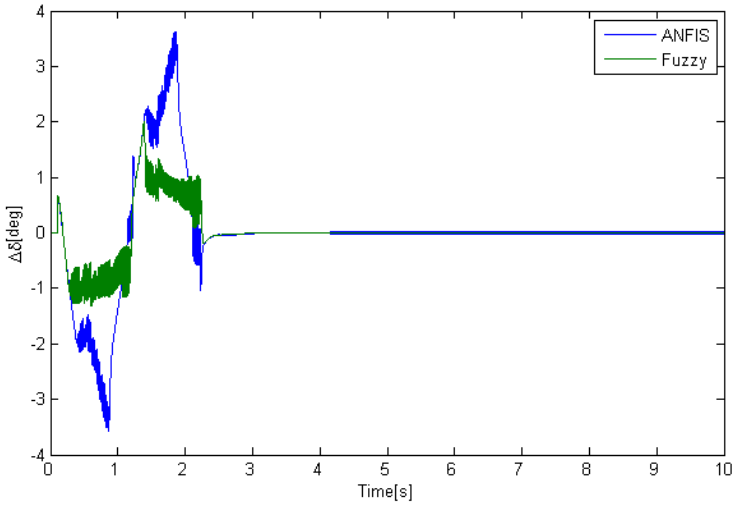

Figure 7.23: Change lane Steering control at 30 m/s

7.1.3 Double change lane maneuver

As for the double change lane trajectories they are shown in figures 7.24 and 7.25 for the speeds of 20 m/s and 30 m/s, respectively. As discussed above, the double-change lane could be regarded as two changing lanes maneuvers, each in a different direction. The simulation of this maneuver could allow us to better view the instability suffered by the vehicle while changing driving lanes rapidly. As seen in figures 7.24 and 7.25 the passive vehicle lost its stability while enduring such a maneuver on the simulated speeds. While both the ANFIS-based and the FLC-based controlled vehicles where able to follow their designated trajectories. Also tables 7.1, B.1 and B.2, show that the ACV yielded the best results in following the designated trajectory.

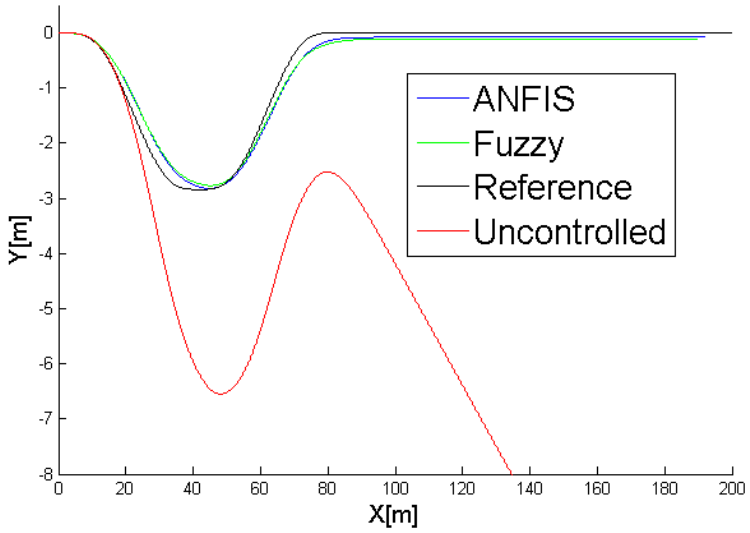

Figure 7.24: Double change lane simulation at a speed of 20 m/s

As by looking to figures 7.26 and 7.27, the yaw rate error of both the ACV and the FCV are almost negligible in comparison to that of the passive vehicle. On the other hand, by looking at figures 7.28 and 7.29, the AFC side-slip angle error is seen bigger. But once more this happens because the ANFIS-based controller avoids the use of the braking moment and limits it to only punctual and necessary uses, as could be seen in figures 7.30 and 7.31. Instead the ANFIS-based controller depends highly on the possible correction that could be generated by the AFS to avoid unnecessary speed deterioration that bothers the drivers. The steering correction used by both the ACV and the FCV is compared in figures 7.32 and 7.33. By carefully watching again

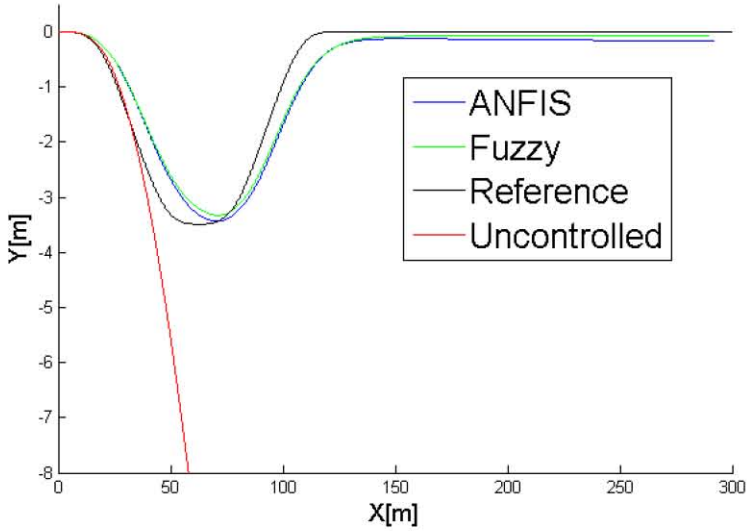

Figure 7.25: Double change lane simulation at a speed of 30 m/s

figures 7.26 and 7.27, the effect of the speed reduction on the FCV is even clearer in the double change lane maneuver than in the change lane maneuver. As for in both trajectories the green line that represent the trajectory made by the FCV in the given time always ends before the blue line which present the trajectory made by the ACV in the same given time. Furthermore, by comparing the maximum X-deviation from the desired path of each of the three vehicles shown in tables B.1 and B.2 the speed maintenance offered by the ACV is more noticeable in the double-change lane maneuver than the change lane one.

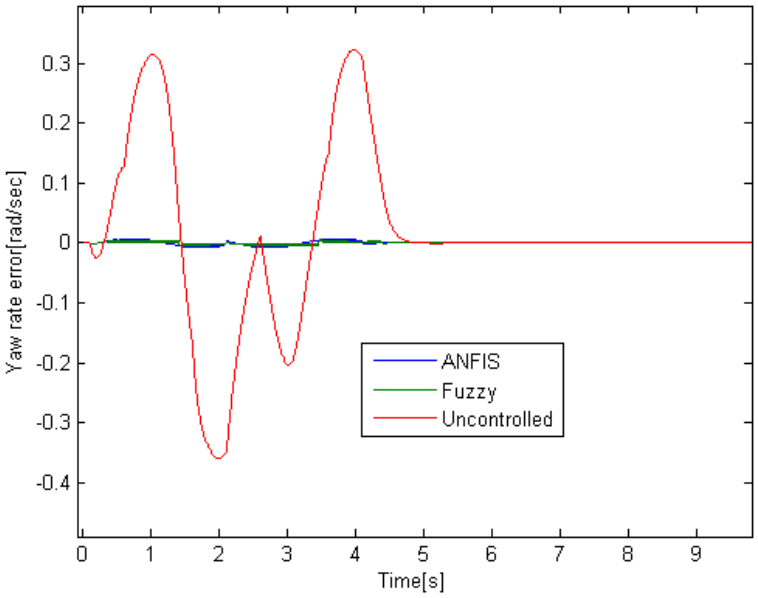

Figure 7.26: Double change lane error of yaw rate at 20 m/s

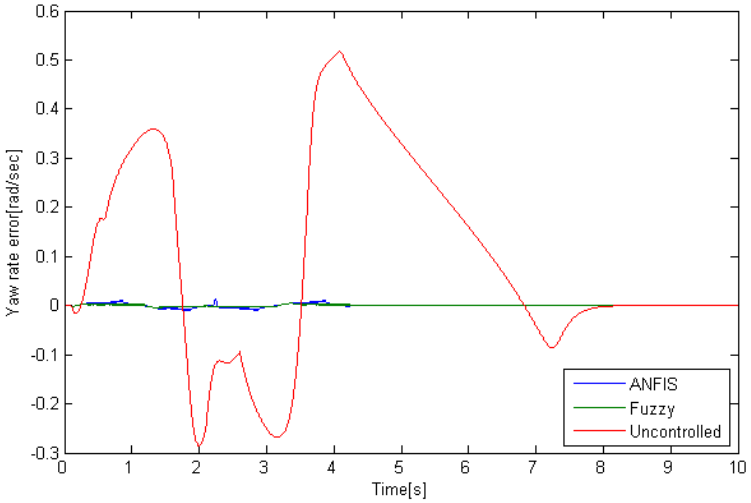

Figure 7.27: Double change lane error of yaw rate at 30 m/s

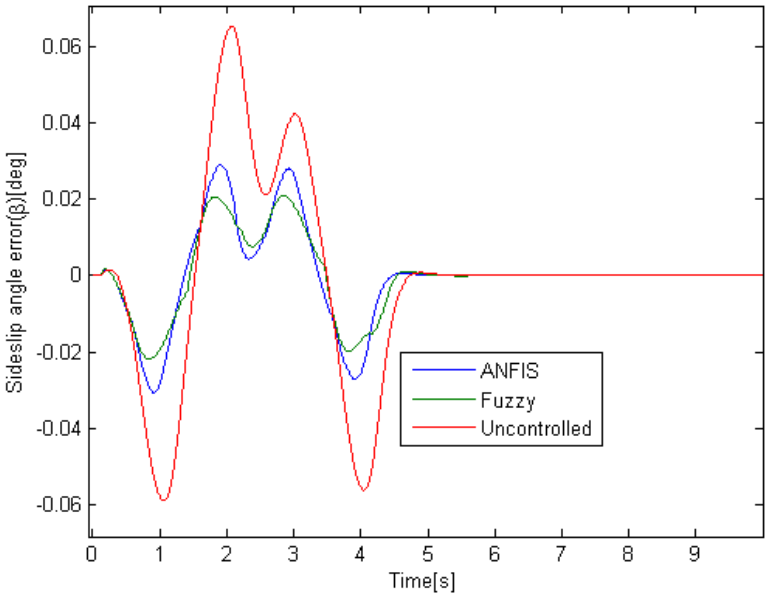

Figure 7.28: Double change lane Side-slip angle performance at 20 m/s

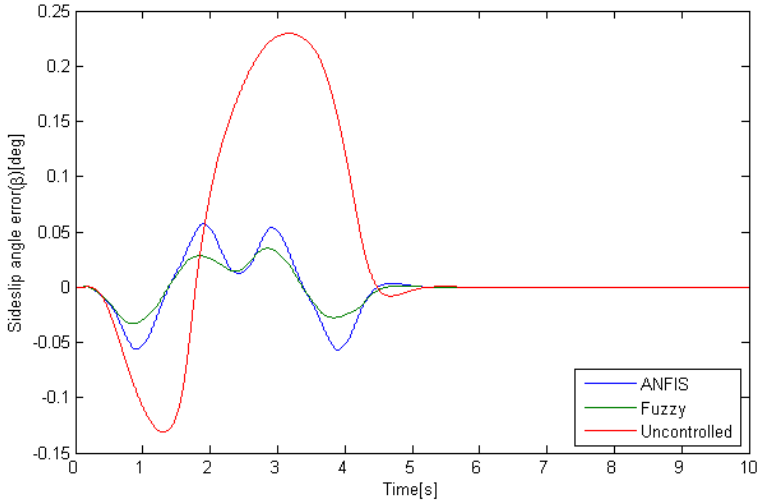

Figure 7.29: Double change lane Side-slip angle performance at 30 m/s

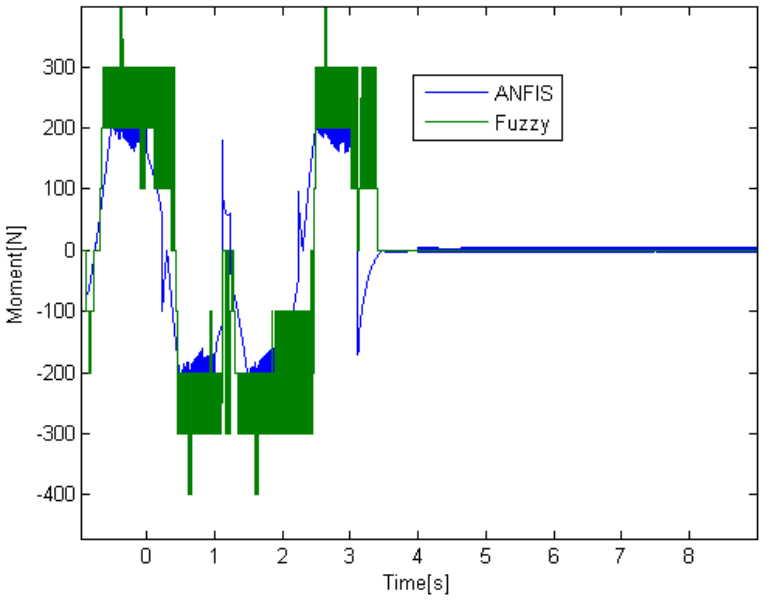

Figure 7.30: Double change lane Yaw-Moment control at 20 m/s

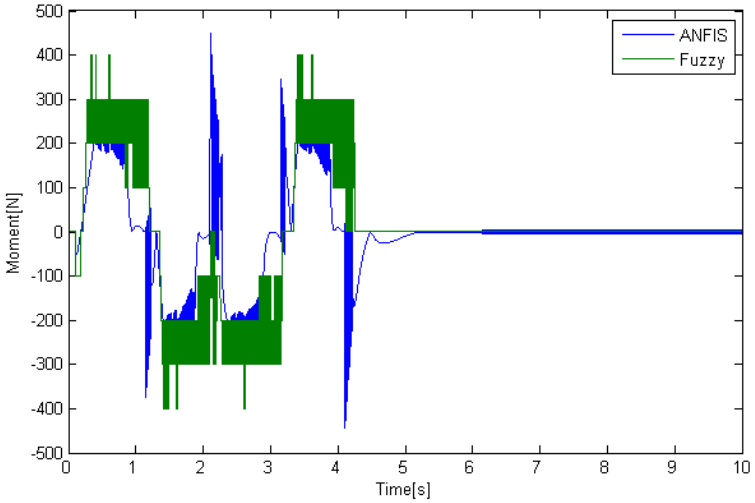

Figure 7.31: Double change lane Yaw-Moment control at 30 m/s

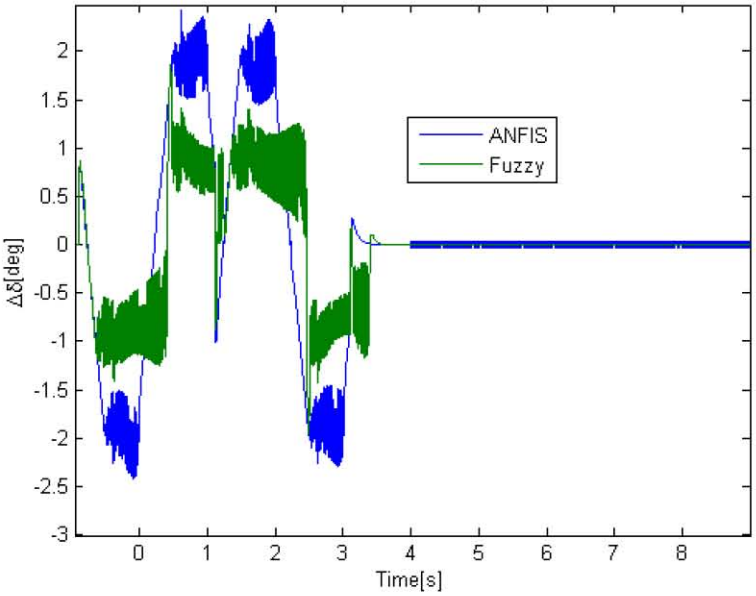

Figure 7.32: Double change lane Steering control at 20 m/s

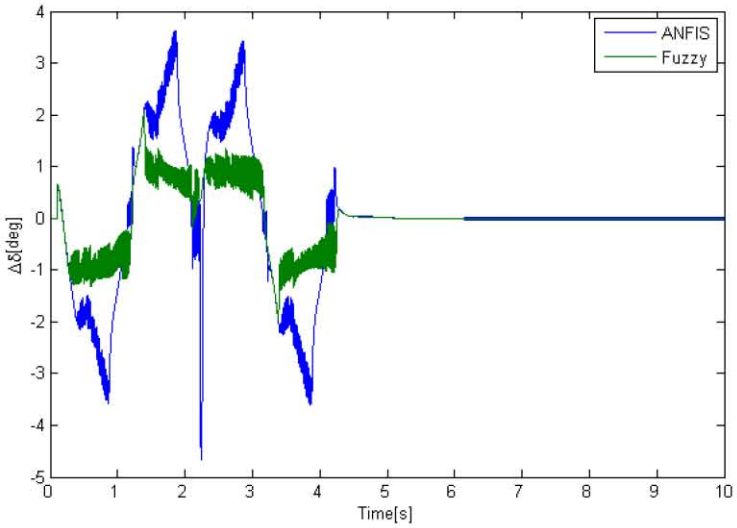

Figure 7.33: Double change lane Steering control at 30 m/s

			RMSD values		
			Trajectory	Yaw rate	Side-slip Angle
20 km/h	Jturn	anfis	24.94	0.0065	0.0328
μ=0.9		fuzzy	28.64	0.0039	0.0219
		passive	71.28	0.14	0.0651
	CL	anfis	4.49	0.002	0.0085
		fuzzy	5.8	0.0011	0.0068
		passive	8.77	0.1143	0.0193
	DCL	anfis	7.8	0.0028	0.0116
		fuzzy	10.07	0.0734	0.0068
		passive	19.04	0.139	0.0247
30 km/h	Jturn	anfis	51.33	0.0759	0.0724
μ=0.9		fuzzy	51.88	0.0023	0.0828
		passive	52.85	0.1045	0.1119
	CL	anfis	4.63	0.0024	0.0166
		fuzzy	5.79	0.0011	0.01
		passive	66.44	0.1147	0.088
	DCL	anfis	8.17	0.0034	0.023
		fuzzy	10.36	0.0015	0.0144
		passive	128.3	0.2261	0.0947

Table 7.1: RMSD values of the 20 and 30 km/h maneuvers on dry surface

7.2 Snowy road conditions

This section describes the evaluation of the same four vehicles in a snowy road condition where the tire-road friction coefficient reduced from $\mu = 0.9$ as in the previous section to a $\mu = 0.5$. This reduction greatly impact the car stability and its response to the driver input. To get a realistic conditions the vehicles are only tested on 20 m/s speed, since a more elevated speed could be extremely dangerous. Also the J-turn maneuver was adapted to be of an elongated turn of 4° in the front wheels inclination along the simulated time. Figure 7.34 shows the new J-turn maneuver, while the change lane and the double change lane maneuvers are kept as in the previous section. Table 7.2 shows the RMSD values of the three comparative aspects, while table B.3 extends the comparison to the maximum and minimum reached values.

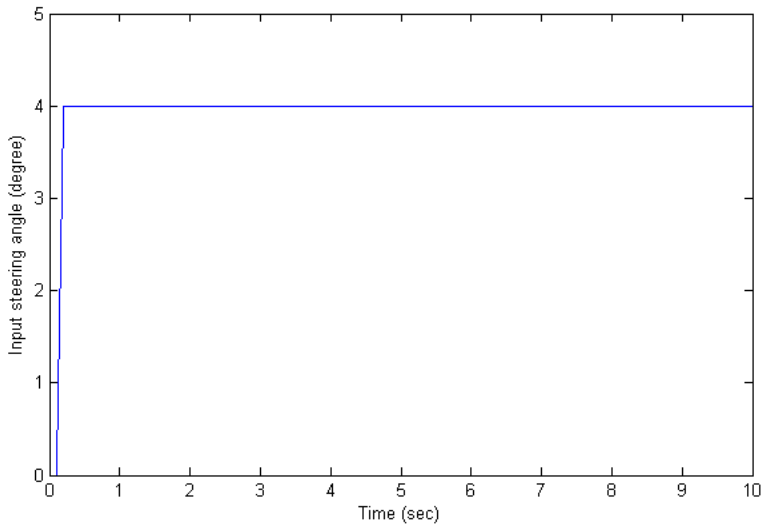

Figure 7.34: Steering input of the J-turn maneuver on snowy surface

7.2.1 J-turn maneuver

Figure 7.35 shows the J-turn maneuver on the described slippery road. The passive vehicle rapidly over-steers and gets extremely unstable as shown by its yaw rate and side-slip angle errors shown in figures 7.36 and 7.37 respectively. As for the ACV and the FCV they both have an under-steering performance, which although is not the most desirable performance, it is preferred more than that of an over steering one, details in section 3.1.5. Between both

controllers performance, as seen in figure 7.35, the AVC approximates much more to the reference trajectory than the FVC, and as calculated in table 7.2. The steering correction and the yaw moment outputs of the two controllers are shown in figures 7.38 and 7.39, respectively. Moreover, as shown in table B.3 the AVC yielded the best RMSD yaw rate and the second best RMSD side-slip angle.

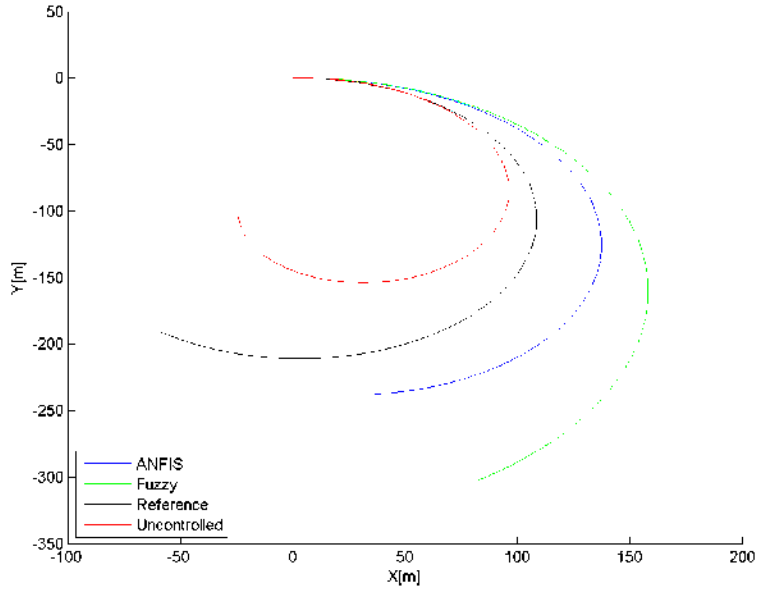

Figure 7.35: J-turn simulation at a speed of 20 m/s on snowy road conditions

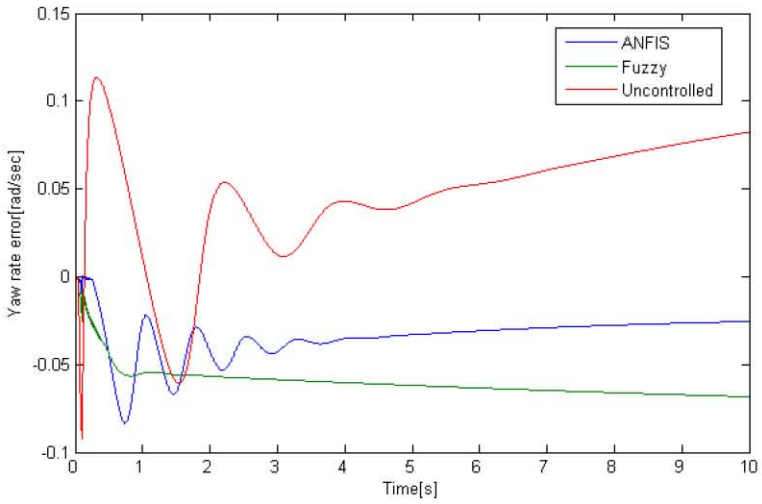

Figure 7.36: J-turn error of yaw rate at 20 m/s on snowy road conditions

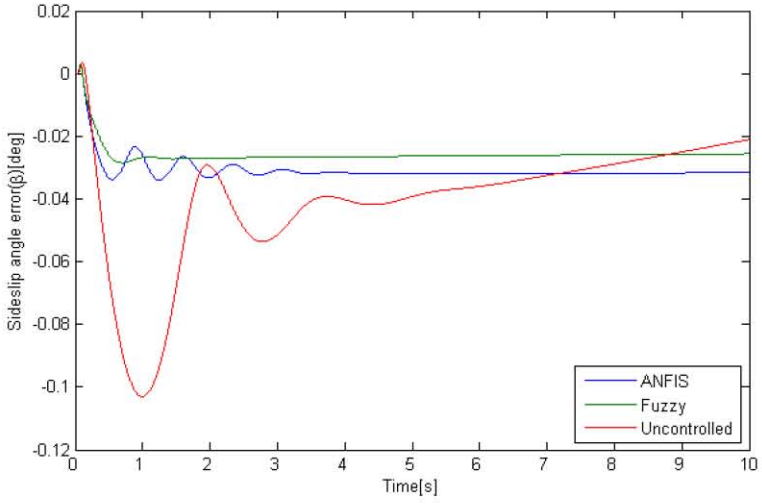

Figure 7.37: J-turn Side-slip angle performance at 20 m/s on snowy road conditions

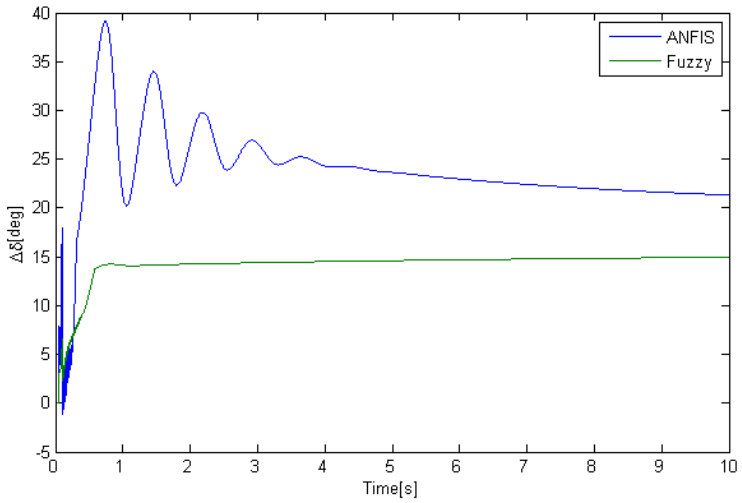

Figure 7.38: J-turn Steering control at 20 m/s on snowy road conditions

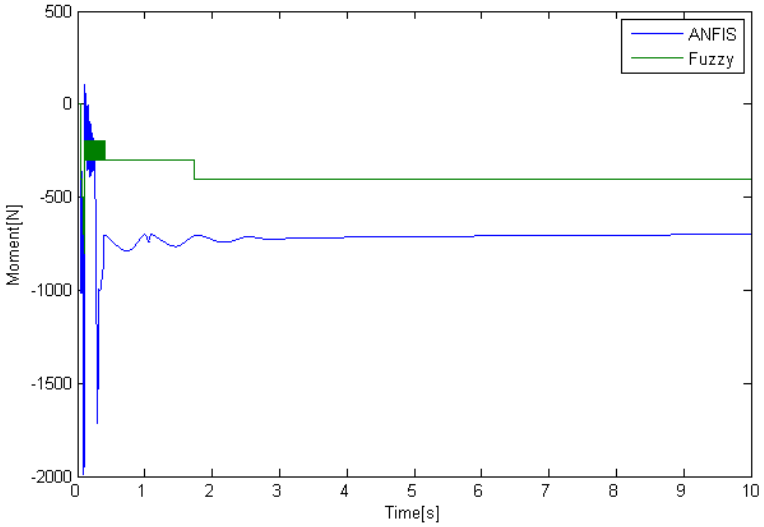

Figure 7.39: J-turn Yaw-Moment control at 20 m/s on snowy road conditions

7.2.2 Change lane maneuver

The trajectory of the change lane maneuver described in figure 7.2 on a slippery road is displayed in figure 7.40. The passive vehicle went out of its course loosing its stability at the beginning of the cornering. While both the ANFIS-based controller and the FLC-based controller maintained their vehicles so close to the desired trajectory. The yaw rate error, the side-slip angle, the steering control and the yaw moment control of the three vehicles are shown in figures 7.41, 7.42, 7.43 and 7.44, respectively. The performance difference of the ACV and the FCV may not be very clear in the trajectory graphs, but the RMSD of the desired path shown in tables 7.2 and B.3, shows that the ACV has the best target following performance. Also figures 7.43 and 7.44 show that the ACV uses more the AFS whenever possible.

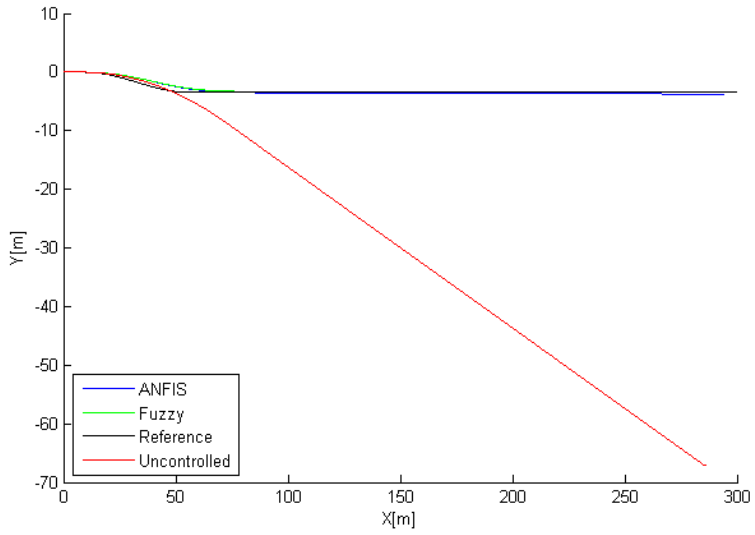

Figure 7.40: Change lane simulation at a speed of 20 m/s on snowy road conditions

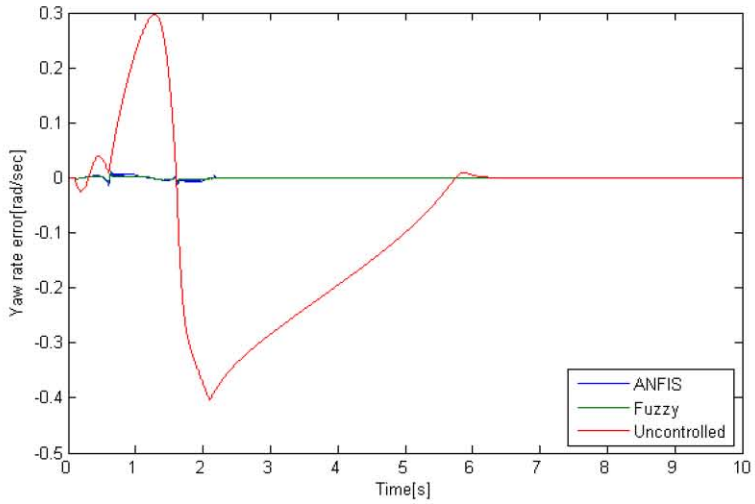

Figure 7.41: Change lane error of yaw rate at 20 m/s on snowy road conditions

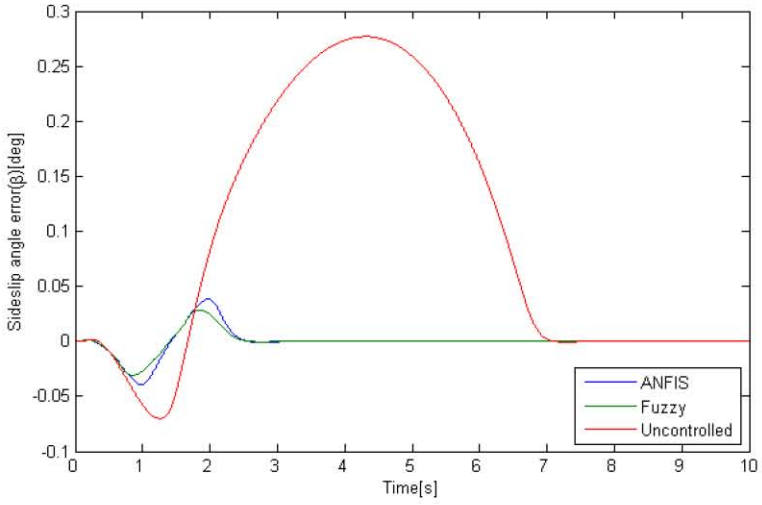

Figure 7.42: Change lane Side-slip angle performance at 20 m/s on snowy road conditions

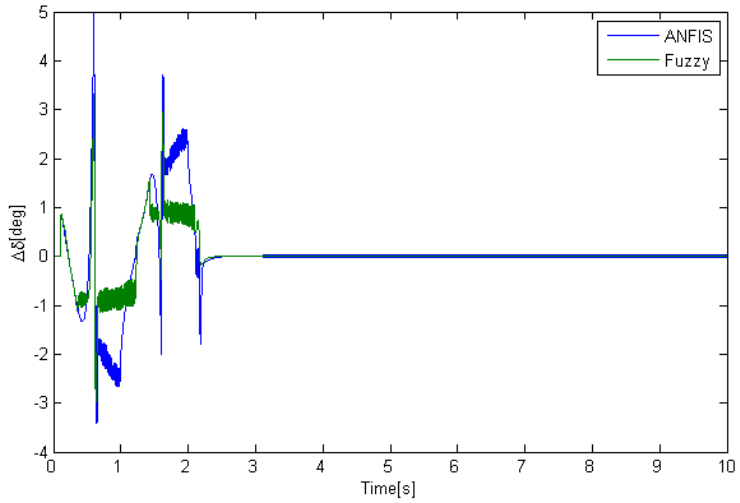

Figure 7.43: Change lane Steering control at 20 m/s on snowy road conditions

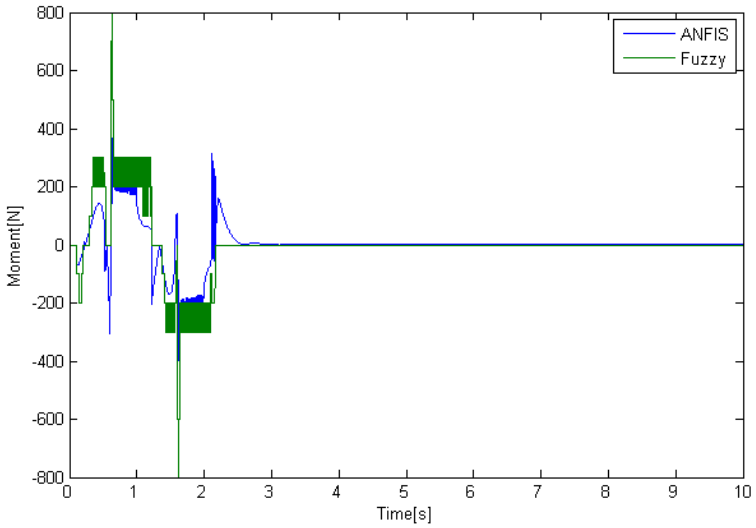

Figure 7.44: Change lane Yaw-Moment control at 20 m/s on snowy road conditions

7.2.3 Double change lane maneuver

Figure 7.45 shows the trajectory drawn by the four vehicles in a snowy road condition on the previously presented double change lane maneuver shown in figure 7.3. Similar to the previous simulation the passive vehicle went out of its course loosing its stability at the beginning of the cornering. While both the ANFIS-based controller and the FLC-based controller kept on maintaining their vehicles so close to the desired trajectory. The yaw rate error, the side-slip angle, the steering control and the yaw moment control of the three vehicles are shown in figures 7.46, 7.47, 7.48 and 7.49, respectively. Similar to the previous maneuver the performance of both the ACV and the FCV is not very clear through looking at the graphs, but it is shown in the RMSD comparison in table B.3, where the ACV shows the best performance in comparison to the FCV and the passive vehicle. Also, figures 7.46 and 7.47 show that the ACV still uses the AFS whenever possible.

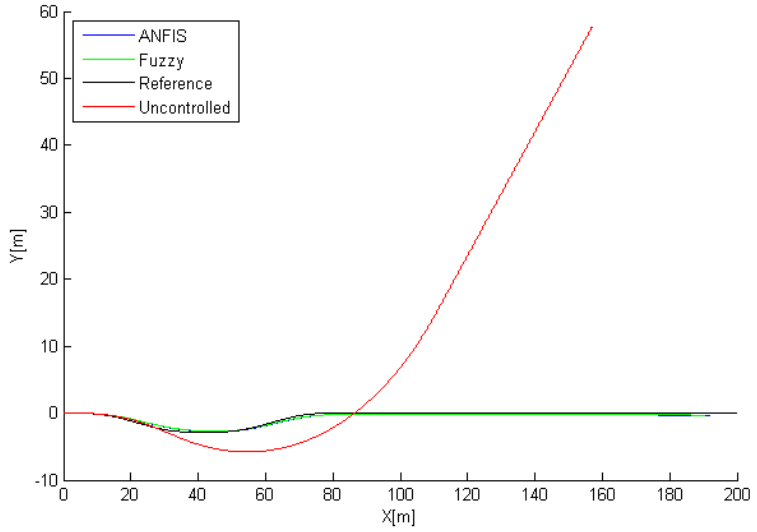

Figure 7.45: Double change lane simulation at a speed of 20 m/s on snowy road conditions

7.3 Discussion

In this chapter the simulation results of the proposed controller were presented in comparison to a passive vehicle and another vehicle controlled by

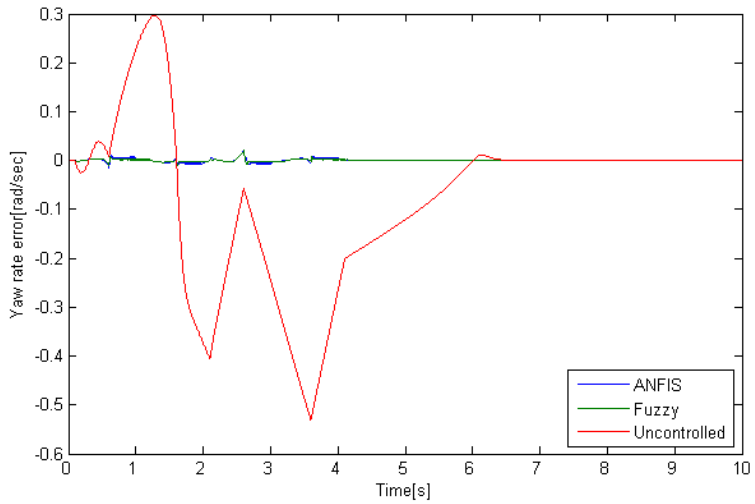

Figure 7.46: Double change lane error of yaw rate at 20 m/s on snowy road conditions

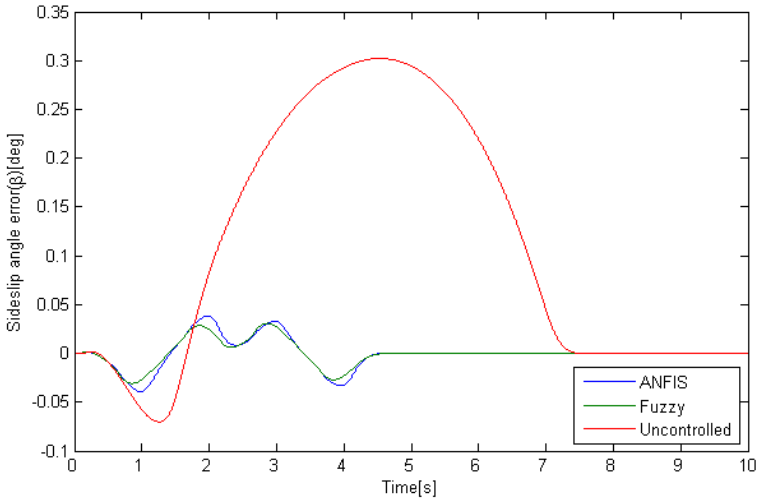

Figure 7.47: Double change lane Side-slip angle performance at 20 m/s on snowy road conditions

a human designed FLC presented in the literature. All of the three vehicles trajectories were evaluated in comparison to the desired trajectory and their stability variables were compared against the optimal ones.

The vehicles were first tested on a dry road of a friction coefficient of $\mu = 0.9$ while negotiating extreme maneuvers of J-turn, change lane and double change lane. All three maneuvers were tested on speeds of 20 and 30 m/s. The presented controller showed the best results in all the experiments made

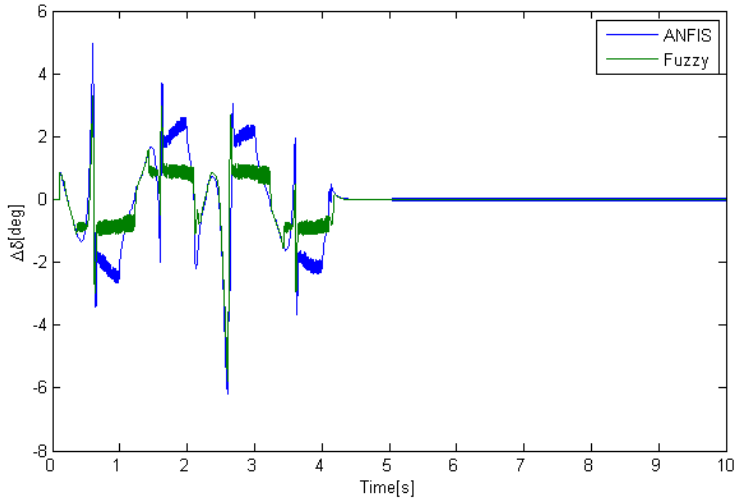

Figure 7.48: Double change lane Steering control at 20 m/s on snowy road conditions

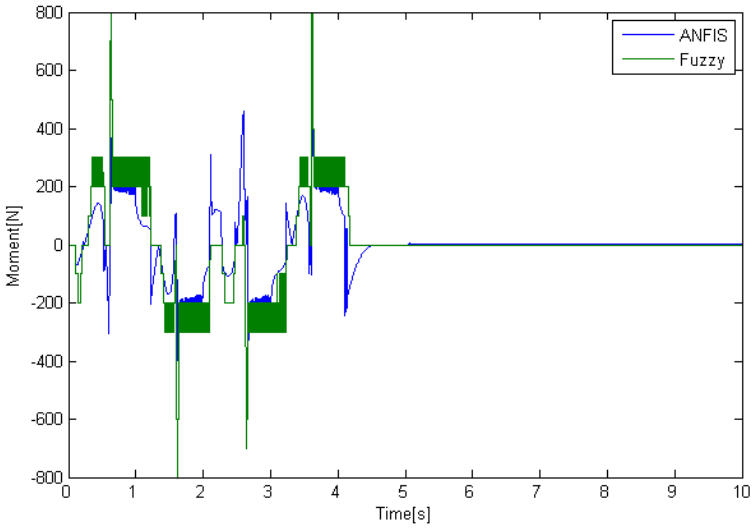

Figure 7.49: Double change lane Yaw-Moment control at 20 m/s on snowy road conditions

on dry surface. Where it was able to handle the stability of the vehicle and approximate its trajectory to the desired one without as much velocity reduction as in the case of the human-designed FLC controller. This behavior was observed due to the fact that the ANFIS-based controller tries to optimally utilize all its available resources, while avoiding to brake whenever possible to reduce the undesirable slowing down effect.

			RMSD values		
			Trajectory	Yaw rate	Side-slip Angle
20 km/h μ=0.5	Jturn	anfis	51.33	0.0759	0.0724
		fuzzy	51.88	0.0023	0.0828
		passive	52.85	0.1045	0.1119
	CL	anfis	4.63	0.0024	0.0166
		fuzzy	5.79	0.0011	0.01
		passive	66.44	0.1147	0.088
	DCL	anfis	8.17	0.0034	0.023
		fuzzy	10.36	0.0015	0.0144
		passive	128.3	0.2261	0.0947

Table 7.2: RMSD values of the 20 km/h maneuvers on slippery surface

Later the three vehicles were tested on a lower friction road with $\mu = 0.5$ to simulate a snowy weather condition. In this weather condition the three previously mentioned maneuvers were simulated on a velocity of 20 m/s. Since circulating in a low friction road condition at a more elevated speed is a highly risky action even in the presence of a DSC system. The ACV showed the best drawn trajectory in the J-turn maneuver. Where it kept the vehicle from oversteering, as what happened to the passive vehicle, or extreme understeering, as what happeed to the FCV. As for the change lane and the double change lane trajectories, both ACV and FCV showed similar results. Yet they both showed great improvement in maintaining the vehicle stability in comparison to the passive vehicle that practically drifts out of track.

Chapter 8

Suspensions systems design and results

This chapter shows the control results of the previously presented algorithm and controlling technique, described in section 6.3. This proposed technique in now tested to control a semi-active suspension system to improve the vehicle riding stability and comfort. The proposed algorithm helps to facilitate the design of semi-active suspension controllers, reduce the design cost and time, and also reduce the human intervention and consequently minimize the human-factor error. In this way different controllers for different suspension systems can be designed by only changing the algorithm input parameters.

The results obtained by controlling the semi-active suspensions were pretty satisfactory, which proves that the presented controlling technique can be very propitious to control more non-linear mechanical systems.

The chapter organization is as follows. Section 8.1 gives a brief background about semi-active suspension control and defines the challenges faced in this area. Then section 8.2 states the main contribution that the proposed algorithm presents. Section 8.3 describes the structure of the used vehicle model. While section 8.4 explains the intelligent algorithm and the adaptive neuro-fuzzy control technique. In section 8.5, the control system performance is evaluated and simulation results are showed and discussed. Finally section 8.6 briefly discusses what the chapter presented.

8.1 Problem statement

In modern vehicles, both the riding comfort and the driving safety are key issues in its design. The suspension systems have a key role in improving these two factors and therefore have received a great attention from both the academia and the industry. There exist three types of suspensions: the traditional suspension that consists of a spring and a damper and known as passive suspensions, since their performance solely determined by the road surface; the second is the fully active suspension that depends on an actuator (usually hydraulic) and are controlled through an electronic controller, these suspensions can work on their own or with the aid of passive spring and damper components; the third type known as semi-active suspension is an intermediate system between the previous two, where the electronic controller only intent to modify the damping rate, by using a special type of dampers along with the rest of the components of a passive suspension. Such dampers are usually Electro or Magneto-Rheological dampers, which use fluids that change their viscosity in the presence of an electrical or magnetic field (Selby, 2003). Between the three types the semi-active suspensions is considered to give the best compromise between the cost in energy consumption, actuators, sensors hardware; and the performance as in safety and ride comfort. And therefore have attracted research attention to improve the technologies of the semi-active damping actuators and the design of the control strategies [139].

Semi-active suspensions use is not limited to automobile vehicles; they are also used in motor vehicles, heavy vehicles, railway vehicles and even to isolate buildings from vibrations. Although active suspension control has been widely researched for decades, by simply looking at the literature, almost no research has focused on designing the damper controller automatically depending on the controlled object characteristics. Such an automatic design can allow the redesign of the suspension controller without human intervention, and therefore increase the portability of the controller from one vehicle to another. This technique could be very useful to redesign a suitable suspension model for each vehicle model and therefore decrease the vehicle designing time.

Artificial intelligence techniques like Fuzzy Logic Control (FLC), Artificial Neural Network (ANN) and Genetic Algorithms (GA) has been used in the literature to control semi-active suspensions and have yielded satisfying results, an excellent review of this use could be found in [140]. Nevertheless, the

presented controllers were designed according to each specific system. Even the controllers that were constructed through an auto-learning technique, like ANN or FLC, used lab-data of the specific suspension for the construction, which at the end imply that this controller could only be used for this specific suspension.

8.2 Main contribution

This chapter presents an adapted version of the intelligent algorithm presented in 6.3.1 that auto-generates the needed suspension data to be used by an ANN to auto-construct a FLC controller. In this way, the designer only enters the main characteristics of the suspension to the algorithm and the algorithm generates the ANN training data automatically. Therefore, the design of each controller would need less time and minimal human intervention. The algorithm uses a simulation model for its design process; which is known to be effective in the field of vehicle design as it reduces the production time and costs while providing a realistic model depending on the model quality [141]. Also the presented algorithm helps to minimize the possible human error and lab data noise effect. The controller is tested on a quarter car model, on four different road profiles, and its results are compared to that of a passive suspension. Simulations show the efficiency of the proposed technique.

8.3 Suspension model

A quarter car's model is used in this study to model the dynamics of the semi-active suspension. Quarter car models is often used to simplify the calculations involved in the model while providing realistic results that can be later adapted to a full model [142]. As its name suggests it's roughly the model of a quarter of a car as shown in 8.1 [143, 144]. The actuator is connected in series with the spring of the passive suspension to control the suspension in order to improve its performance. The tire is modeled by a simple spring with stiffness (k_2) and the unsprung mass (m_u). It is assumed that the tire does not leave the ground. The sprung mass (m_s) of the vehicle body is considered as a rigid body. The spring (k_1), damper (C_s) and actuator between sprung mass (m_s) and unsprung mass (m_u) constitute a semi-active suspension model.

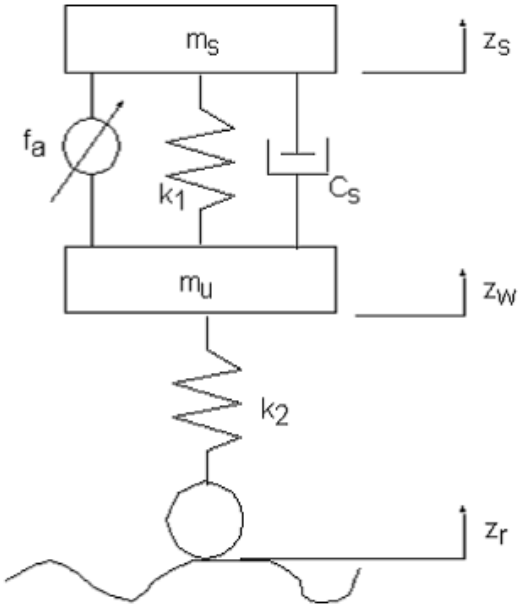

Figure 8.1: Quarter suspension vehicle model [14]

The dynamics equations of the quarter suspension model are:

- Sprung mass:

$$m_s \cdot \ddot{z}_s = k_1 \cdot (z_w - z_s) + C_s \cdot (\dot{z}_w - \dot{z}_s) - f_a \tag{8.1}$$

- Unsprung mass:

$$m_u \cdot \ddot{z}_w = -k_1 \cdot (z_w - z_s) - C_s \cdot (\dot{z}_w - \dot{z}_s) - k_2 \cdot (z_w - z_r) + f_a \tag{8.2}$$

From equations 8.1 and 8.2 the following state space equations can be formulated:

$$\dot{X} = A \cdot X + B \cdot u \tag{8.3}$$

$$Y = C \cdot X + D \cdot u \tag{8.4}$$

where X is an the independent variable, u is the input vector and Y is the output vector:

$$X = \begin{bmatrix} z_s \\ z_w \\ \dot{z}_s \\ \dot{z}_w \end{bmatrix}; A = \begin{bmatrix} 0 & 0 & 1 & 0 \\ 0 & 0 & 0 & 0 \\ -\frac{k_1}{m_s} & \frac{k_1}{m_s} & -\frac{C_s}{m_s} & \frac{C_s}{m_s} \\ \frac{k_1}{m_u} & -\frac{k_1+k_2}{m_u} & \frac{C_s}{m_u} & -\frac{C_s}{m_u} \end{bmatrix}; B = \begin{bmatrix} 0 & 0 \\ 0 & 0 \\ -\frac{1}{m_s} & 0 \\ \frac{1}{m_u} & \frac{k_2}{m_u} \end{bmatrix} \tag{8.5}$$

$$u = \begin{bmatrix} f_a \\ z_r \end{bmatrix}; C = \begin{bmatrix} 1 & 0 & 0 & 0 \\ 0 & 1 & 0 & 0 \\ 0 & 0 & 1 & 0 \\ 0 & 0 & 0 & 1 \end{bmatrix}; D = \begin{bmatrix} 0 & 0 \\ 0 & 0 \\ 0 & 0 \\ 0 & 0 \end{bmatrix} \tag{8.6}$$

The input vector u consists of actuator force f_a and road disturbance z_r.

There are three main parameters for the design and evaluation of the vehicle suspensions [145, 95]:

- Sprung mass vibration isolation, which determines the ride comfort.
- Suspension stroke, which indicates the limit of the vehicle body motion.
- Tire road contact which provides proper lateral and braking force.

To observe these parameters, the following variables have to be examined:

- Vertical acceleration of sprung mass ($\ddot{z}_s$).
- Deflection of the suspension ($z_w - z_s$).
- Deflection of the tire ($z_r - z_w$).

The decreased responses of these parameters indicate better suspension quality. Therefore, a good controller should actuate a controlling force f_a that gives the minimum possible values for the previous variables.

8.4 The Neuro-Fuzzy Controller

As explained before with the Integrated Chasis Dynamics controller explained in section 6.3, to construct the proposed control system, two steps has to be carried out. The first is to construct the intelligent algorithm that auto-generates the needed suspension data to be used afterward by the neural

network. This phase is carried out once and then this algorithm can be run on different suspensions without any need of its modification. The algorithm mainly search for the optimum acceleration and wheel adhesion values that could be obtained at different road conditions and the adequate force that yields such results. These values are then stored in a database, to be learnt by the ANN that automatically constructs the appropriate fuzzy controller for the given suspension.

This section will start by explaining the proposed intelligent algorithm, then it will briefly explain the special type of ANN that is used for the FLC construction and finally will explain the controller construction characteristics and the used values in the given experiment.

8.4.1 Intelligent Algorithm

The first step in the proposed idea is to search for the optimum force control input (f_a), which can yield the best performance of the vertical acceleration, the tire deflection and the suspension deflection. To find the optimum control force input f_a, the proposed algorithm replaces the control system and tests the suspension performance on different road conditions; and each condition of which is tested along different time instances. Each test case is then tried with different input force magnitudes, and the input that gives the best performance, at this certain case, is stored in a database as the best control input for this certain case.

The final output of this algorithm is a quadruple set that can be written as: $\{(z_w - z_s), \ddot{z}_s, (z_r - z_w), f_a\}$ and it represents the best decision output to be taken by the control system when it gets these inputs. A table filled of these quadruple sets at different riding conditions is then passed to the ANN so that it can construct the fuzzy logic controller. The algorithm was written using MATLAB's m-code.

8.4.2 ANFIS

The ANN used to construct the FLC is also a part of the technique called Adaptive Neuro-Fuzzy Inference System (ANFIS) mentioned before. For a brief summarization, ANFIS is an advanced AI technique that uses a special ANN and trains it on the given data to construct automatically a FLC that

mimics this given data and can be installed in the system to be controlled (in this case the suspension). The advantage of using ANFIS is that it combines the benefits of both: Neural Networks and Fuzzy logic; where the first have the quality of being adaptive and can learn by generalization and pattern recognition, and the latter allows soft and steady performance [114].

Unlike the traditional linguistic Mamdani FLC technique, ANFIS uses a Takagi-Sugeno fuzzy inference method. The Takagi-Sugeno is a more compact and computationally more efficient than the Mamdani system, furthermore, it is more flexible to the use of adaptive techniques [13]. For a detailed explanation of the ANFIS training process, please refer to section 3.4.

8.4.3 Controller characteristics

To construct the learning data 2200 quadruple sets were constructed through the previously explained algorithm. This data were then divided in 3 groups; estimation, validation and testing in the ratio of 2:1:1 respectively. Where the network goes training cycle by cycle on the training data and checking its performance on the validation set, while the testing set is to prevent the learning algorithm to fall in a global minima. By means of the MATLAB ANFIS toolbox, the neural network was constructed and taught on the given data, see figure 8.2. The ANN design was chosen through trial and error by varying the toolbox options, such as, the number and type of the fuzzy logic membership functions, the number of the ANN learning epochs (cycles), the error tolerance, etc. And accordingly the fuzzy logic systems were chosen as the one that yields the least error percentage.

Figure 8.3 shows the performance of the new ANFIS-constructed FLC on the training data, where the blue 'o's are the testing data that the system should follow and the red '*'s are the output of the control system. The new FLC has 19 gauss membership functions, and was trained over 50 epochs.

8.5 Simulation results and analysis

A simulation study was realized to verify the efficiency of the proposed controller before experiments are carried out on a real vehicle. Simulation was carried on two identical quarter vehicle's model one using a passive suspension and the other a semi-active suspension model, explained in section 8.3. The

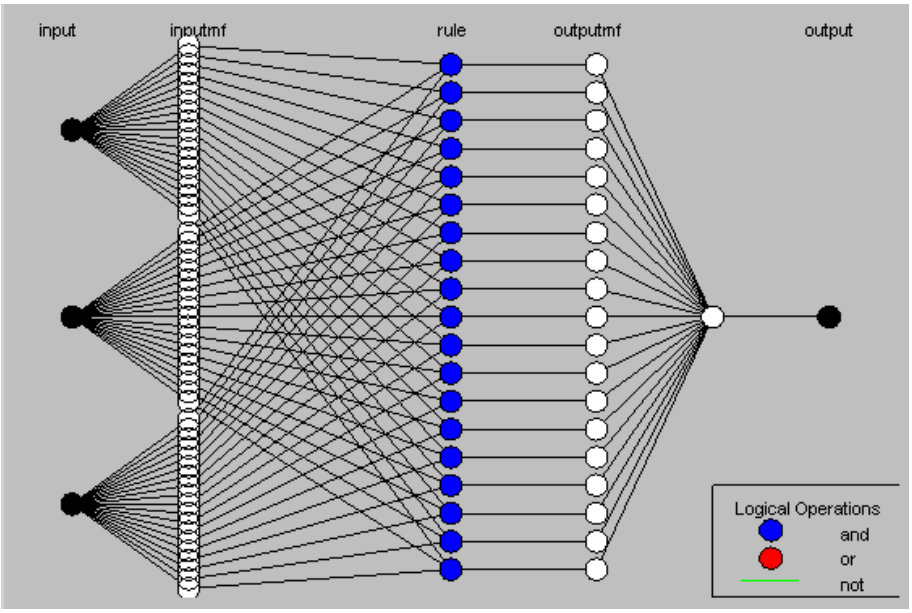

Figure 8.2: Neural Network structure

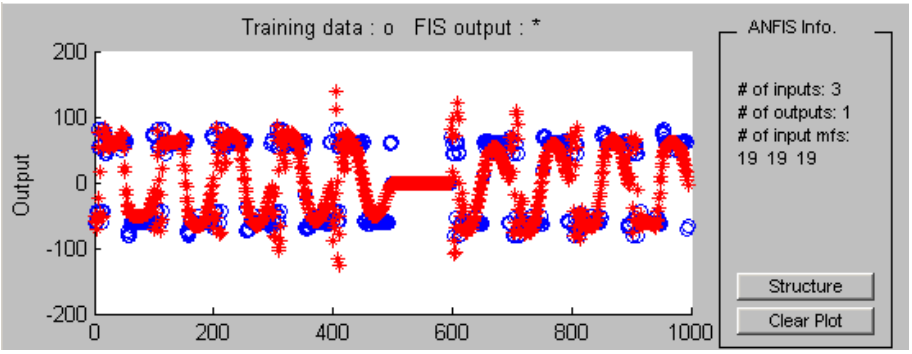

Figure 8.3: FLC-controller performance

models were implemented using MATLAB SIMULINK simulation software and the chosen parameters of the simulated model are shown in table 8.1.

Sprung mass (m_s)	250 kg
Unsprung mass (m_u)	35 kg
Stiffness of tyre (k_2)	160000 N/m
Spring (k_1)	1600 N/m
Damper (C_s)	980 Ns/m

Table 8.1: Parameters of vehicle suspension

To evaluate the model efficiency four road profiles were considered: a step up step down of 0.1 meter each, a bump of 0.05 meter, a bump of 0.11 meter

and a highly uneven road profile. The time domain response of the vehicle in each of the cases is simulated for a period of four seconds, with sampling time intervals of 0.001 seconds.

Figure 8.4 shows the road profile drew by the step up step down case, then a comparison between the performances of the passive suspension (represented by an uncontinuous line) and the semi-active suspension presented in this paper (represented by a solid line). The graphs include the suspension evaluation criteria; the vertical acceleration of sprung mass ($\ddot{z}_s$), the deflection of the suspension ($z_w - z_s$) and the deflection of the tire ($z_r - z_w$).

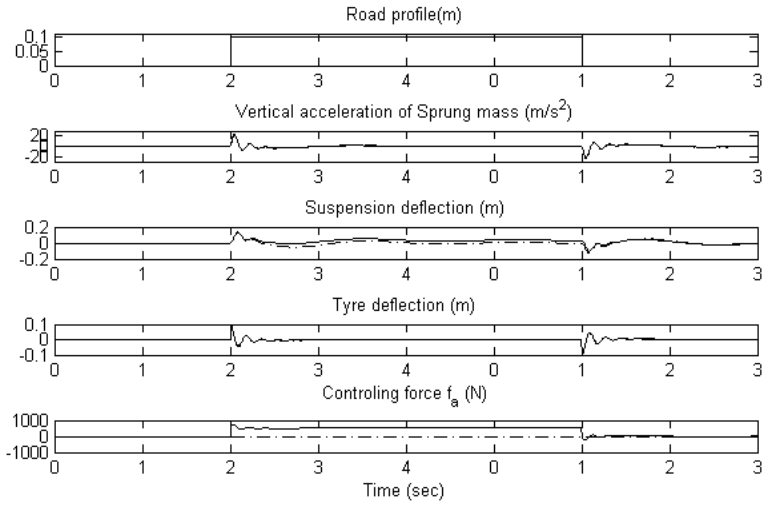

Figure 8.4: Step up step down simulation: passive suspension (solid line); semi-active suspension (dotted line)

The vehicle's ride comfort or the ability of vibration isolation is evaluated by the level of acceleration that the passengers or the suspended mass are subjected to. And since the vibration affect the comfort basicly through frequency, frequency weighting functions are used to evaluate the passengers comfort [146, 96]. Therefore for a fair judgment of the results, Figure 8.5 shows the spectral densities of the suspended mass of the body vertical displacement and the body vertical acceleration, respectively. Frequencies near 1 Hz are known to be sensitive to the human body and therefore the frequency zone below 2 Hz has a great impact on the ride comfort [95], figure 8.5 shows the effectiveness of the semi-active suspension system reduction in this area.

Figures 8.6 and 8.8 show the 0.05 and the 0.11 meter bumps road profile,

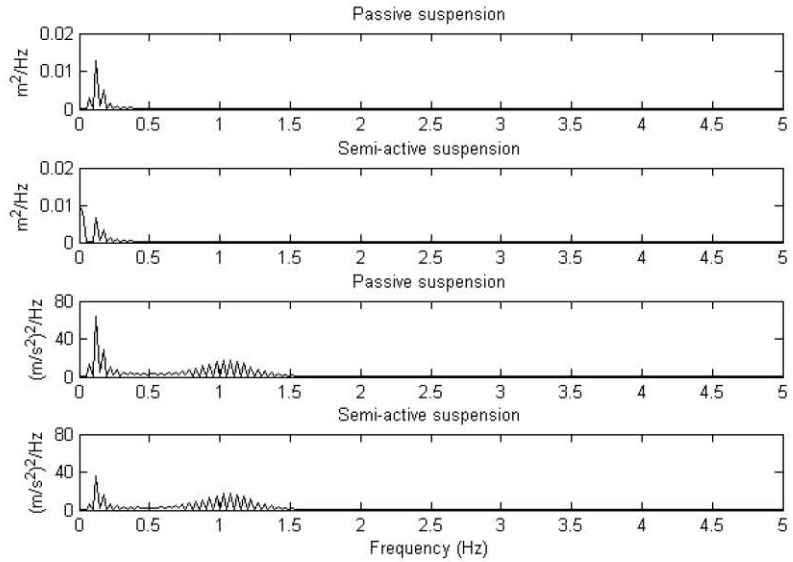

Figure 8.5: Spectral densities of the step up step down simulation of the body vertical displacement (first two graphs) and the body vertical acceleration (later two graphs)

respectively, with each of its corresponding sprung mass acceleration, suspension and tire deflections. While figure 8.7 and 8.9 compares the effectiveness of the suspension systems from the point of spectral densities of the suspended mass of the body vertical displacement and acceleration, of each of these road profiles. The semi-active suspension shows a considerable reduction in the displacement and acceleration frequencies, in both situations.

Finally the suspensions were tested on a rough road where a random road profile is modelled as a filtered white noise suggested by Roh and Park (1998) and could be described as:

$$w' + avw = av\xi$$

where a is a positive constant, v is the vehicle speed, and ξ is a zero-mean Gaussian random process with the covariance $cov[\xi(t)] = 2\sigma^2$. In this simulation, the following values are considered to simulate a road that is rougher than asphalt $a = 1.35$ and $\sigma^2 = 1.10^{-2}$.

Figures 8.10 and 8.11 shows this road profile along with the suspension evaluation criteria mentioned above and the evaluation frequencies, respectively. The figures also prove the efficiency of the proposed semi-active suspension controlling technique. Also it can be seen from figures 8.4, 8.6, 8.8 and

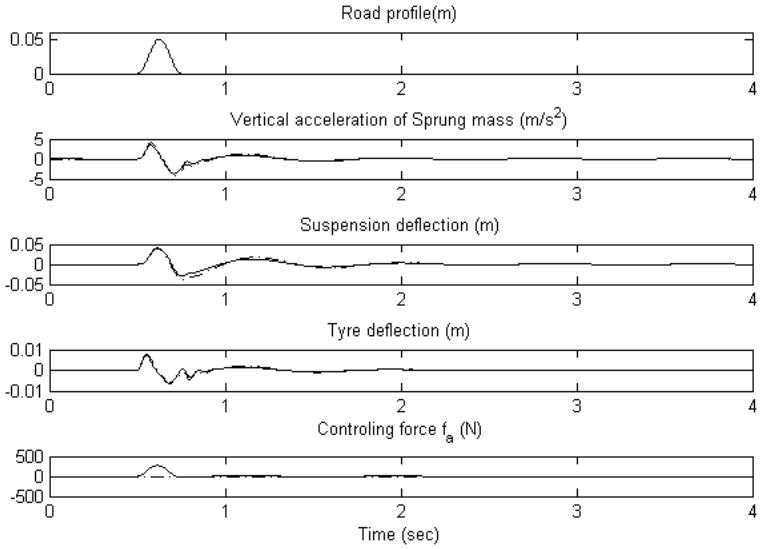

Figure 8.6: 0.05 meter bump simulation: passive suspension (solid line); semi-active suspension (dotted line)

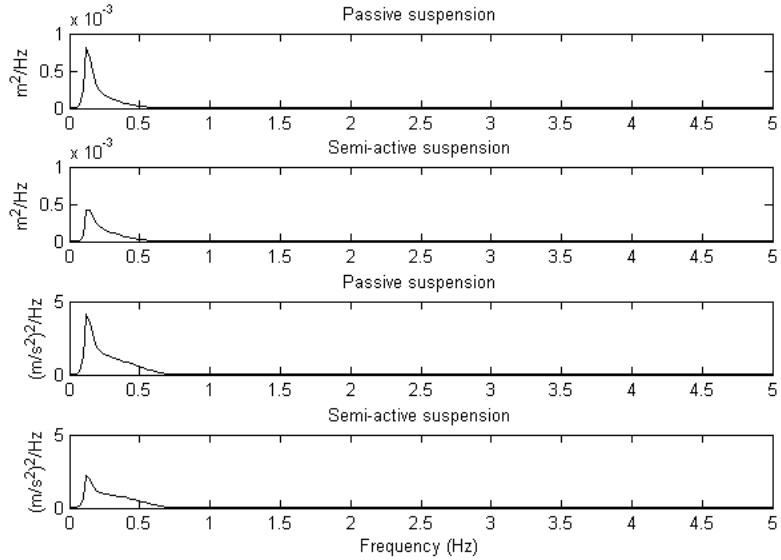

Figure 8.7: Spectral densities of the 0.05 meter bump simulation of the body vertical displacement (first two graphs) and the body vertical acceleration (later two graphs)

8.10, that the controlling force f_a doesn't exceed ± 1000 N which implies lower energy consumption in comparison to the standard limit of ± 8000 N [147].

For a better judgment of the performance of both studied suspensions

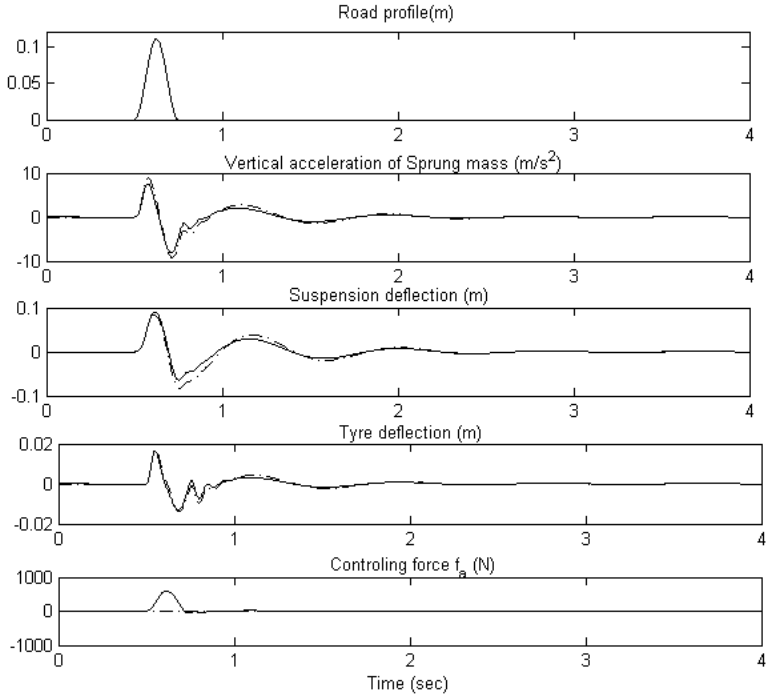

Figure 8.8: 0.11 meter bump simulation: passive suspension (solid line); semi-active suspension (dotted line)

table 8.2 shows the Root Mean Square (RMS) values of the time responses of the three main suspension evaluation criteria; the vertical acceleration of sprung mass ($\ddot{z}_s$), the deflection of the suspension ($z_w - z_s$) and the deflection of the tire ($z_r - z_w$). From this table it can be observed that the semi-active suspension system reduces all the evaluation parameters except for: the tire deflection in the step-up step down and the uneven road; and the suspension deflection of the uneven road. Yet this increase is almost negligible in comparison to the considerable reduction in the other parameters.

8.6 Discussion

In this chapter an intelligent algorithm was presented to facilitate the design of semi-active suspension controllers. The proposed algorithm constructs the needed training data that is later passed to an ANN that auto construct a FLC-based controller that is used to control the suspension.

The presented technique aims to reduce the cost and design time of the controller and make it more portable to be reused for different suspension

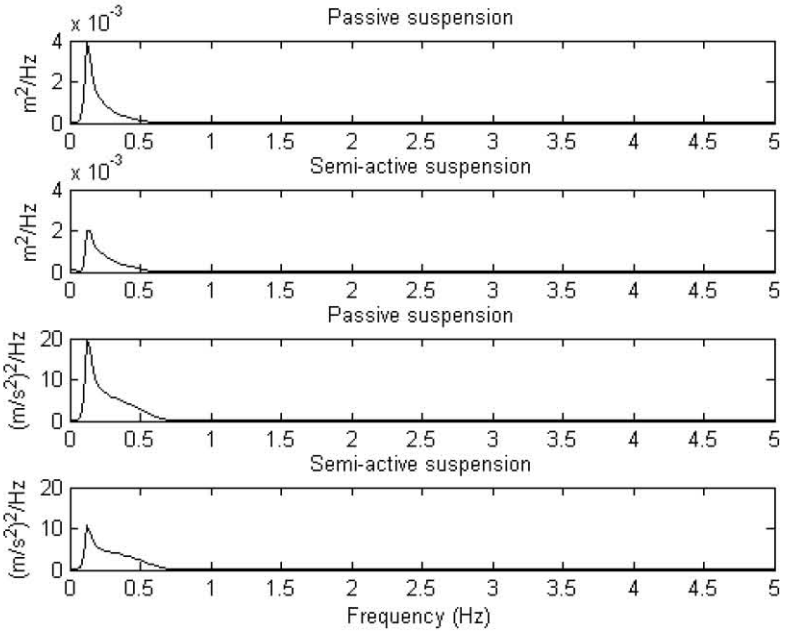

Figure 8.9: Spectral densities of the 0.11 meter bump simulation of the body vertical displacement (first two graphs) and the body vertical acceleration (later two graphs)

		RMS values		
Road profiles		$\ddot{z}_s(m/s^2)$	$(z_w - z_s)$ (m)	$(z_r - z_w)$ (m)
Step-up Step-down	Passive	3.0501	0.0272	0.0100
	Semi-Active	2.7635	0.0302	0.0102
Bump 0.05	Passive	0.8332	0.0097	0.0013
	Semi-Active	0.6825	0.0082	0.0012
Bump 0.11	Passive	1.8329	0.0213	0.0029
	Semi-Active	1.5018	0.0180	0.0026
Uneven road	Passive	1.5923	0.0092	0.0060
	Semi-Active	1.2920	0.0114	0.0075

Table 8.2: RMS values of vertical acceleration of sprung mass ($\ddot{z}_s$), the deflection of the suspension $(z_w - z_s)$ and the deflection of the tyre $(z_r - z_w)$ for different road profiles

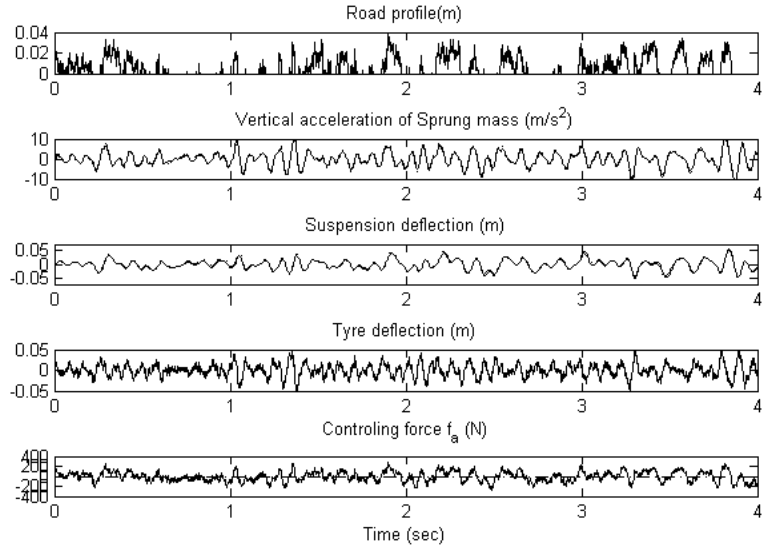

Figure 8.10: Uneven road simulation: passive suspension (solid line); semi-active suspension (dotted line)

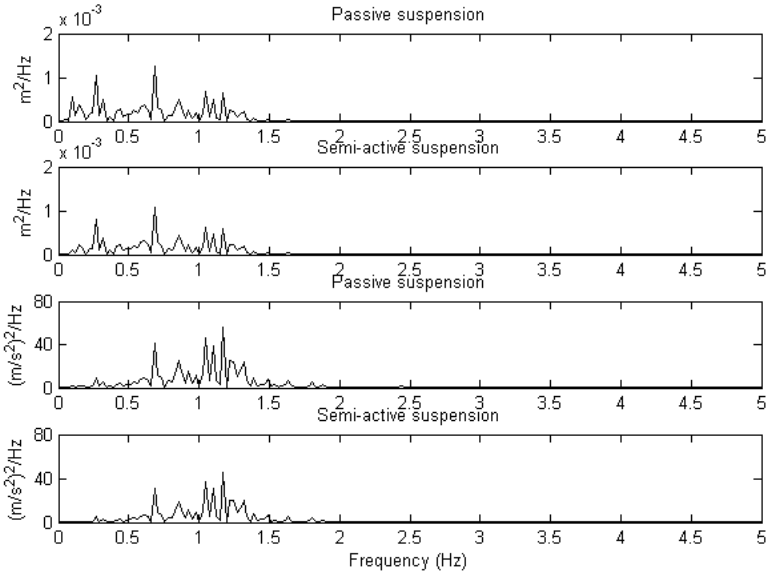

Figure 8.11: Spectral densities of the uneven road simulation of the body vertical displacement (first two graphs) and the body vertical acceleration (later two graphs)

mechanism. This technique also helps to reduce the human-factor error, by minimizing the human intervention, and also eliminate the possible lab-data noise experienced by the similar techniques.

Simulation results on a quarter vehicle model, show the efficiency of the presented controller through testing it over four different road profiles. For a realistic evaluation, the controller's results were compared to the results obtained by a passive suspension, by means of parameters evaluation, spectral density and root mean squared values.

Chapter 9

Conclusions and Future Work

This chapter summarizes the results and the achievements of the presented work. It first reviews briefly the thesis contents and the contribution to the proposed solution. Then it verifies that all the thesis objectives were met. Finally, the chapter presents recommendations for future work.

9.1 Conclusions

Active control of the vehicle dynamics have been proved to have a great impact on improving the vehicle stability. In the literature, different control approaches were reviewed. Where some of these controllers aims to control the longitudinal vehicle forces, others the lateral forces and others the vertical ones. While all the reviewed controllers have been shown to improve the vehicle's stability. Each one of them had its advantage and disadvantages. So in order to compensate for these disadvantages, different controllers have to be grouped together to make up for each other's flaws.

Nevertheless this grouping can not be made simply by an arithmetic operation. Due to the fact that the controlling objectives and/or decisions can conflict and/or overlap, resulting in undesired control outputs. Therefore, a careful integration have been proved to be crucial. Lately, integration trials have been a hot research topic and was defined under the name Integrated Vehicle Dynamics Control (IVDC). Consequently, different approaches have been used in the literature to try to improve the vehicle stability by integrating two or more controllers.

Yet, the proposed controllers were human-designed and depended solely

on human information that is highly error prone. Also, the presented controller have been tested on the same maneuvers used for their design, hence their reliability and predictability were questionable which is a great problem in a safety critical system like the treated one.

Therefore, this thesis presents an auto-generated controller, that could be automatically constructed through artificial intelligence techniques. Such that, an intelligent algorithm is developed to search for the optimum control decision in the control variables space and store it in a database that contains control inputs and their corespondent optimum output. This database is then passed to an Artificial Neural Network that is trained on these data, and from what it have learned, it constructs a Fuzzy Logic Controller that mimics these optimum control decisions. This FLC is the final controller that is used to control the vehicle.

The presented automated-approach have various advantages over the others in literature. The most important of which are the minimization of the human-intervention that cannot be reliable in a safety critical system. It guarantees the inclusion of the maneuvers that a car can go through. It can be easily auto-construct and auto-adapt and therefore can be easily adapted to any vehicle model or any changes in the vehicle characteristics. It almost fully exploits the available control hardware. And the use of the ANNs together with the FLCs helps to combine the advantages of both techniques were the first have auto-learning and adaption capability while the other provides a smooth control performance.

To test the proposed controller, a non linear full vehicle model was designed. And by controlling this vehicle through Active Front Steering and Brake-based Direct Yaw moment Control the controller performance was evaluated. To fairly judge the proposed controller, its performance was compared to the performance of a reference model, another controller from the literature and passive vehicle. All the four vehicles were tested on three different maneuvers: a J-turn, a change lane and a double change lane. Where these maneuvers were tested in dry weather conditions at speeds of 20 and 30 m/s^2 and on a slippery road condition at a speed of 20 m/s^2.

Simulation results shows the effectiveness of the proposed approach. Also, as the controlling approach seems to be promising in controlling other mechanical systems. It is tested on a semi-active suspensions, that also yielded

very satisfactory results.

9.2 Thesis objectives Fulfillment

This section is dedicated to verify that all the thesis objectives were met. It will discuss how all the work break down of objectives points were fulfilled.

First, the proposed IVDC effectively combined between two different stand-alone vehicle chassis controllers that compliment each other: the AFS and the brake-based DYC. Such that, as discussed in section 3.2, that while the AS systems improves the vehicle stability in normal circulating conditions, they became less effective as the vehicle reaches its handling limits. On the other hand, the brake-based DYC is the most efficient as the vehicle approaches its handling limits, but in normal circulating conditions it produces undesired velocity reduction that decreases the driver controllability feel. Therefore, both controllers were integrated to compensate the drawbacks of each other. Also the decision of choosing these controllers over their competitors was supported by their hardware simplicity, relatively low cost and their availability in the market, so that the study could be based on realistic and achievable implementation goals. Such that, the brake-based DYC shares its sensors and actuators with the ABS system that is available in almost all modern cars. And the AFS system adds electric motors to the traditional front wheels steering system with minimal extra sensors and actuators.

Second, the presented IVDC approach tends to exploit the advantages of each of the two integrated control systems through the proposed intelligent algorithm. Such that, the algorithm has extensively varied the possible control input of each of the two controllers until the optimal control combination was reached. In this way the IVDC insures to make the best use of the available hardware resources.

Third, the reliability and predictability of the controller was shown by training the ANN on the data collected through extensive generic maneuvers to cover any driving situation that the driver might go through. And finally, unlike the proposed systems in the literature, the controller was tested on a completely new and different maneuvers, as shown in chapter 7.

Fourth, the system design approach makes it of a high repetitiveness since all the learning is done offline. Therefore, the system will not be affected

later by a certain road characteristic and forget about another. Neither would it change if a certain driver uses the car more frequently than the other and hence provides worse performance with the driver that rides less frequently. On the contrary, the system learns the vehicle characteristics and behavior at the beginning and repeats the learned control actions.

Fifth, the system effectively needs minimal human intervention to learn the vehicle characteristics and behavior. Which makes it easily portable from one vehicle model to another or from one suspension model to another. Such that the data generation and the learning phases are done automatically through intelligent systems with the minimal human aid.

Sixth, a high quality non-linear full vehicle model is developed with 13 degrees of freedom to model the necessary vehicle characteristics to simulate the and evaluate the performance of the proposed controller.

Seventh, the thesis also defines the control objectives that the controller should achieve. And described the equations that calculates their desired values. And finally evaluated the obtained control results against the desired values for a better insight of the results.

Eighth, the model have effectively shown results improvements in the vehicle handling and control in comparison to an exact uncontrolled vehicle and another vehicle controlled by a controller from the literature.

9.3 Recommendations for Further Work

The results yielded by the proposed algorithm and control strategy shows very promising results, which encourages to make a long list of future work and research. Some of which are:

- Test the model using a real-time hardware to verify its correct response timing.
- Test the system on a Hardware-in-the-Loop (HIL) systems to test the whole model as a vehicle-driver closed loop model. Such that, the controller can be tested at the presence of unpredictable driver reactions.
- Finally, mount the controller on a real vehicle for a production prototype.
- Last but not least, apply the same techniques on more nonlinear systems, other than the semi-active suspensions, and test the controller

performance on them.

Bibliography

[1] Body and chassis controls. `http://www.neweagle.net/support/wiki/index.php?title=Body_and_Chassis_Controls`, June 2012. [Online; accessed 21-April-2013].

[2] Observatorio Nacional de Seguridad Vial. Información de accidentes. Technical Report 25, Dirección general de Tráfico, Ministerio del interior, August 2010.

[3] M. Aga and A Okada. Analysis of vehicle stability control (vscs) effectiveness from accident data. In *Proceedings of the 18th International Technical Conference on the Enhanced Safety of Vehicles*, Washington, DC, 2003. NHTSA.

[4] Pierre Duysinx. Introduction to vehicle dynamics. e-publish University of Liege, 2012.

[5] D Gillespie Thomas. Fundamentals of vehicle dynamics. *Society of Automotive Engineering Inc*, pages 168–193, 1992.

[6] Thomas Kenneth Garrett, Kenneth Newton, and William Steeds. *Motor Vehicle*. Butterworth-Heinemann, 13 edition, 2000.

[7] Willy Klier, Gerd Reimann, and Wolfgang Reinelt. Concept and functionality of the active front steering system. *SAE paper*, 20042212:0073, 2004.

[8] Rolf Isermann. Mechatronic systems–innovative products with embedded control. *Control Engineering Practice*, 16(1):14 – 29, 2008.

[9] Junjie He. *Integrated Vehicle Dynamics Control Using Active Steering, Driveline and Braking*. Phd dissertation, University of Leeds, UK, 2005.

[10] Masao Nagai, Yutaka Hirano, and Sachiko Yamanaka. Integrated control of active rear wheel steering and direct yaw moment control. *Vehicle System Dynamics*, 27(5-6):357–370, 1997.

[11] Rainer Busch, Klaus Webers, and Achim Seibertz. Ford integrated vehicle dynamics control: concept. *Vortrag*, 3:2003, 2003.

[12] Fan Yu, Dao-Fei Li, and DA Crolla. Integrated vehicle dynamics control state of the art review. In *Vehicle Power and Propulsion Conference, 2008. VPPC'08. IEEE*, pages 1–6. IEEE, 2008.

[13] Michael Negnevitsky. *Artificial Intelligence: A Guide to Intelligent Systems*. Addison Wesley, 2005.

[14] M.J.L. Boada, B.L. Boada, C. Castejon, and V. Diaz. A fuzzy-based suspension vehicle depending on terrain. *Int. J. of Vehicle Design*, 37(4):311–326, 2005.

[15] Christof Ebert and Capers Jones. Embedded software: Facts, figures, and future. *Computer*, 42(4):42–52, 2009.

[16] Amos Albert. Comparison of event-triggered and time-triggered concepts with regard to distributed control systems. *Embedded World*, 2004:235–252, 2004.

[17] K Senthilkumar and R Ramadoss. Designing multicore ecu architecture in vehicle networks using autosar. In *Advanced Computing (ICoAC), 2011 Third International Conference on*, pages 270–275. IEEE, 2011.

[18] DA Crolla, G Firth, and D Horton. *An introduction to vehicle dynamics*. University of Leeds, Department of Mechanical Engineering, 1992.

[19] Mark Albert Selby. *Intelligent vehicle motion control*. Phd dissertation, University of Leeds, UK, 2003.

[20] Tim Gordon, Mark Howell, and Felipe Brandao. Integrated control methodologies for road vehicles. *Vehicle System Dynamics*, 40(1-3):157–190, 2003.

[21] Choose-ESC. Bringing life-saving vehicle technology to market. Electronic, Gaby Roosen, Campaign Manager, Square de Meeus 37 - B-1000 Brussels.

[22] Insurance Institute for Highway Safety, editor. *Status Report*, number 6 in 45, 1005 N. Glebe Rd., Arlington, VA 22201, June 19 2010.

[23] Department of Transportation. Federal motor vehicle safety standards; electronic stability control systems; controls and displays. Final rule 27662, National Highway Traffic Safety Administration, USA, 2007.

[24] Observatorio Nacional de Seguridad Via. Indicador rÁpido de accidentalidad en carretera año 2010. Cómputo de las víctimas a 24 hora, DIRECCIÓN GENERAL DE TRÁFICO, MINISTERIO DEL INTERIO, 1 2011.

[25] C.M. Farmer. Effects of electronic stability control on fatal crash risk. Technical report, Insurance Institute for Highway Safety, Arlington, VA:22201, May 2010.

[26] *TEXTS ADOPTED*, P6_TA-PROV(2009)03-10. EUROPEAN PARLIAMENT, 2009-2010.

[27] Regulation of the european parliament and of the council concerning type-approval requirements for the general safety of motor vehicles, May 2008.

[28] choose esc. Esc compulsory form 2011. Electronic, November 2010.

[29] David Burton, Amanda Delaney, Stuart Newstead, David Logan, and Brian Fildes. Effectiveness of abs and vehicle stability control systems. Technical report, Royal Automotive Club of Victoria, April 2004.

[30] Tejas Shrikant Kinjawadekar. Model-based design of electronic stability control system for passenger cars using carsim and matlab-simulink. Masters thesis, The Ohio State University, US, 2009.

[31] Jo Yung Wong. *Theory of ground vehicles*. Wiley-Interscience, 3 edition, 2001.

[32] Rajesh Rajamani. *Vehicle dynamics and control*. Mechanical Engineering Series. Springer, 2006.

[33] M. Abe and W. Manning. Chapter 3 - fundamentals of vehicle dynamics. In *Vehicle Handling Dynamics*, pages 47 – 118. Butterworth-Heinemann, Oxford, 2009.

[34] Vicente Diaz. *Automóviles y ferrocarriles*. Universidad Nacional de Educación a Distancia, 2012.

[35] Moustapha Doumiati, Olivier Sename, Luc Dugard, John Jairo Martinez Molina, Peter Gaspar, Zoltan Szabo, et al. Integrated vehicle dynamics control via coordination of active front steering and rear braking. *European Journal of Control*, 2013.

[36] RS Sharp and DA Crolla. Controlled rear steering for cars-a review. In *Proceeding of the ImechE, International Conference" Advanced Suspensions C*, volume 437, 1988.

[37] Yoshimi Furukawa, Naohiro Yuhara, Shoichi Sano, Hideo Takeda, and Yoshinobu MATSUSHITA. A review of four-wheel steering studies from the viewpoint of vehicle dynamics and control. *Vehicle System Dynamics*, 18(1-3):151–186, 1989.

[38] Masao Nagai. Active four-wheel-steering system by model following control. *Vehicle System Dynamics*, 18:428–439, 1989.

[39] Bilin Aksun Guvenc, Tilman Bunte, Dirk Odenthal, and Levent Guvenc. Robust two degree-of-freedom vehicle steering controller design. *Control Systems Technology, IEEE Transactions on*, 12(4):627–636, 2004.

[40] Moustapha Doumiati, Olivier Sename, John Jairo Martinez Molina, Luc Dugard, Peter Gaspar, Zoltan Szabo, Jozsef Bokor, et al. Vehicle yaw control via coordinated use of steering/braking systems. In *Preprints of the 18th IFAC World Congress*, pages 644–649, 2011.

[41] Philip Koehn and Michael Eckrich. Active steering - the bmw approach towards modern steering technology. Technical Paper 2004-01-1105, SAE, 2004.

[42] Yasuji Shibahata, K Nakamura, Hideo Itoh, and N Irie. *The development of an experimental four-wheel-steering vehicle*. 1986.

[43] T Takiguchi, H Inoue, H Kanazawa, S Furutani, and N Yasuda. *Improvement of vehicle dynamics by vehicle-speed-sensing four-wheel steering system*. 1986.

[44] Shoiehi Sano, S Shiraishi, and Y Furukawa. *Four wheel steering system with rear wheel steer angle controlled as a function of steering wheel angle*. 1986.

[45] S Sano, Y Furukawa, T Nihei, M Abe, and M Serizawa. Handling characteristics of steer angle dependent four wheel steering system. *SAE Paper*, 885034, 1988.

[46] K Fukui, H Hasegawa, Y Hayashi, and K Miki. *Analysis of Driver and a" four Wheel Steering Vehicle" System Using a Driving Simulator*. 1988.

[47] H Sato, A Hirota, H Yanagisawa, and T Fukushima. Dynamic characteristics of a whole wheel steering vehicle with yaw velocity feedback rear wheel steering. In *Road Vehicle Handling, I Mech E Conference Publications 1983-5*, number C124/83, 1983.

[48] John C Whitehead. Four wheel steering-maneuverability and high speed stabilization. 1988.

[49] Shin Koike, Hiroki Sato, Hiroyuki Kawai, and Masaru Ishikawa. Development of four wheel steering system using yaw rate feedback control. 1991.

[50] X Xia and EH Law. Nonlinear analysis of closed loop driver/automobile performance with four wheel steering control. *ITS technology collection on CD-ROM: SAE's essential resource for ITS vehicle applications, 1998*, 1992.

[51] Kiyoshi Wakamatsu, Yoshimitsu Akuta, Manabu Ikegaya, and Nobuyoshi Asanuma. Adaptive yaw rate feedback 4ws with tire/road friction coefficient estimator. *Vehicle System Dynamics*, 27(5-6):305–326, 1997.

[52] A Szosland. Fuzzy logic approach to four-wheel steering of motor vehicle. *International Journal of Vehicle Design*, 24(4):350–359, 2000.

[53] Wolfgang Reinelt, Willy Klier, Gerd Reimann, Wolfgang Schuster, and Reinhard Groβheim. Active front steering (part 2): Safety and functionality. *SAE paper*, 01(1102), 2004.

[54] Bin Li and Fan Yu. Optimal model following control of four-wheel active steering vehicle. In *Information and Automation, 2009. ICIA'09. International Conference on*, pages 881–886. IEEE, 2009.

[55] IAN AUSTEN. Drive by wire, an aerospace solution. Electronically, The New York Times, March 29 2013. [Online; accessed 31-April-2013] `http://www.nytimes.com/2013/03/31/automobiles/drive-by-wire-an-aerospace-solution.html?smid=pl-share`.

[56] Y Wang and M Nagai. Intelligent vehicle motion control by adaptive front steering system. In *International Symposium on Advanced Vehicle Control, 1992, Yokohama, Japan*, 1992.

[57] Y Tagawa, H Ogata, K Morita, M Nagai, and H Mori. Robust active steering system taking account of nonlinear dynamics. *Vehicle System Dynamics*, 25(S1):668–681, 1996.

[58] Eiichi Ono, Shigeyuki Hosoe, Hoang D Tuan, et al. Robust stabilization of vehicle dynamics by active front wheel steering control. In *Decision and Control, 1996., Proceedings of the 35th IEEE*, volume 2, pages 1777–1782. IEEE, 1996.

[59] E Ono, S Hosoe, S Doi, K Asano, and Y Hayashi. Theoretical approach for improving the vehicle robust stability and maneuverability by active front wheel steering control. *Vehicle system dynamics*, 29(S1):748–753, 1998.

[60] Jürgen Ackermann, Tilman Bünte, Wolfgang Sienel, Holger Jeebe, and Karl Naab. Driving safety by robust steering control. In *in Proc. Int. Symposium on Advanced Vehicle Control*. Citeseer, 1996.

[61] Juergen Ackermann. Robust control prevents car skidding. *Control Systems, IEEE*, 17(3):23–31, 1997.

[62] Jrgen Ackermann and T Bünte. Yaw disturbance attenuation by robust decoupling of car steering. *Control Engineering Practice*, 5(8):1131–1136, 1997.

[63] Jürgen Ackermann. Active steering for better safety, handling and comfort. In *Proceedings of Advances in Vehicle Control and Safety*. Citeseer, 1998.

[64] Long Wang and J Ackermann. Robustly stabilizing pid controllers for car steering systems. In *American Control Conference, 1998. Proceedings of the 1998*, volume 1, pages 41–42. IEEE, 1998.

[65] Ryouhei Hayama, Katsutoshi Nishizaki, Shirou Nakano, and Kazuhiro Katou. The vehicle stability control responsibility improvement using steer-by-wire. In *Intelligent Vehicles Symposium, 2000. IV 2000. Proceedings of the IEEE*, pages 596–601. IEEE, 2000.

[66] Paul Yih and J Christian Gerdes. Steer-by-wire for vehicle state estimation and control. In *Proceedings of AVEC*, pages 785–790, 2004.

[67] Paul Yih and J Christian Gerdes. Modification of vehicle handling characteristics via steer-by-wire. *Control Systems Technology, IEEE Transactions on*, 13(6):965–976, 2005.

[68] Yung-Hsiang Judy Hsu and J Christian Gerdes. Stabilization of a steer-by-wire vehicle at the limits of handling using feedback linearization. In *Proceedings of the 2005 ASME International Mechanical Engineering Congress and Exposition*, 2005.

[69] Nagai M., Shino M., and Gao F. Study on integrated control of active front steer angle and direct yaw moment. *JSAE Review*, 23:309–315(7), July 2002.

[70] M. J. Boada, B. L. Boada, A. Muñoz, and V. Díaz. Integrated control of front-wheel steering and front braking forces on the basis of fuzzy logic. *Proceedings of the Institution of Mechanical Engineers – Part D – Journal of Automobile Engineering*, 220(3):253 – 267, 2006.

[71] M Nagai and M Ohki. Theoretical study on active four wheel steering system by virtual vehicle model following control. *JSAE Review*, 9(4), 1988.

[72] M Aga, H Kusunoki, Y Satoh, R Saitoh, and M Ito. Design of 2-degree-of-freedom control system for active front-and-rear-wheel steering. *SAE transactions*, 99(6):1529–1536, 1990.

[73] Y Lin. Improving vehicle handling performance by a closed-loop 4ws driving controller. *SAE transactions*, 1992.

[74] Sven Kleine and JOHANNES L VAN NIEKERK. Modelling and control of a steer-by-wire vehicle. *Vehicle System Dynamics*, 29(S1):114–142, 1998.

[75] Feng Du, Ji-shun Li, Lun Li, and Dong-hong Si. Robust control study for four-wheel active steering vehicle. In *Electrical and Control Engineering (ICECE), 2010 International Conference on*, pages 1830–1833. IEEE, 2010.

[76] Norhazimi Hamzah, Yahaya Md Sam, Hazlina Selamat, M Khairi Aripin, and Muhamad Fahezal Ismail. Yaw stability improvement for four-wheel active steering vehicle using sliding mode control. In *Signal Processing and its Applications (CSPA), 2012 IEEE 8th International Colloquium on*, pages 127–132. IEEE, 2012.

[77] Khisbullah Hudha, Mohd Hafidz Zakaria, and Noreffendy Tamaldin. Hardware in the loop simulation of active front wheel steering control for yaw disturbance rejection. *International Journal of Vehicle Safety*, 5(4):356–373, 2011.

[78] Infiniti g coupe specs. `http://www.infiniti-me.com/en/shopping_tools/buildtool.selecttrim.g_coupe.html`. [Online; accessed 1-May-2013].

[79] Masato Abe, Naoto Ohkubo, and Yoshio Kano. A direct yaw moment control for improving limit performance of vehicle handling-comparison and cooperation with 4ws. *Vehicle System Dynamics*, 25(S1):3–23, 1996.

[80] Kenneth R Buckholtz. Use of fuzzy logic in wheel slip assignment–part i&ii. *SAE paper*, (2002-01):1220, 2002.

[81] T Yoshioka, T Adachi, T Butsuen, H Okazaki, and H Mochizuki. Application of sliding-mode control to control vehicle stability. In *Proceedings of AVEC*, volume 98, pages 455–60, 1998.

[82] Tohru Yoshioka, Tomohiko Adachi, Tetsuro Butsuen, Haruki Okazaki, and Hirotaka Mochizuki. Application of sliding-mode theory to direct yaw-moment control. *JSAE review*, 20(4):523–529, 1999.

[83] Masato Abe, Yoshio Kano, Yasuji Shibahata, and Yoshimi Furukawa. Improvement of vehicle handling safety with vehicle side-slip control by direct yaw moment. In *IAVSD Symposium (16th: 1999: Pretoria, South Africa). The dynamics of vehicles on roads and on tracks: proceedings of the 16th IAVSD Symposium*, 1999.

[84] Masato Abe, Yoshio Kano, Kazuasa Suzuki, Yasuji Shibahata, and Yoshimi Furukawa. Side-slip control to stabilize vehicle lateral motion by direct yaw moment. *JSAE review*, 22(4):413–419, 2001.

[85] Shoji Inagaki, Ikuo Kshiro, and Masaki Yamamoto. Analysis on vehicle stability in critical cornering using phase-plane method. In *International Symposium on Advanced Vehicle Control (1994: Tsukuba-shi, Japan). Proceedings of the International Symposium on Advanced Vehicle Control 1994*, 1994.

[86] Ken Koibuchi, Masaki Yamamoto, and Yoshiki Fukada. Vehicle stability control in limit cornering by active brake. 1996.

[87] Yoshiyuki Yasui, Kenji Tozu, and Noriaki Hattori. Improvement of vehicle directional stability for transient steering maneuvers using active brake control. 1996.

[88] V Alberti and E Babbel. Improved driving stability by active braking of the individual wheels. In *Proc. of the International Symposium on Advanced Vehicle Control*, pages 717–732, 1996.

[89] Jong Hyeon Park and Woo Sung Ahn. H¡ sub¿8¡/sub¿ yaw-moment control with brakes for improving driving performance and stability. In *Advanced Intelligent Mechatronics, 1999. Proceedings. 1999 IEEE/ASME International Conference on*, pages 747–752. IEEE, 1999.

[90] Koji Uematsu and J Christian Gerdes. A comparison of several sliding surfaces for stability control. In *Proceedings of International Symposium on Advanced Vehicle Control,(AVEC)*, pages 601–608, 2002.

[91] Sumio Motoyama, H Uki, K ISODA Manager, and H YUASA Manager. Effect of traction force distribution control on vehicle dynamics. *Vehicle System Dynamics*, 22(5-6):455–464, 1993.

[92] Damrongrit Piyabongkarn, John Grogg, Qinghui Yuan, Jae Lew, and Rajesh Rajamani. Dynamic modeling of torque-biasing devices for vehicle yaw control. In *Automotive Dynamics, Stability and Controls Conference and Exhibition*, 2006.

[93] Hilding Elmqvist, Sven Erik Mattsson, Hans Olsson, Johan Andreasson, Martin Otter, Christian Schweiger, and Dag Bruck. Realtime simulation of detailed vehicle and powertrain dynamics. *SAE SP*, pages 63–76, 2004.

[94] M YAMAMOTO. Active control strategy for improved handling and stability. *SAE transactions*, 100(6):1638–1648, 1991.

[95] MJL Boada, BL Boada, B Munoz, and V Diaz. Neural control for a semi-active suspension of a half-vehicle model. *International journal of vehicle autonomous systems*, 3(2):306–329, 2005.

[96] Jun Wang, David A Wilson, Wenli Xu, and David A Crolla. Active suspension control to improve vehicl0e ride and steady-state handling. In *Decision and Control, 2005 and 2005 European Control Conference. CDC-ECC'05. 44th IEEE Conference on*, pages 1982–1987. IEEE, 2005.

[97] Junjie He, DA Crolla, MC Levesley, and WJ Manning. Coordination of active steering, driveline, and braking for integrated vehicle dynamics control. *Proceedings of the Institution of Mechanical Engineers, Part D: Journal of Automobile Engineering*, 220(10):1401–1420, 2006.

[98] Masao Nagai, Yutaka Hirano, and Sachiko Yamanaka. Integrated robust control of active rear wheel steering and direct yaw moment control. *Vehicle System Dynamics*, 29(S1):416–421, 1998.

[99] Masao Nagai, Sachiko Yamanaka, Yutaka Hirano, et al. Integrated control of active rear wheel steering and yaw moment control using braking forces. *JSME International Journal-Series C-Mechanical Systems Machine Elements and Manufact*, 42(2):301–308, 1999.

[100] BA Guvenc, T Acarman, and L Guvenc. Coordination of steering and individual wheel braking actuated vehicle yaw stability control. In *Intelligent Vehicles Symposium, 2003. Proceedings. IEEE*, pages 288–293. IEEE, 2003.

[101] J. Jo, S. You, J. Joeng, K. Lee, and K. Yi. Vehicle stability control system for enhancing steerabilty, lateral stability, and roll stability. *International Journal of Automotive Technology*, 9:571–576, 2008. 10.1007/s12239-008-0067-9.

[102] T. Yoshimura and Y. Emoto. Steering and suspension system of a full car model using fuzzy reasoning based on single input rule modules. *International Journal of Vehicle Autonomous Systems*, 1:237–255(19), 8 October 2003.

[103] T Yoshimura and K Watanabe. Active suspension of a full car model using fuzzy reasoning based on single input rule modules with dynamic absorbers. *International journal of vehicle design*, 31(1):22–40, 2003.

[104] R. Karbalaei, A. Ghaffari, R. Kazemi, and S.H. Tabatabaei. Design of an integrated afs/dyc based on fuzzy logic control. In *Vehicular Electronics and Safety, 2007. ICVES. IEEE International Conference on*, pages 1–6, 2007.

[105] Liang Chu, Xinzhao Gao, Jianhua Guo, Hongwei Liu, Libo Chao, and Mingli Shang. Coordinated control of electronic stability program and active front steering. *Procedia Environmental Sciences*, 12:1379–1386, 2012.

[106] Junjie He, David A Crolla, Martin C Levesley, and Warren J Manning. Integrated active steering and variable torque distribution control for

improving vehicle handling and stability. *SAE transactions*, 113(6):638–647, 2004.

[107] J He, DA Crolla, MC Levesley, and WJ Manning. Integrated chassis control through coordination of active front steering and intelligent torque distribution. In *Proc. AVEC*, volume 333339, 2004.

[108] Eiichi Ono, Yoshikazu Hattori, Y Muragishi, and K Koibuchi. Vehicle dynamics integrated control for four-wheel-distributed steering and four-wheel-distributed traction/braking systems. *vehicle system dynamics*, 44(2):139–151, 2006.

[109] A Goodarzi, A Sabooteh, and E Esmailzadeh. Automatic path control based on integrated steering and external yaw-moment control. *Proceedings of the Institution of Mechanical Engineers, Part K: Journal of Multi-body Dynamics*, 222(2):189–200, 2008.

[110] Xiujian Yang, Zengcai Wang, and Weili Peng. Coordinated control of afs and dyc for vehicle handling and stability based on optimal guaranteed cost theory. *Vehicle System Dynamics*, 47(1):57–79, 2009.

[111] Nenggen Ding and Saied Taheri. An adaptive integrated algorithm for active front steering and direct yaw moment control based on direct lyapunov method. *Vehicle System Dynamics*, 48(10):1193–1213, 2010.

[112] B Li and F Yu. Design of a vehicle lateral stability control system via a fuzzy logic control approach. In Professional Engineering Publishing, editor, *Proceedings of the Institution of Mechanical Engineers - D*, page 313, 2010.

[113] Michael Negnevitsky. *Artificial Intelligence: A Guide to Intelligent Systems*. Addison-Wesley Longman Publishing Co., Inc., Boston, MA, USA, 2nd edition, 2004.

[114] P.P. Cruz, J.M. Aquino, and M.R. Elizondo. Vector control using anfis controller with space vector modulation [induction motor drive applications]. In *Universities Power Engineering Conference, 2004. UPEC 2004. 39th International*, volume 2, pages 545 – 549 vol. 1, sept. 2004.

[115] Hany Hagras. Unpublished lecture notes on fuzzy logic. Presented in the German University in Cairo.

[116] Hany Hagras. Unpublished lecture notes on artificial neural networks. Presented in the German University in Cairo.

[117] L. Zadeh. Fuzzy sets. *Information and Control*, 8(3):338–353, 1965.

[118] Perambur S. Neelakanta. In search of a cyberspace, to launch biologically-inspired advanced computing strategies. In *International Conference on Advanced Computing*. ICAC 2009, August 2009.

[119] John A. Bullinaria. Biological neurons and neural networks, artificial neurons. Lecture 2 on: Neural Computation, 2008.

[120] Graham Kendall. Introduction to artificial intelligence. Lecture Notes: G5AIAI, University of Nottingham, September 2001.

[121] Simon Haykin. *Neural Networks: A Comprehensive Foundation*. Prentice-Hall, 2 edition, 1999.

[122] L. Fausett. *Fundamentals of Neural Networks : Architectures, Algorithms and Applications*. Prentice-Hall, 1994.

[123] T. Takagi and M. Sugeno. Derivation of fuzzy control rules from human operator's control actions. In *Knowledge Representation and Decision Analysis*, pages 55–60. IFAC Symposium of Fuzzy Information, July 1983.

[124] E.H. Mamdani and S. Assilian. An experiment in linguistic synthesis with a fuzzy logic controller. *International Journal of Man-Machine Studies*, 7(1):1 – 13, 1975.

[125] H. Dugoff, C. Fancher, and L. Segel. An analysis of tire traction properties and their influence on vehicle dynamic performance. *SAE Transaction*, 3(700377):1219–1243, 1970.

[126] Håvard Fjír Grip, Lars Imsland, Tor A. Johansen, Thor I. Fossen, Jens C. Kalkkuhl, and Avshalom Suissa. Nonlinear vehicle side-slip estimation with friction adaptation. *Automatica*, 44(3):611–622, 2008.

[127] Y. Furukawa and M. Abe. Direct yaw moment control with estimating side-slip angle by using on-board-tire-model. In *International Symposium on Advanced Vehicle Control*. SAE, 1998.

[128] H. Kim and J. Ryu. Sideslip angle estimation considering short-duration longitudinal velocity variation. *International Journal of Automotive Technology*, 12:545–553, 2011. 10.1007/s12239-011-0064-2.

[129] H.F. Grip, L. Imsland, T.A. Johansen, J.C. Kalkkuhl, and A. Suissa. Vehicle sideslip estimation. *Control Systems, IEEE*, 29(5):36 –52, oct. 2009.

[130] G. Zhengqi, L. Yufeng, and W. Seemann. The performance of a vehicle with four-wheel steering control in crosswind. *International Journal of Vehicle Autonomous Systems*, 1:256–269(14), 8 October 2003.

[131] Tang-Hsien Chang. Field performance assessment of the advance-f automatic steering control vehicle. *Control Engineering Practice*, 12(5):569 – 576, 2004. Fuzzy System Applications in Control.

[132] Dirk E. Smith and John M. Starkey. Effects of model complexity on the performance of automated vehicle steering controllers: Model development, validation and comparison. *Vehicle System Dynamics: International Journal of Vehicle Mechanics and Mobility*, 24(2):163 – 181, March 1995.

[133] Horiuchi S., Okada K., and Nohtomi S. Improvement of vehicle handling by nonlinear integrated control of four wheel steering and four wheel torque. *JSAE Review*, 20:459–464(6), October 1999.

[134] A. El Hajjaji and S. Bentalba. Fuzzy path tracking control for automatic steering of vehicles. *Robotics and Autonomous System*, 43:203–213, 2003.

[135] Rana Farag, Beatriz Boada, Vicente Diaz, and Maria Jesus Boada. A neuro-fuzzy-based controller to improve the efficiency of a semi-active suspension depending on terrain. In *13th EAEC European Automotive Congress*, 2011.

[136] J.-S.R. Jang. Anfis: adaptive-network-based fuzzy inference system. *Systems, Man and Cybernetics, IEEE Transactions on*, 23(3):665 –685, may/jun 1993.

[137] J. Wesley Hines, Lefteri H. Tsoukalas, and Robert E. Uhrig. *MATLAB Supplement to Fuzzy and Neural Approaches in Engineering,*. John Wiley & Sons, Inc., New York, NY, USA, 1997.

[138] Jeffery Anderson. Fuzzy logic approach to vehicle stability control. Master's thesis, Mechanical Engineering, Clemson University, August 2010.

[139] Charles Poussot-Vassal, Cristiano Spelta, Olivier Sename, SM Savaresi, and Luc Dugard. Survey and performance evaluation on some automotive semi-active suspension control methods: A comparative study on a single-corner model. *Annual Reviews in Control*, 2012.

[140] Jiangtao Cao, Honghai Liu, Ping Li, and David J Brown. State of the art in vehicle active suspension adaptive control systems based on intelligent methodologies. *Intelligent Transportation Systems, IEEE Transactions on*, 9(3):392–405, 2008.

[141] Tejas Shrikant Kinjawadekar. Model-based design of electronic stability control system for passenger cars using carsim and matlab-simulink. Master's thesis, The Ohio State University, 2009.

[142] K Kamalakannan, A ElayaPerumal, S Mangalaramanan, and K Arunachalam. Performance analysis and behaviour characteristics of cvd (semi active) in quarter car model. *JJMIE*, 5(3), 2011.

[143] Salah G Foda. Neuro-fuzzy control of a semi-active car suspension system. In *Communications, Computers and signal Processing, 2001. PACRIM. 2001 IEEE Pacific Rim Conference on*, volume 2, pages 686–689. IEEE, 2001.

[144] Shiuh-Jer Huang and Wei-Cheng Lin. Adaptive fuzzy controller with sliding surface for vehicle suspension control. *Fuzzy Systems, IEEE Transactions on*, 11(4):550–559, 2003.

[145] Y-J Lin, Joseph Padovan, and Y-Q Lu. Toward better ride performance of vehicle suspension system via intelligent control. In *Systems, Man and*

Cybernetics, 1992., IEEE International Conference on, pages 1470–1475. IEEE, 1992.

[146] ISO. Mechanical vibration and shock: Evaluation of human exposure to whole-body vibration. part 1, general requirements: International standard iso 2631-1: 1997 (e). Technical report, ISO, 1997.

[147] Jun Wang, David A Wilson, Wenli Xu, and David A Crolla. Active suspension control to improve vehicl0e ride and steady-state handling. In *Decision and Control, 2005 and 2005 European Control Conference. CDC-ECC'05. 44th IEEE Conference on*, pages 1982–1987. IEEE, 2005.

Appendix A

Back-propagation learning algorithm: equations

Equations from [116, Hagras Lecture Notes]:

Notation:

Output nodes: $y_k = \varphi(v_k), k = 1, 2, ..., l.$
Hidden nodes: $h_i = \varphi^h(v_i^h), i = 1, 2, ..., n.$
Inputs: $x_j, j = 1, 2, ..., m.$
Output weights: w_{ki}
Hidden weights: w_{ij}^h

Network formulation: $y_k = \varphi[\sum_{i=0}^{n} w_{ki} h_i] = \varphi[\sum_{i=0}^{n} w_{ki} \varphi^h(\sum_{j=0}^{m} w_{ij}^h x_j)]$

$x_o = h_0 = +1$, w_{ko} and w_{io}^h **are biases.**

Training data: $\{x(s), d(s)\}_{s=1}^{M}$, $x(s) = [x_1(s)x_2(s)...x_m(s)]^T$,

$d(s) = [d_1(s)d_2(s)...d_l(s)]^T$.

Error training: $\varepsilon(t) = \frac{1}{2} \sum_{k=1}^{l} e_k^2(t)$, $e_k(t) = d_k(s(t)) - y_k(s(t))$.

Weight updating: Instantaneous error gradient-descent:

Local gradients $\delta_k(t)$, $\delta_t^h(t)$:

$$\Delta w_{ki}(t) = -\eta \frac{\partial \varepsilon(t)}{\partial w_{ki}(t)} = \eta \delta_k(t) h_i(t)$$

$$\Delta w_{ij}^h(t) = -\eta \frac{\partial \varepsilon(t)}{\partial w_{ij}^h(t)} = \eta \delta_i^h(t) x_j(t)$$

To speed up the convergance, a moment term is added:

$$\Delta w_{ki}(t) = \eta \delta_k(t) h_i(t) + \alpha \Delta w_{ki}(t-1)$$

$$\Delta w_{ij}^h(t) = \eta \delta_i^h(t) x_j(t) + \alpha \Delta w_{ij}^h(t-1)$$

$$0 < \alpha < 1$$

$$k = 1, 2, ..., l;\ i = 0, 1, 2, ..., n;\ j = 0, 1, 2, ..., m.$$

Appendix B

RMSD, maximum and minimum values of the tested maneuvers

This section provides the Root Mean Squared Deviation (RMSD) of the ANFIS Controlled Vehicle (ACV), Fuzzy Controlled Vehicle (FCV) and the passive vehicle described in chapters 6 and 7. And they are referred to as *anfis*, *fuzzy* and *passive*, respectively. Each of the three vehicles are compared based on the deviation from their desired trajectory, from their desired yaw rate, and from their desired side-slip angle. Where the deviation of the desired trajectory is described as the RMSD of the XY-coordinate, the maximum X-coordinate reached deviation and the maximum Y-coordinate reached deviation. While both the yaw rate and the side-slip angles are evaluated through the RMSD of each and the maximum and minimum deviations calculated by each.

The three evaluation trajectories: the Jturn, the Change Lane (CL) and the Double-change Lane (DCL) are described in chapter 7. Tables B.1 and B.2 show the described results on a dry surface with initial velocities of 20 and 30 km/h, respectively. While table B.3 shows the results on a 20 km/h in a snowy weather condition.

		Trajectory			Yaw rate			Side-slip Angle		
		RMSD	Max X	Max Y	RMSD	Max	Min	RMSD	Max	Min
Jturn	anfis	24.94	-6.741	-24.94	0.0065	0.0096	-0.0201	0.0328	0.0047	-0.0532
	fuzzy	28.64	-9.981	-26.84	0.0039	0.0062	0.0279	0.0219	0.004	-0.0368
	passive	71.28	24.03	-67.1	0.14	0.2153	-0.1311	0.0651	0.0056	-0.142
CL	anfis	4.49	4.49	0.045	0.002	0.0068	-0.0071	0.0085	0.029	-0.0307
	fuzzy	5.8	5.8	0.0457	0.0011	0.0038	-0.0052	0.0068	0.0207	-0.022
	passive	8.77	7.72	-4.17	0.1143	0.3147	-0.3593	0.0193	0.0654	-0.059
DCL	anfis	7.8	7.80	0.068	0.0028	0.0068	-0.0071	0.0116	0.0291	-0.0307
	fuzzy	10.07	10.07	0.1049	0.0734	0.2845	-0.2845	0.0068	0.0207	-0.022
	passive	19.04	13.18	13.74	0.139	0.3231	-0.359	0.0247	0.0654	-0.059

Table B.1: Results of the 20 km/h maneuvers on dry surface

		Trajectory			Yaw rate			Side-slip Angle		
		RMSD	Max X	Max Y	RMSD	Max	Min	RMSD	Max	Min
Jturn	anfis	51.33	-41.46	-30.26	0.0759	0.0136	-0.3059	0.0724	0.0024	-0.1282
	fuzzy	51.88	-9.548	-51	0.0023	0.0089	-0.0105	0.0828	0.0020	-0.1331
	passive	52.85	50.75	-52.61	0.1045	0.2418	-0.2466	0.1119	0.0019	-0.2243
CL	anfis	4.63	4.63	0.1065	0.0024	0.0099	-0.01	0.0166	0.057	-0.056
	fuzzy	5.79	5.79	-0.0567	0.0011	0.0035	-0.0056	0.01	0.0282	-0.0329
	passive	66.44	17.07	64.21	0.1147	0.3591	-0.2852	0.088	0.21	-0.1312
DCL	anfis	8.17	8.17	0.1674	0.0034	0.013	-0.0101	0.023	0.0574	-0.0568
	fuzzy	10.36	10.36	0.0722	0.0015	0.0054	-0.0056	0.0144	0.0351	-0.0329
	passive	128.3	73.83	105.00	0.2261	0.5188	-0.2852	0.0947	0.2295	-0.1311

Table B.2: Results of the 30 km/h maneuvers on dry surface

		Trajectory			Yaw rate			Side-slip Angle		
		RMSD	Max X	Max Y	RMSD	Max	Min	RMSD	Max	Min
Jturn	anfis	41.71	-32.57	-26.06	0.0418	0.0003	-0.0835	0.03	0.0029	-0.034
	fuzzy	52.65	-47.92	-21.81	0.0557	0.00	-0.0619	0.0259	0.0027	-0.0284
	passive	23.15	17.36	-15.32	0.0478	0.1134	-0.0922	0.0556	0.0034	-0.103
CL	anfis	4.51	4.51	-0.12	0.00	0.01	-0.01	0.01	0.04	-0.04
	fuzzy	5.4	5.398	-0.1228	0.00	0.01	-0.01	0.01	0.03	-0.03
	passive	69.65	38.13	-58.28	0.17	0.30	-0.40	0.15	0.28	-0.07
DCL	anfis	7.99	7.99	0.30	0.00	0.02	-0.01	0.01	0.04	-0.04
	fuzzy	9.40	9.40	0.28	0.00	0.02	-0.01	0.01	0.03	-0.03
	passive	71.79	42.82	-57.62	0.18	0.30	-0.53	0.17	0.30	-0.07

Table B.3: Results of the 20 km/h maneuvers on snowy surface